

## **APPENDIX A**

### **CHINESE TECHNICAL REPORTS**

**Note:** Throughout the Chinese Technical Reports, **B** stands for the multinational organization that this study chose. **H** stands for one of the rival companies of this multinational organization.

# **WIRE BONDING PROCESS**

*C1*

## **FINE PITCH WIRE BONDING ON 56L SDIP PRODUCTS**

## BACKGROUND:

Shortly after inventing the transistor, Bell laboratories developed a technique called thermocompression bonding, Bell then began contact equipment designers to provide the production machines. The year was 1957.

Kulicke & Soffa Company manufactured the first commercially available bonding Machines for the infant semiconductor industry. The wire bonding technique became generally applied.

Differently from the original way, today, the thermosonic welding method is the most often used way of wire bonding. It used ultrasonic energy and heat to weld the gold or copper wire from the bond pad of die to the lead of lead frame, thus, the internal connection of electronic circuit formed. Ball bonding takes its names from the shapes of the wire's end just prior to welding.

The requirements of today's high performance products have made fine pitch wire bonding a key semiconductor assembly capability. The introduction of fine pitch not only reduces the cost and raise the output, but also, make the device precision than ever before. It make it possible to bring customer more precious goods with smaller IC.

## EFFECTIVE:

To access the capability of current wirebond models available in MCEL to bone fine pitch devices, an evaluation of fine pitch wire bond on 56l SDIP conducted from Jun/98 to Aug/98. Following is the evaluation reports.

## PRODUCTION:

The evaluation divide into 3 phases, evaluation vehicle by 68H08MQ16, wire bond machine is KNS1488 TURBO and 1488 PLUS. From phase 2, 1488 TURBO is the only tested machine. By the end of phase 3, a Qual lot of XC device was conducted.

## EVALUATION FLOW:

### Phase 1:

To confirm the capability of 1488 wire bonder on handling material on 103 pad pitch; determine the important parameters.

### Phase 2:

Optimize the wire bond machine parameters for better in process responses.

### Phase 3:

Run evaluation lot by shift by operator, to determine the possibility of production.

### XC Qual Lot:

Per request of  $\beta$  a Qual lot was conducted for test the reliability of material.

## EVALUATION INFORMATION:

*wire bond machine:* 1488 Turbo & 1488 Plus

1488 Turbo is the continuous improve program version of 1484LXQ, through redesign of the microprocessor architecture, this machine could make long, straight, low loops in 120 milliseconds.

*evaluation schedule:*

PHASE 1	PHASE 2	PHASE 3	XC QUAL
3/JUN/98	3/JUL/98	31/JUL/98	2/AUG/98

*new material and tool:*

Lead Frame: H00662A507 pad size 300\*300mil  
Epoxy: SUMITOMO CRM-1078



Mold Compound: NITTO MP8000CH  
Capillary: MICROSWISS 484FD-2093-R35

**Assembly Information:**

Die P/N: D5046000J55G  
Die Size: 173.9\*177.9 mil  
Min pitch: 103.6 micron  
Pass opening: 86.2 micron  
Bond Diagram: 67ASE04727W  
Package: 56L SDIP

**EVALUATION:**

**PHASE 1**

Evaluation conducted on two model of wire bond machine: 1488plus and turbo  
GW is Sumitomo NL3, the experiment is debugged in two sections:

*\* Parameters set for 1488 plus:*

	<i>First bond(pad)</i>	<i>Second bond</i>
<i>Pre head temperature</i>	190 deg C	190 deg C
<i>Bond site temperature</i>	200 deg C	200 deg C
<i>Tip offset</i>	50 tenth-mil	50 tenth-mil
<i>Bond velocity</i>	60 tenth-mil	60 tenth-mil
<i>Bond time</i>	15 msec	15 msec
<i>Bond force</i>	35 g	40 g
<i>Bond power</i>	48 mwatt	40 mwatt
<i>Power profile</i>	1-sqr	1-sqr
<i>USG I/V select</i>	1-volt	1-volt
<i>USG delay</i>	0	0
<i>Ramp up</i>	0	0
<i>Ramp down</i>	0	0
<i>Initial force</i>	0	0
<i>First force time</i>	0	0
<i>Force ramp time</i>	0	0

<i>Looping:</i>	<i>LF2 worked</i>		
<i>Loop height</i>	60	<i>Wire size</i>	1.0 mil
<i>Loop factor</i>	150 percent	<i>Ball size ratio</i>	1.5
<i>Theta</i>	45	<i>LF4</i>	75
<i>Contact threshold</i>	50	<i>Kink height</i>	55 tenth-mil
<i>Delta loop</i>	0 tenth-mil	<i>Reverse loop</i>	55 tenth-mil
<i>EFO gap</i>	15	<i>Loop trajectory</i>	5
<i>Loop factor 2</i>	10	<i>Contact angle</i>	0
<i>Loop factor 3</i>	0	<i>Tol correction</i>	0
<i>Impact profile</i>	200	<i>Impact time</i>	0

*\* Result of 1488 plus: (g)*

	MAX	MIN	AVER	RANGE	S	Cpk
<b>Wire pull</b>	11.0	7.5	9.1	3.5	.8	2.13
<b>Ball shear</b>	46.3	29.7	35.8	16.6	4.0	1.73
<b>Wire peer</b>	8.5	5.5	7.1	3.0	.62	1.67

*Other data such as wire sweep, and die shear are under spec.*

*\* Parameters set for 1488 turbo:*

	<i>First bond(pad)</i>	<i>Second bond</i>
<i>Pre head temperature</i>	190 deg C	190 deg C
<i>Bond site temperature</i>	200 deg C	200 deg C
<i>Tip offset</i>	60 tenth-mil	60 tenth-mil
<i>Bond velocity</i>	10 tenth-mil	10 tenth-mil
<i>Bond time</i>	15 msec	20 msec
<i>Bond force</i>	35 g	40 g
<i>Bond power</i>	33 mwatt	40 mwatt
<i>Power profile</i>	1-sqr	1-sqr
<i>USG I/V select</i>	1-volt	1-volt
<i>USG delay</i>	0	0

<i>Looping:</i>	<i>LF2 worked</i>
-----------------	-------------------

Theta	23	LF4	35
Contact threshold	50	Kink height	55 tenth-mil
Delta loop	-30 tenth-mil	Reverse loop	55 tenth-mil
EFO gap	15	Loop trajectory	5
Loop factor 2	10	Contact angle	0
Loop factor 3	0	Tol correction	0
Impact profile	200	Impact time	2

\* Result of 1488 turbo: (g)

	MAX	MIN	AVER	RANGE	S	Cpk
Wire pull	9.8	7.5	8.7	2.3	0.53	2.95
Ball shear	35.6	24.3	29.1	11.3	2.79	1.68
Wire peer	8.3	5.8	6.9	2.5	0.55	1.76

Result of ball placement: (micron)

Bx	69.95	Sx	1.06	Tx	2.13	Cx	4.42
By	67.95	Sy	1.06	Ty	0.62	Cy	1.59
Cpk(X)	0.52			Cpk(Y)	1.64		

Bx: Ball size(x)      Sx: Ball size std dev(x)  
 By: Ball size(y)      Sy: Ball size std dev(y)  
 Tx: Target error      Cx: Target error std dev(x)  
 Ty: Target error      Cy: Target error std dev(y)

*The result shows that: besides the ball placement, other data all above the requirement of spec. Further evaluation needed for improve the ball placement performance.*

## PHASE 2:

Second phase evaluation emphasized on improving the performance of ball placement, with two kind of wire: Tanaka FA type: Sumitomo NH 2 type

	<i>First bond(pad)</i>	<i>Second bond</i>
<i>Pre head temperature</i>	190 deg C	190 deg C
<i>Bond site temperature</i>	200 deg C	200 deg C
<i>Tip offset</i>	70 tenth-mil	70 tenth-mil
<i>Bond velocity</i>	6 tenth-mil	6 tenth-mil
<i>Bond time</i>	20 msec	15 msec
<i>Bond force</i>	35 g	40 g
<i>Bond power</i>	40 mwatt	40 mwatt
<i>Power profile</i>	1-sqr	1-sqr
<i>USG I/V select</i>	1-volt	1-volt
<i>USG delay</i>	0	0

<i>Looping:</i>	<i>LF2 worked</i>		
<i>Loop height</i>	50	<i>Wire size</i>	1.0 mil
<i>Loop factor</i>	140 percent	<i>Ball size ratio</i>	1.85
<i>Theta</i>	23	<i>LF4</i>	50
<i>Contact threshold</i>	40	<i>Kink height</i>	50 tenth-mil
<i>Delta loop</i>	-30 tenth-mil	<i>Reverse loop</i>	55 tenth-mil
<i>EFO gap</i>	10	<i>Loop trajectory</i>	5
<i>Loop factor 2</i>	10	<i>Contact angle</i>	0
<i>Loop factor 3</i>	0	<i>Tol correction</i>	0
<i>Impact profile</i>	80	<i>Impact time</i>	2

*Compare with phase 1, the most important parameters of bond force, bond time, and bond power were changed as same with impact profile.*

*\* Result of Sumitomo NL3 type: (g)*

	MAX	MIN	AVER	RANG	S	Cpk
--	-----	-----	------	------	---	-----

Ball shear	35.9	26.5	30.5	9.4	1.99	1.76
Wire peer	7.5	5.3	6.4	2.2	0.56	1.42
Loop height(mil)	8.82	7.34	8.25	1.48	0.27	N/A
Ball height(mil)	0.66	0.48	0.55	0.18	0.06	N/A

*Result of ball placement: (mil)*

<i>Bx</i>	2.69	<i>Sx</i>	0.08	<i>Tx</i>	0.06	<i>Cx</i>	0.04
<i>By</i>	2.63	<i>Sy</i>	0.06	<i>Tx</i>	0.10	<i>Ty</i>	0.10
<i>Cpk(X)</i>	0.52			<i>Cpk(Y)</i>	1.64		

*Bx*: Ball size(x)      *Sx*: Ball size std dev(x)  
*By*: Ball size(y)      *Sy*: Ball size std dev(y)  
*Tx*: Target error      *Cx*: Target error std dev(x)  
*Ty*: Target error      *Cy*: Target error std dev(y)

*\* Result of Sumitomo FA type: (g)*

	MAX	MIN	AVER	RANG E	S	Cpk
Wire pull	9.5	6.5	8.2	3.0	.71	1.95
Ball shear	38.5	26.7	31.2	11.8	2.65	2.1
Wire peer	6.8	5.0	5.9	1.8	.41	1.55
Loop height(mil)	8.7	7.2	8.0	1.5	.28	N/A
Ball height(mil)	0.6	0.4	0.5	0.1	0.04	N/A

*Result of ball placement: (mil)*

<i>Bx</i>	2.75	<i>Sx</i>	0.07	<i>Tx</i>	0.06	<i>Cx</i>	0.05
<i>By</i>	2.61	<i>Sy</i>	0.07	<i>Tx</i>	0.13	<i>Ty</i>	0.06
<i>Cpk(X)</i>	1.00			<i>Cpk(Y)</i>	1.09		

By: Ball size(y)      Sy: Ball size std dev(y)  
 Tx: Target error      Cx: Target error std dev(x)  
 Ty: Target error      Cy: Target error std dev(y)

*Result shows that the Cpk of ball placement were improved compared with phase 1, the difference between were reduced.*

### PHASE 3 and XC Qualification lot:

With the same parameters set as phase 2, the third evaluation lot was released to production line, besides F/E process, the assembly data tests were taken also

The operation of the lot was conducted by production line operators instead of engineers in phase 1 and 2, the purpose is to examine the capability of process.

Since the Gold wire of FA type shows the same performance with NL3 type, and FA type is the qualified G/W in TianJin plant, we used only FA type in phase 3 and qual lot.

### *\* Result of Phase 3: (g)*

	MAX	MIN	AVER	RANGE	S	Cpk
Wire pull	9.3	7.5	8.4	1.8	0.45	3.26
Ball shear	37.4	25.6	30.5	11.8	2.98	1.73
Wire peer	8.0	5.3	6.9	2.7	0.56	1.76
Loop height(mil)	8.48	7.20	7.86	1.28	0.23	N/A
Package warpage(mil)	2.9	2.7	2.8	0.2	N/A	N/A
Plating thickness(u-inch)	581.18	410	170	494	N/A	1.72
Composition(%)	84	80	4.02	82.7	N/A	2.37
Solderability						Pass
Physical dimension test						Pass

### *Result of ball placement: (mil)*

Rv	2.64	Cv	0.05
----	------	----	------

<i>By</i>	2.57	<i>Sy</i>	0.06	<i>Tx</i>	0.01	<i>Ty</i>	0.07
<i>Cpk(X)</i>		1.51		<i>Cpk(Y)</i>		1.47	

*\* Result of Qual lot: (g)*

	MAX	MIN	AVER	RANGE	S	Cpk
Wire pull	8.8	7.3	8.1	1.5	0.39	>3
Ball shear	38.7	26.0	31.4	12.7	3.19	1.71
Wire peer	8.0	6.0	7.1	2.0	0.49	2.11
Loop height(mil)	8.06	7.02	7.67	1.04	0.25	N/A
Package warpage(mil)	2.94	2.15	2.628	0.79	N/A	N/A
Plating thickness(u-inch)	581.1	410.8	170.38	494	3.1	1.72
Composition(%)	84.24	80.22	4.02	82	3.27	2.37
Solderability	Pass					
Physical dimension test	Pass					

*Result of ball placement: (mil)*

<i>Bx</i>	2.68	<i>Sx</i>	0.05	<i>Tx</i>	0.02	<i>Cx</i>	0.06
<i>By</i>	2.67	<i>Sy</i>	0.06	<i>Tx</i>	0.06	<i>Ty</i>	0.04
<i>Cpk(X)</i>		1.42		<i>Cpk(Y)</i>		1.52	

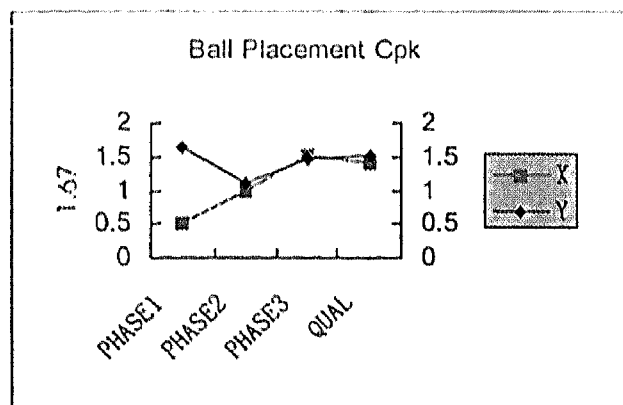
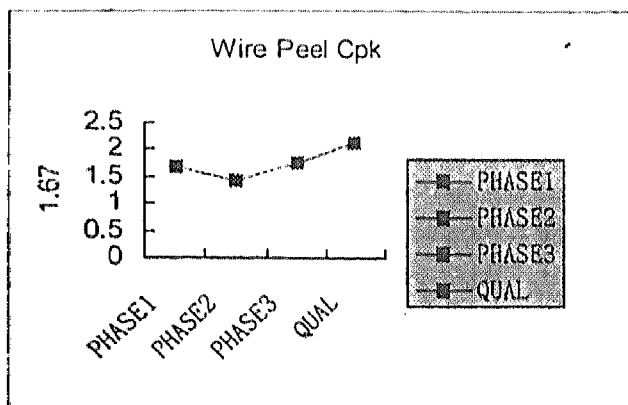
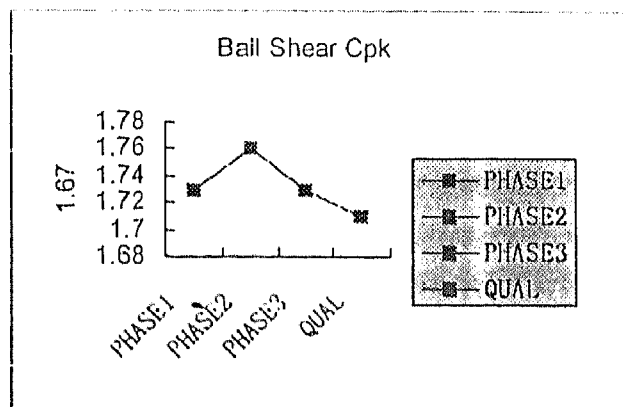
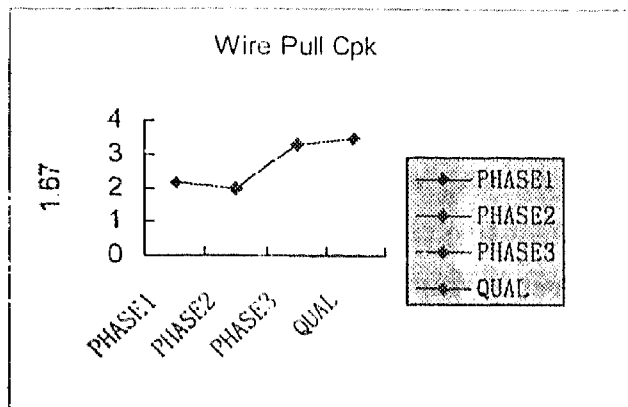
*Bx: Ball size(x)      Sx: Ball size std dev(x)*  
*By: Ball size(y)      Sy: Ball size std dev(y)*  
*Tx: Target error      Cx: Target error std dev(x)*  
*Ty: Target error      Cy: Target error std dev(y)*

*Result shows significant improve of ball placement Cpk, the trial run & production is successfully.*

*Following analysis will show the Cpk trend of the three phase evaluations and XC Qual lot.*

## ANALYSIS OF EVALUATION:

The data trend of the key data value shown as following charts.



Based on the confirmation run on 1488 turbo, significant difference on die placement capability was seen on 56L SDIP product, the trial run also shows that the assembly line can deal the production of 100 micron level pad pitch device, it is the first lot of fine pitch material tested in TianJin plant, this experience is very helpful for further evaluation.

## MARK:

- \* Although the evaluation shows good result, there still some points need improve. Ball placement still need improve. and if OK DCA...



- 
- \* The assembly parameter definition requires more study on DOE.
  - \*.The gold wire of FA type is not a finepitch type, so, it better to evaluate a finepitch type wire.
  - \*.The overall performance of material still expect the XC Qual lot result.

#### VERLOOK:

*The definition of what is considered fine pitch has changed very quick. A few years ago, manufacturers were struggling to reach 115  $\mu$  m bonding pitch; today, 90  $\mu$  m is a growing application that is producing excellent yield in many production environments. An 80  $\mu$  m process is in qualification for QFPs, and feasibility studies for 70  $\mu$  m QFPs and BGAs have produced very good results. So, the evaluation of our plant is low level study compare with the fashion, it is urgent for MCEL to catch up with the leader level.*

## **No PMC Study on SOIC28WB Package with Fast Cure Molding Compound**

## Background

As we know, PMC process has much contribution to our assembly cycle time as well as it to the quality of our products. Many investigations are being performed aiming to eliminate this process. TJ plant had passed the BOM standardization qualification with No PMC process on 08/14/16 last year and no additional process was required. Molding compound used in equal is MP8000 series and EME6600CS series which are both categorized in fast cure type. For SOIC28WB, same project will be launched. Before this, we have to determine if we can eliminate PMC or how many hours it can be shortened through study on compound properties based on current process.

In this industry, we must go through the validation test for major process/material change. In other words, we must pass reliability test. The reliability performance has close relationship with mechanical interaction between the plastic package and the silicon device it surrounds. Thermal expansion, dynamic modulus and adhesion studies are used to describe this interaction. So, our investigation was divided into two stages, one is compound properties comparison between PMC and No PMC, another is the reliability test.

## Performance of Molding Compound Before and After Postcure

Due to the high glass filler content of the IC encapsulant compound are very stiff, high modulus, brittle material. Although the coefficient of expansion for this type of material is low, the combination of high curing temperature and high modulus can lead to serious thermally induced stress that can damage the silicon device or result in cracking of the epoxy package during temperature cycling. Any fissure in the IC package can provide a path for the ingress of moisture contaminants that can cause failure of the device. Thermally induced stress can also cause adhesive bond failure between the epoxy and the copper lead frame, which allows another means for moisture to reach the device. Therefore, the heat history is very important in order to get elements with high reliability. Economics is the driving force for industry interest in no postcure epoxy packages. At the same time, microelectronic performance requirements remain high. Thus, these key characteristics need special scrutiny regarding to no-postcure and postcure.

This study is mainly on comparing the performance of molding compound before and after postcure. Four types of commercial molding compound were selected for evaluation and named as A, B, C, M. A, C and M are all belong to fast cure family.

## Test and analysis (I) - effect on Tg

Besides epoxy chemistry, its heat history is an important crosslink factor. Up to 95% of potential crosslinks may be established during molding of integrated circuits. Additional crosslink occurs during postcuring of molded parts in an oven for 4-16 hours. Mold and postcure temperature may vary from 160 - 190degree. Most often, postcure conditions of 2 hours at 170degree are employed.

Table 1 and Fig. 1 presents Tg data versus postcure time. It is always significantly higher after postcure. Therefore, high Tg-specification generally can not be served without postcure

Table 1 postcure effect on Tg

Table 1 Postcure effect on Tg

cure condition	Tg degree			
	A	B	C	M
NPMC	103	129	130	111
170@2 hrs	127	154	142	132
170@4hrs	149	167	149	155

Remark: Tg is measured by DMA which is defined the temperature at the peak of the tan delta.

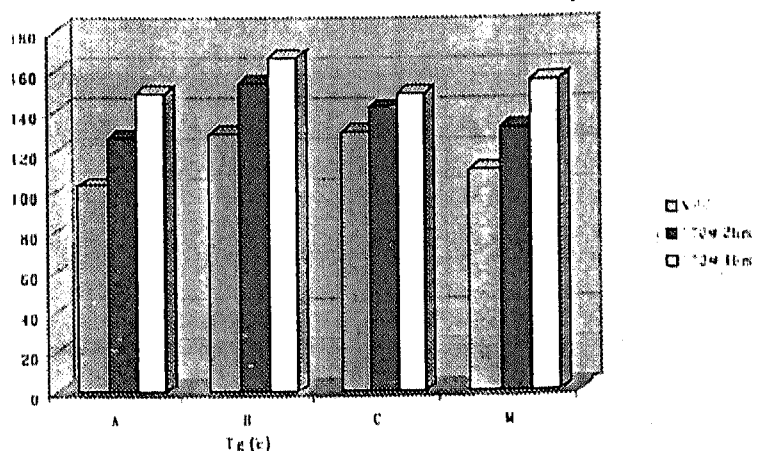


Fig. 1 The postcure effect on Tg

and analysis (2) - effect on adhesion properties

importance of good adhesion of the epoxy to the silicon device for excellent package cra-  
 stance was discovered as the result of a special test design to simulated the stress  
 concentrations at chip corners to observe epoxy cracking. If there is good epoxy-silicon  
 adhesion the thermal stress that develops at low temperature in the element of epoxy will  
 plate into the silicon. However, if there is poor adhesion over the surface leading up to th  
 corner, the stress in the element no longer couples into the silicon but will cause an  
 ease in the stress at the corner.

how in table 2 and Fig. 2, the effect of postcure on adhesion to metal lead frames is  
 evident on the compound type. The adhesion of Molding compound A with postcure to  
 ver leadframe was found lower than that of no-postcure, while Molding compound C  
 ved higher adhesion to copper leadframe after postcure.

Table 2 Postcure effect on adhesion to Copper lead frame

Table 2 Postcure effect on adhesion to cu lead frame

cure condition	adhesion(kgf)	
	A	C
NPMC	129	111
170@2hrs	167	155

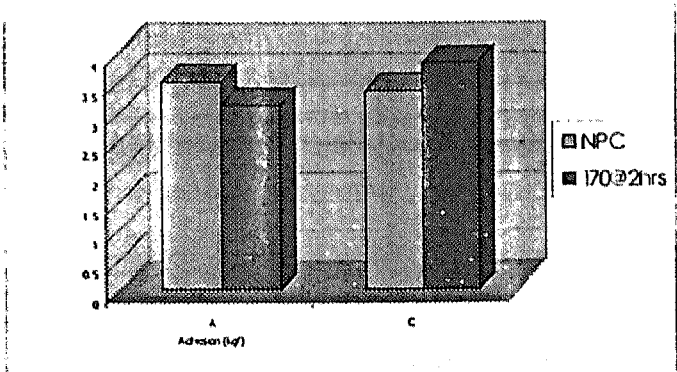


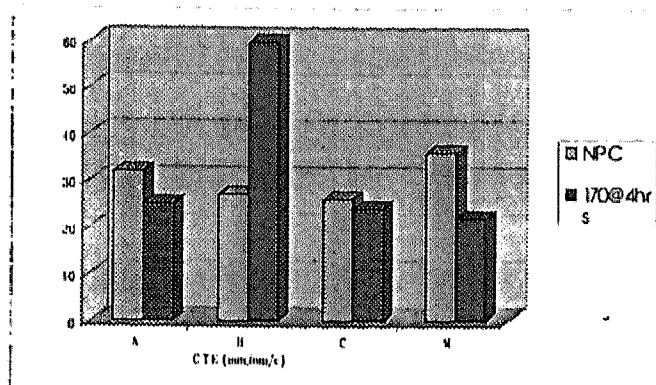
Fig. 2 Adhesion to cu lead frame

### and analysis (3) - effect on CTE

efficient of expansion (CTE) are generally governed by filler type and level, not by postcure or postcure conditions. As displayed in Table 3 and Fig. 3, however lower CTE after postcure have been noticed except B.

Table 3 Postcure effect on CTE(25 - T<sub>g</sub>)

cure condition	CTE (mm/mm/degree)			
	A	B	C	M
NPMC	32	27	26	36
170@4hrs	25	60	24	22



### g) Coefficient of thermal expansion of no-postcure versus postcure

### and analysis (4) - effect on moisture absorption

ed fully cured by various mechanical measurements, there remains, in fact, a measurable amount of unreacted epoxy groups. This phenomenon, we believe, has its origin in the physical constraints in highly crosslinked networks that render inaccessible to a fraction of

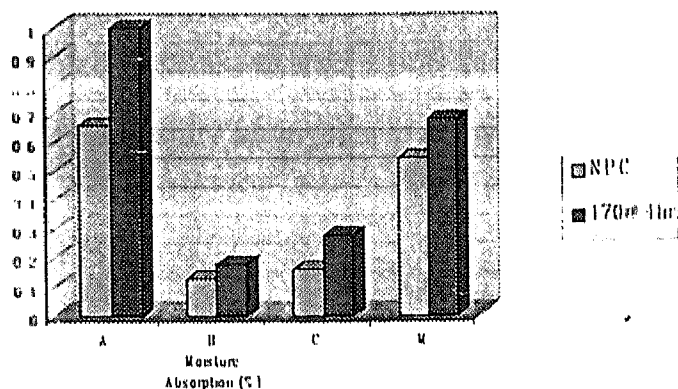
groups during the final stages of cure. The postcure step in the stoichiometric and y-rich formulations caused an additional crosslink.

effect of postcure on moisture absorption depends on it's moisture condition. Moisture rption in Fig. 4 and table 4 showed that postcure increase moisture absorption. The omenon has been explained an increase in free volume with postcure.

Table 4 Postcure effect on moisture absorbtion

(dipped in deion water at room temperature for 10 days)

cure condition	Moisture Absorption(%)			
	A	B	C	M
NPMC	0.66	0.13	0.16	0.55
170@4hrs	1	0.18	0.28	0.68



#### 4Moisture absorption of no-postcure versus poscure

Table 5 Postcure effect on moisture absorbtion

(Exposure to hast 85degree/85% RH)

cure condition		
	A	C
Cured at 180°C /40s	0.33	0.41
Cured at 180°C /60s	0.43	0.56
2hrs PMC 40s	0.39	0.55
4hrs PMC 40s	0.47	N/A

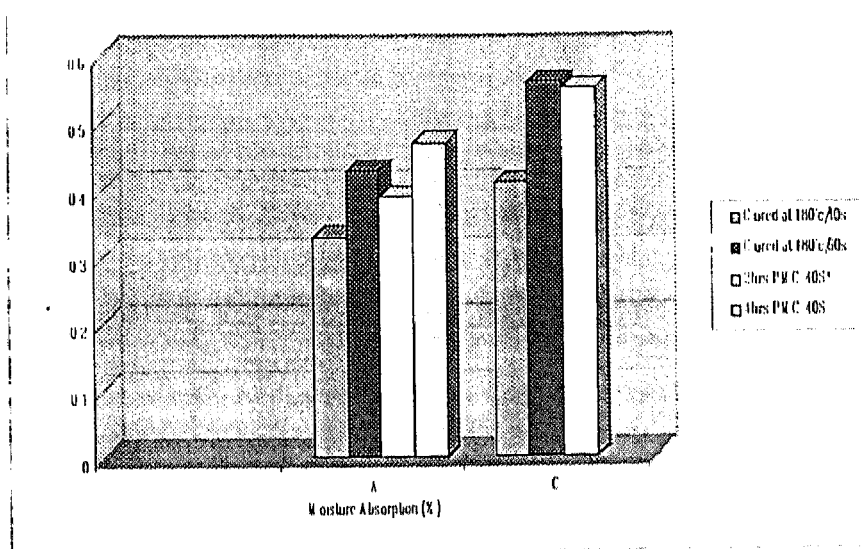


Fig.5 Moisture absorption of no-postcure versus postcure

and analysis (5) - effect on modulus

As the CTE, the modulus is governed by the filler content, since filler is the predominant component with a high modulus in the order of 69Gpa(10Mpsi), compared to only 0.5Gpa(0.5Mpsi) for the organic portion of the compound.

Table 6 Postcure effect on storage modulus

cure condition	Storage Modulus(Gpa)			
	A	B	C	M
NPMC	13.5	4.9	12.6	10.5
170@2hrs	12.9	5.4	12.8	12.6
170@4hrs	12.4	4.9	14	11.4



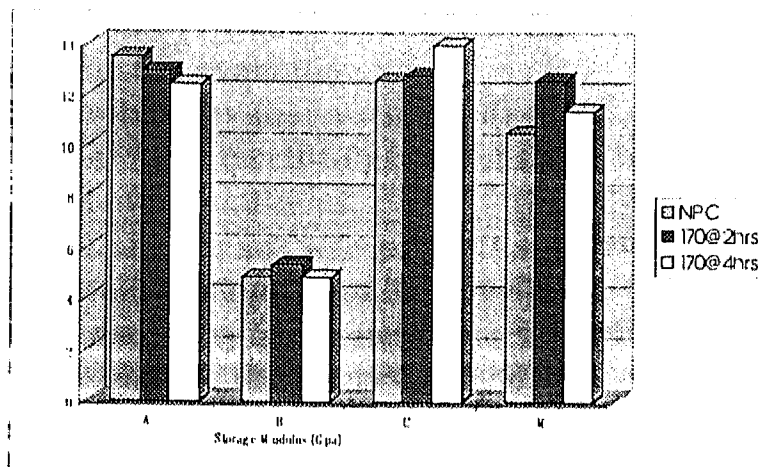


Fig.6 The effect of postcure on storage modulus

Table 7 Postcure effect on flexural strength

cure condition	Flexural Strength(Kgf/mm2)			
	A at 140°C	A at 170°C	C at 190°C	C at 240°C
PMC 2 hrs	2.1	1.13	0.82	0.75

### Reliability Performance Evaluation

From above investigation on molding compound, we build 7 lots with different mold condition to compare the impact of no-postcure and postcure process on IC reliability performance. The different molding conditions are as following:

Compound type	in mold cure time	post mold cure time
C	60s	0 hour
	40s	0 hour
	40s	2 hours
A	60s	0 hour
	40s	0 hour
	40s	2 hours
	40s	4 hours

Compound C&A are both fast cure type. Vendor

his evaluation was aimed to choose appropriate molding condition for further no or less  
 sture qualification on SOIC28 wide body. One type of micro controller MC68HC705P6  
 open as vehicle for this evaluation.

Reliability is the probability that a semiconductor device will perform its specified function  
 given environment for a specified period of time . In other words, reliability is quality over  
 time and environmental conditions. Reliability has always stressed reliability and quality  
 considerations in designing any new product and developing new process.

It has no expectation this time. But, how to choose reliability test for this evaluation? It has  
 time and is not necessary for us to finish a full reliability test table designed for a formal  
 qualification. According to the requirements of AEC-Q100 & MIL-standards, we choose  
 TH(AUTOCLAVE) and HAST(pressure-Temperature-Humidity-Bias) as the test items.

Condition of PTH: 121degree, 15psig, 100% relative humidity, 144hours.

Condition of HAST: 85%RH/121degree/15psig plus abias level which is the nominal rating  
 of device.

Sides, for surface mount package, preconditioning process is required before standard  
 environment test is performed. The procedure for preconditioning test is as following:

1. -65 degc; 10cycles) --->Backing (125degc; 24hrs) --->T(85degc/85%RH; 168hrs)  
 2. IR(245 degc)

According to AEC-Q100, pre and post stress electrical test must be performed on samples at  
 room and hot temperature.

#### Reliability result:

IR(245 degc) precondition	precondition	pass
HAST	48hrs	pass
	96hrs	pass
IR(245 degc) precondition	precondition	pass
PTH	96hrs	pass
	144hrs	pass

#### Conclusion

Through above investigation on compound properties, we have further understanding upon  
 molding compound that we are using. To some aspect, we can see there is no significant  
 change between after and before PMC to fast cure type compound. In the other hand, the  
 compound vendors had their products achieved low stress by rubber type elastomer, achieved

high reliability by special additive, and so on. This can offset the influence of no-PMC proc  
 some extent. And all lots under different

ability test with no failure was detected. This gives us more confidence on qualifying the MC process on SOIC WB package.

# **WIRE BONDING PROCESS**

## **PPF STUDY ON D/B PROCESS**

# PPF STUDY ON D/B PROCESS

## - Background

CRM-1064M/MA epoxy are used for PCIC/SOIC PPF. Their outgassing is less and is reported having better die adhesive characteristic. But 1064MA was found having low die shear problem during production. This will affect other following process (such as wire bond) and reliability feature of device

Many works have been done to search the root causes and resolve them.

## - PPF Epoxy Die Shear Characteristic

The die shear characteristics of CRM-1064M/MA provided by epoxy vendor are shown as figure1 and figure2. From the figures we can see:

1. Die shear strength for PPF is lower than that for Ag-plated copper L/F which is being used by now
2. Die shear strength will obviously reduce at high temperature(hot shear feature)

So, die shear should be focused on during production evaluation, which is also the most important characteristic of die bond process.

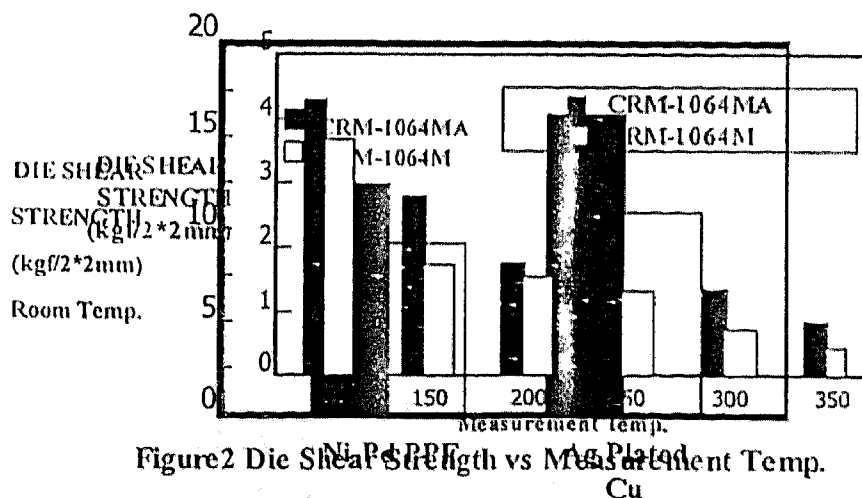


Figure2 Die Shear Strength vs Measurement Temp.

Figure1 Die Shear Strength for PPF and Ag-plated L

## *- Problem Description*

Our problem occurred to CRM-1064MA used for SOIC 8/14/16LD package.

SOIC 16LD (H00980A706) PPF and SOIC 8LD (H00976A704) PPF was first used on production line. Their die shear quality was found not acceptable. For example, our first evaluation results for H00976A704 are as follow:

Device: MC34119

Die Size: 49\*58mils

D/S Spec: 2.26kg

L/F Vendor: Mitsui/DCI

Die Bonder: ESEC 2006HR

Die shear raw data: (Unit: kg)

Mitsui: 1.60 1.26 2.56 1.99 3.92 2.68

DCI: 2.83 1.22 0.81 1.03 3.93 2.10

All the data with underline are lower than SPEC.

The same thing was found to H00980A706, too.

An experiment was done to compare different die shear feature of PPF and Ag-plated copper L/F. It shows that PPF has worse die shear strength than Ag-plated just as figure1 shows.

Experiment information:

Device: MC 34119

Die Size: 49\*58mils

SPEC: 2.26kg

Die Shear raw data (Unit: kg):

1. PPF (H00976A704):

2.46 4.01 4.35 3.19 5.81 2.24 4.32 4.09 3.95 3.92

max: 5.81 min: 2.24 average: 3.83

2. Ag-plated (H00976A502):

4.81 5.75 7.17 4.73 6.14 7.22 5.13 7.28 4.89 5.86

max: 7.28 min: 4.73 average: 5.90

Besides die shear data is lower for PPF than Ag-plated L/f, it's observed that there is almost no epoxy residual on L/f flag for PPF while there is always more than 60% residual on flag for Ag-plated. This also means that epoxy has less adhesive strength with PPF.

## **- *Solution***

Through our former experiment and analysis, below respects were found having heavy impact and should be pay attention:

1. cure method, cure temperature and epoxy
2. epoxy thickness between die and flag pad
3. test method for die shear

Our experiment design is based on these three respects.

## **Experiment1**

### **-----Feature of snap cure:**

First, experiment was conducted on H00980A706. It focuses on the effects of snap cure temperature, epoxy and deference between snap cure and oven cure.

Snap cure has big difference from oven cure. Its temperature profile was measured as Figure1. It can't provide the same stable temperature profile as oven cure: the temperature readings at different positions in tunnel are different from each other and for one L/F, the temperature at side strands is lower than that at center strand. This is a potential root cause of unstable die shear strength.

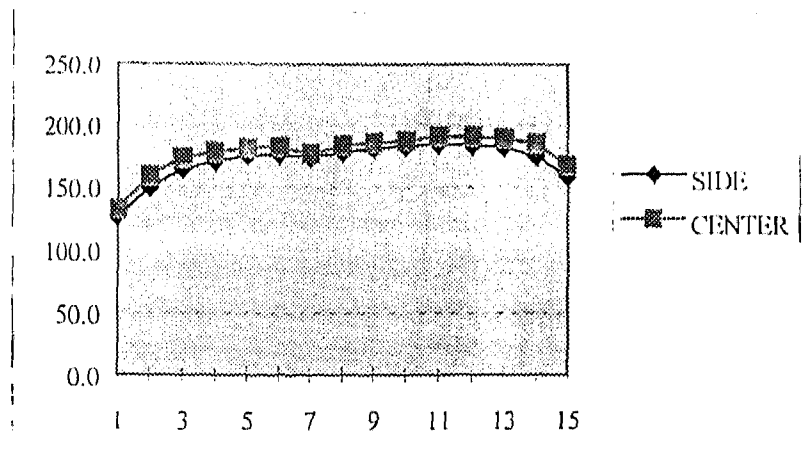


Figure3 Temperature profile of snap cure

Experiment information:

Die/Bonder: ESEC 2006HR

Wire/Bonder: UTC-105 with snap cure

L/F: H00980A706 (PPF)

Die Attachment: CRM-1064MA

Device: SC78202DR2

Die Size: 80\*95mils

D/S SPEC: 5.0kg

Experiment results and conclusion:

Table1

Unit: kg

	Max	Min	Average
1. Tunnel cure vs Oven cure:			
Cure condition			
180degree C/140s+200degree C/140s	7.17	3.43	5.86
175degree C/140s+175degree C/140s	7.23	4.08	6.05
175degree C(280s)Oven Cure	13.22	8.66	10.77
2. Different epoxy lot:(200degree C/180s+200degree C/180s)			
Lot# 712153	9.62	3.61	6.87
Lot# 801121	10.76	3.74	7.25
Lot# 801282	9.33	4.11	7.04
Conclusion: 1.Oven cure has much better die shear strength than tunnel cure.			
2.There's no significant difference between different epoxy lot			



## Experiment2

### -----Comparison of different l/f:

This experiment was done to compare different l/f from Mitsui and DCI respectively.

Die size: 50\*53mils

SPEC: 2.12kg

Mitsui l/f :					max	min	avg
7.49	10.86	8.85	5.48	4.28			
8.38	5.32	2.33	4.21	2.54	10.86	2.33	5.96
DCI l/f :							
7.80	4.69	4.31	4.15	4.72			
3.64	2.69	1.12	3.04	4.22	7.80	1.12	4.04

The results show that die bond performance of Mitsui l/f is better than DCI, so our following evaluation experiment focus on l/f from Mitsui.

## Experiment3

### -----Die Attach Thickness

Although snap cure has negative effect on die shear, but we don't think it's the only and the most important root cause for a so bad die shear problem. Our next focus is on epoxy thickness.

Two functions executed by epoxy is:

1. Attach die to flag
2. Cushion internal stress

Epoxy thickness is the most important parameter to these two functions. If epoxy is not thick enough, the functions could not be achieved.

Motorola SPEC about epoxy thickness is 0.3-2mils. But by checking our status on production line, the thickness range is only 0.2-0.3mil, which is even lower than SPEC. It does need to be improved.

Experiment information:

Device: MC34119

L/F: H00976A704

L/F Vendor: Mitsui

Die Size: 49\*58mils

Die Bonder: ESFC 2006HR

D/S SPEC: 2.26kg

Experiment results is as Table2.

Table2:

Thin Epoxy: ( 0.2-0.3mil, not meet SPEC )												
	1	2	3	4	5	6	max	min	range	std	cpk	avrg
1	8.48	6.85	8.94	9.36	4.40	10.08	10.08	3.67	6.41	1.99	0.88	7.54
2	8.05	8.48	9.28	8.58	6.80	6.82						
3	4.68	9.22	10.00	8.11	9.95	7.91						
4	4.77	7.32	4.32	4.70	9.80	10.00						
5	5.73	3.67	8.31	5.25	8.18	8.06						
Thick epoxy: ( 0.4-0.6mil, meet SPEC )												
1	9.57	9.15	8.11	6.42	9.11	10.37	11.91	5.25	6.66	1.71	1.34	9.13
2	10.93	9.13	6.65	10.05	11.91	8.15						
3	9.97	10.50	9.38	9.97	5.25	10.60						
4	8.46	9.97	11.03	9.96	9.59	10.29						
5	8.45	10.81	6.44	10.48	5.47	7.58						

JMP analysis was used for above data.

t-Test

	Difference	t-Test	DF	Prob> t
Estimate	0.92722	2.234	118	0.0273
Std Error	0.41497			
Lower 95%	0.10546			
Upper 95%	1.74898			

Assuming equal variances

Epoxy thickness is an important parameter according to the above result.

## Experiment4

### -----Cure Temperature

Three different cure temperatures were selected to determine the impact.

Table3:

cure temp		1	2	3	4	5	max	min	range	sld	avg
180-200	1	9.57	9.15	8.11	7.42	9.11	11.60	5.25	6.35	1.66	9.16
	2	10.93	9.13	6.65	10.05	10.91					
	3	8.15	10.81	6.41	10.48	5.17					
	4	10.37	9.97	10.50	9.38	9.97					
	5	8.15	8.16	9.97	10.03	9.96					
	6	7.58	5.25	11.60	9.59	11.29					
200-220	1	10.27	8.06	10.66	8.57	10.72	12.23	4.80	7.43	1.92	8.31
	2	5.94	6.79	7.80	4.80	8.29					
	3	7.46	11.53	12.23	8.34	10.49					
	4	6.23	6.27	9.13	7.64	8.36					
	5	6.53	6.42	9.30	9.70	9.28					
	6	10.80	7.68	5.02	6.67	8.25					
175-175	1	10.37	6.15	7.29	5.37	8.51	12.66	5.37	7.29	2.11	7.96
	2	11.18	6.96	7.72	12.66	7.98					
	3	8.10	7.87	9.86	6.84	7.02					
	4	6.02	7.46	6.28	9.32	6.05					
	5	7.23	12.20	11.10	11.74	6.11					
	6	5.95	6.35	6.02	6.84	6.22					

Unit: kg

Above data was analyzed using JMP.

### Analysis of Variance

Source	DF	Sum of Squares	Mean Square	F Ratio
Model	2	21.49158	10.7458	2.9122
Error	87	321.02796	3.6900	Prob>F
C Total	89	342.51954	3.8485	0.0597

### Means for Oneway Anova

Level	Number	Mean	Std Error
high	30	8.30767	0.35071
low	30	7.95900	0.35071
medium	30	9.12500	0.35071

Std Error uses a pooled estimate of error variance

From the ANOVA result,  $H_0$  is failed to reject. But, Prob>F is very close to the critical value of 0.05. So the cure temperature is an important input variable.

## Experiment 5

### -----Comparison of measurement method

During our experiment, we find that unproper test method is also affecting our results.

One L/F with die attached was separated into two parts for MCEL and Mitsui to measure respectively. The test results were quite different.

#### Experiment information:

Device: MC34072

Die Size: 65\*74mils

D/S Spec: 3.78kg

L/F: H00976A704 (SOIC 8LD)

#### TEST 1:

Test Location : MCEL

Equipment : Bondtest-30

Raw data(kg) : 0.72, 1.73, 2.48, 2.58, 3.28, 3.45, 3.81, 4.04, 4.04,  
5.03, 5.18, 5.28, 5.87, 6.69, 6.71, 7.27, 8.22, 9.67

Below spec : 6 out of 18

Within spec : 12 out of 18

Total average : 5.5 kg

#### TEST 2:

Test Location : Mitsui Japan

Equipment : Dage BT100 (Arctek)

Raw data(kg) : 9.0, 10.0, 10.0, 11.0, 11.0, 11.0, 11.5, 12.0, 12.0, 12.0,  
12.0, 12.5, 12.5, 12.5, 12.5, 12.5, 12.5, 13.0, 14.0, 15.0

Below spec : none

Within spec : 20 out of 20

Total average : 11.9 kg

The possible causes for the large discrepancy:

- (1) Different measurement equipment
- (2) Variation (decreased strength) introduced by clamping methods.

Comparison of measurement methods

MCFI.

Equipment :	Bondtest-30	Dage BT100
Clamping :	One-direction clamp	Vacuum on bottom of pad
Separation:	Die pad not separated from leadframe	Die pad separated from leadframe before test
Tool :	Manual positioning	Automatic positioning 10 um above die pad surface

The sketch of the two testing set ups shown as figure4 and figure5.  
Comparison of measurement results (See Figure6 ):

Visual examination of the die pads after testing shows that the gripping clamps of the Bondtest-30 machine leave strong dent marks on the underside of the die pad, and cause the die pad to warp. Mitsui currently uses a fixture jig that pulls a vacuum on the bottom of the die pad, but previously used a similar clamping machine to that of MCEL. In past experience, it was shown that excess clamping of the die pad may cause deformation that weakens the bond between the epoxy. In extreme cases, pressure from the clamp can cause the die to pop off even before the test is run. Same phenomena was observed by us, too.

Experiment results show that PPF is stiffer than copper l/f, the die is more likely tend to separate from the flag pad when the flag is clamped heavily. So, operators are noticed to use as small clamp force as possible to avoid it. New jig is being designed which don't need clamp force to fix the flag pad.

In order to eliminate the negative effect of jig, we use another jig to conduct experiment. The new one just press the l/f around leads instead of clamping the flag pad, so no direct force is used on flag.

We got the die shear data as below:

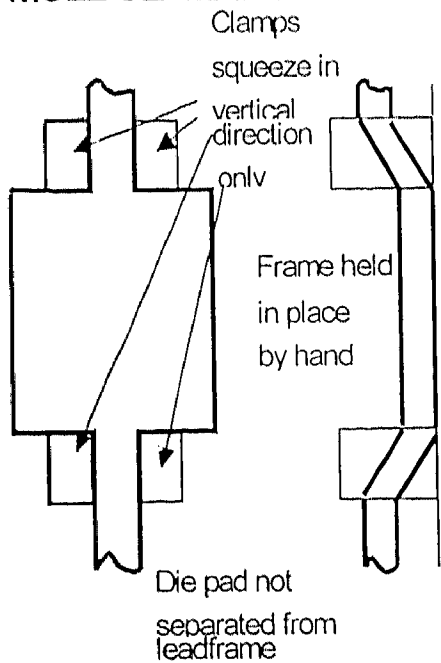
Unit: kg

Old jig:	1.60	1.29	2.56	1.99	3.92	2.68
New jig:	7.49	10.86	8.85	5.48	4.28	8.38

Using JMP to analyze the raw data and the result is:

t-Test

## MCEL CLAMPING



## mitsui clamping

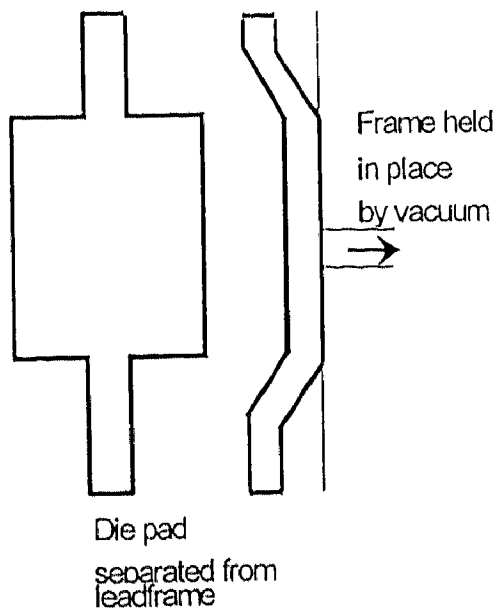
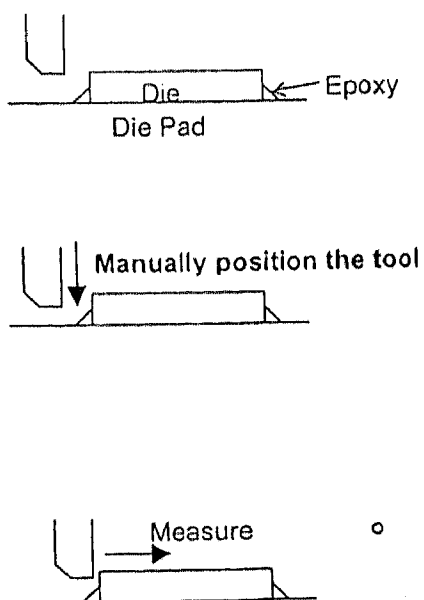


Figure4 Different clamp method

## MCEL MEASURING



## MITSUI MEASURING

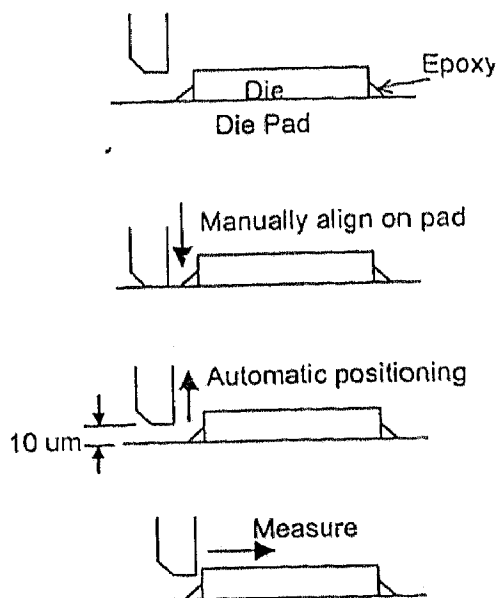


Figure5 Different Shear Method

1. Experiment Design

According to the result of previous study, three input variables are selected, they are epoxy thickness, cure temperature and jig. Mean of die shear strength before & after wire bonding and their stand deviation are selected to be output responses. The experiment design is as below:

Pattern	Epoxy thickness	Cure time	Jig	Standard Order	
---	-1	-1	-1	1	
+--	1	-1	-1	2	
-+-	-1	1		-1	3
++-	1	1		-1	4
--+	-1	-1	1	5	
+ - +	1	-1	1	6	
- + +	-1	1	1	7	
+++	1	1		1	8

Note: level choice:

Epoxy thickness:	thick	-1
	thin	1
Cure temp.:	180/200degreeC	-1
	175/175degreeC	1
Jig:	old	-1
	new	1

The epoxy thickness was measured as:

Table4:

Unit: mil

	Unit1		Unit2		Unit3		Mean
	1	2	1	2	1	2	
Thick	0. 68	0. 78	0. 42	0. 54	0. 40	0. 48	0. 55
Thin	0. 12	0. 22	0. 16	0. 24	0. 18	0. 16	0. 18

2. Raw Data

**Table5: Raw data of experiments**

Before W/B(ds1)												
Order	1	2	3	4	5	6	7	8	9	10	range	mean
1	5.68	6.05	8.22	8.24	11.27	5.37	6.85	7.06	7.09	7.72	5.90	7.36
2	8.58	4.27	5.63	5.02	3.37	4.89	5.47	3.00	4.92	5.45	5.58	5.06
3	8.16	9.00	7.12	9.87	7.85	8.69	5.55	6.95	6.52	12.41	6.86	8.21
4	4.33	5.19	2.40	3.05	3.51	7.66	3.20	2.88	3.48	3.26	5.26	3.90
5	7.35	8.86	8.08	10.39	8.04	11.68	14.54	12.86	11.17	11.35	7.19	10.43
6	7.79	9.49	7.08	10.19	6.33	5.61	7.33	7.60	5.70	8.86	4.58	7.60
7	11.48	6.10	6.47	13.64	6.73	7.97	11.55	12.29	15.60	13.38	9.50	10.52
8	8.85	10.36	8.95	6.00	4.96	4.73	6.80	10.18	9.40	9.53	5.63	7.98
After W/B(ds2)												
Order	1	2	3	4	5	6	7	8	9	10	range	mean
1	5.11	5.08	3.51	4.24	5.37	6.21	4.20	3.53	3.98	8.09	4.58	4.93
2	3.21	1.34	3.36	4.06	3.17	4.89	3.16	2.80	2.55	2.57	3.55	3.11
3	2.58	5.27	2.94	2.82	3.11	3.71	4.32	3.59	3.17	4.72	2.69	3.62
4	4.01	3.00	4.88	3.79	4.35	3.73	2.23	3.14	2.11	3.58	2.77	3.48
5	6.62	7.78	5.28	7.70	6.28	6.64	5.46	6.74	2.71	6.79	5.07	6.20
6	5.65	4.10	5.37	6.32	5.61	5.58	6.73	7.47	7.08	6.59	3.37	6.05
7	4.33	5.59	7.10	5.96	5.63	4.74	7.22	5.30	6.21	10.94	6.61	6.30
8	4.14	4.24	2.79	5.45	5.11	5.16	5.80	5.89	6.27	3.73	3.48	4.86

**Table 6: Raw data array for DOE**

Std Order	Random Order	Epoxy	cure thickness	jig time	mean of d/s1	stdev of d/s1	mean of d/s1	stdev of d/s2	d/s2
1	1	-1	-1	-1	7.36	1.69	4.93	1.40	
2	5	1	-1	-1	5.06	1.52	3.11	0.94	
3	6	-1	1	-1	8.21	1.95	3.62	0.89	
4	4	1	1	-1	3.90	1.54	3.48	0.88	
5	8	-1	-1	1	10.43	2.33	6.20	1.47	
6	3	1	-1	1	7.60	1.54	6.05	0.99	
7	7	-1	1	1	10.52	3.43	6.28	1.87	
8	2	1	1	1	7.98	2.15	4.80	1.19	

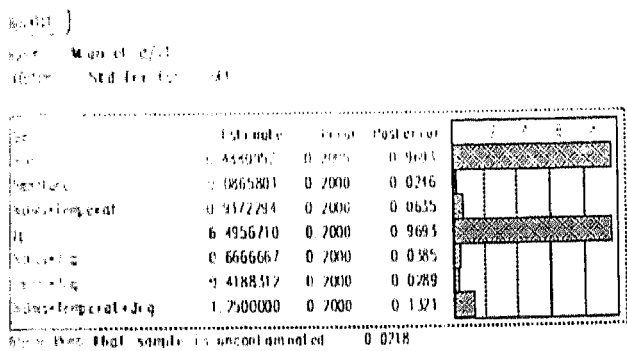
**Note: d/s1 is die shear strength before wire bonding**  
**d/s2 is die shear strength after wire bonding**



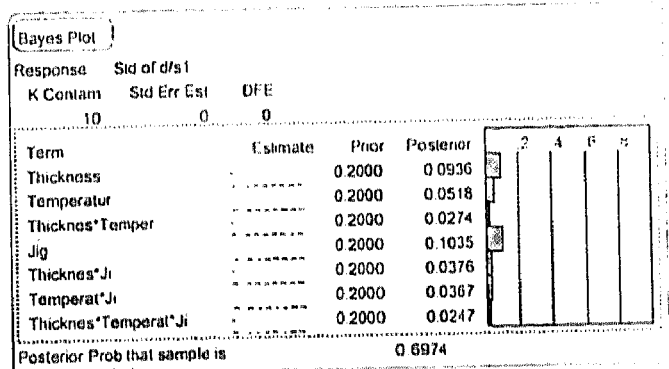
### 3. Data Exploring

Table 1 is the data of experiment. According to the Bayes Plot (Figure7), epoxy thickness, cure temperature, jig and thickness\*temperature\*jig is significant to the die shear. For stand deviation, no factor is significant. It indicates that the variance of die shear is same within the experimental region.

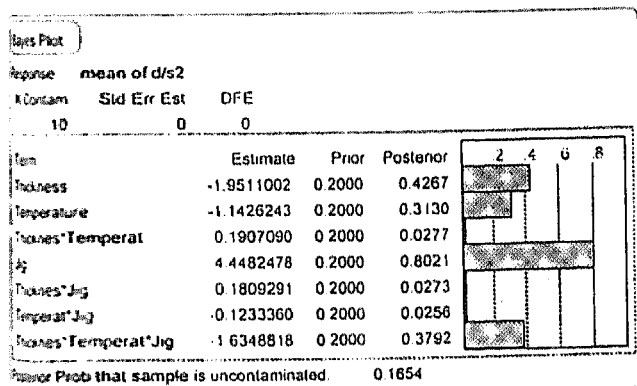
**Figure7: Bayes Plot**



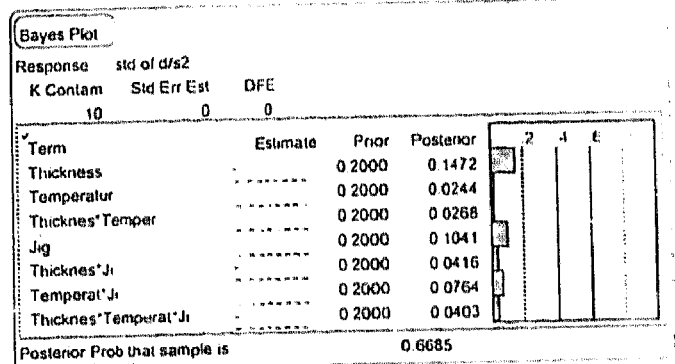
**1a: Bayes Plot of d/s before w/b**



**1c: Bayes Plot of stdev of d/s1**



**1b: Bayes Plot of d/s after w/b**



**1d: Bayes Plot of stdev of d/s2**

Before w/b, the significant factors is thickness and measurement method. But after w/b, thickness\*temp. and thickness\*temp.\*jig also become noticeable inputs besides the two above. This doesn't mean these two input factors really have so much effects on output. A reasonable explanation should be that wire bonding affects the die adhesive strength. Of course this effect is unstable. So, a very bad wire bonding machine

an extreme example is that die will “fly off” from flag pad during wire bonding.

The wire bonder status includes: heat block temperature, window clamp pressing status, heat block mechanical dimension and etc.

Exclude non-significant input & output variables, and refit the model, the result is as below:

### Mean of d/s1:

#### Summary of Fit

RSquare	0.982849
RSquare Adj	0.959981
Root Mean Square Error	0.461732
Mean of Response	7.63125
Observations (or Sum Wgts)	8

#### Analysis of Variance

Source	DF	Sum of Squares	Mean Square	F Ratio
Model	4	36.652227	9.16306	42.9793
Error	3	0.639591	0.21320	Prob>F
C Total	7	37.291818		0.0056

#### Parameter Estimates

Term	Estimate	Std Error	t Ratio	Prob> t
Intercept	7.63125	0.163247	46.75	<.0001
Thickness	-1.49875	0.163247	-9.18	0.0027
Temperature	0.02	0.163247	0.12	0.9102
Jig	1.5005	0.163247	9.19	0.0027
Thicknes*Temp	0.28875	0.163247	1.77	0.1751

\*Jig

#### Effect Test

Source	Nparm	DF	Sum of Squares	F Ratio	Prob>F
Thick	1	1	17.970013	84.2884	0.0027
Temp	1	1	0.003200	0.0150	0.9102
Jig	1	1	18.012002	84.4853	0.0027
Thick*	1	1	0.667013	3.1286	0.1751
Temp*jg					

### Summary of Fit

RSquare	0.996951
RSquare Adj	0.992886
Root Mean Square Error	0.109091
Mean of Response	4.810375
Observations (or Sum Wgts)	8

### Analysis of Variance

Source	DF	Sum of Squares	Mean Square	F Ratio
Model	4	11.674868	2.91872	245.2540
Error	3	0.035702	0.01190	Prob>F
C Total	7	11.710570		0.0004

### Parameter Estimates

Term	Estimate	Std Error	t Ratio	Prob> t
Intercept	4.810375	0.038569	124.72	<.0001
Thickness	-0.448875	0.038569	-11.64	0.0014
Temperature	-0.262875	0.038569	-6.82	0.0065
Jig	1.023375	0.038569	26.53	0.0001
Thick*Temp	-0.376125	0.038569	-9.75	0.0023
*Jig				

### Effect Test

Source	Nparm	DF	Sum of Squares	F Ratio	Prob>F
Thick	1	1	1.6119101	135.4456	0.0014
Temp	1	1	0.5528261	46.4529	0.0065
Jig	1	1	8.3783711	704.0180	0.0001
Thick*	1	1	1.1317601	95.0996	0.0023
Temp*Jig					

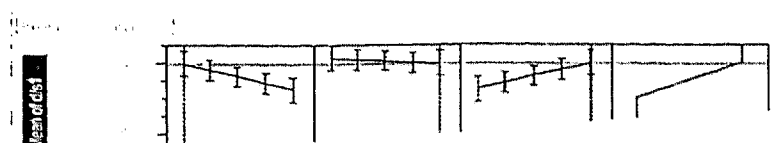


## Figure8 Prediction Profile

Using Prediction Profile (Figure8), we can find the most desirable die shear value and corresponding inputs levels. From the Cube Plot (Figure9), we also can find the point of (-1,1,1) is the most desirable.

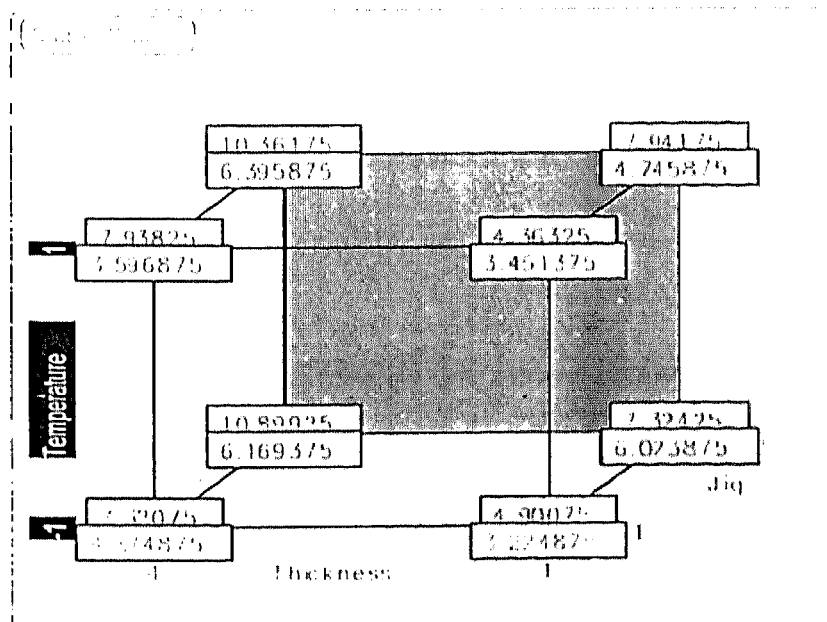


Figure9 Cube Plot

## 4. Conclusion

1. Epoxy thickness and jig have significant impact on die shear value.
2. The stand deviation of die shear is same within experimental region.
3. The most desirable value is appeared on the point of (-1,1,1).

## 5. Confirmation Run

The confirmation experiment results is as table 6. It correlated with the DOE results very well.

Table 6

Unit: kg

thick thickness									SPEC: 2.26
13.34	8.49	8.68	12.12	9.83	12.77	10.24	9.93	12.19	9.41
8.81	7.94	10.04	11.82	10.67	11.98	10.32	9.49	12.90	7.56
9.34	12.99	9.92	14.75	10.91	6.88	8.49	9.36	9.43	8.47
max	14.75		min	6.88			mean	10.30	
thin thickness									
6.70	9.44	8.67	5.82	8.99	4.38	3.94	4.69	8.30	4.30
8.02	7.21	9.35	5.54	5.92	3.23	3.15	6.72	7.03	5.40
4.69	7.45	5.51	5.57	4.09	3.85	3.30	5.68	9.51	6.23
max	9.51		min	3.15			mean	6.09	

## - Conclusion

Three root causes were proved to be negatively affect the die shear feature of PPF. Different method was adopted to resolve them:

1. According to the results above, a thick epoxy can provide better die shear feature than thin epoxy. It's important for production line to control epoxy thickness to overcome PPF low die shear problem. It's also the requirement of SPEC.
2. Wire bonder status must keep good to reduce its negative impact on die bond feature.
3. Design new jig to eliminate measurement error.

# **WIRE BONDING PROCESS**

(

## **PPF STUDY ON W/B PROCESS**

# PPF STUDY ON W/B PROCESS

## BACKGROUND

Pre-plated L/F calls for quite different equipment and process setup, due to its special plating structure compared with current silver plated copper L/F. Because gold wire will be bonded to the inner lead of L/F and metal intermetallic is formed to provide the mechanical and electrical connection, the change to the plating material of L/F surface can lead to a changed nature of wire bonding. Study and evaluation is necessary and has been conducted.

## SOLUTION

### 1. Material

#### (1) Leadframe

Actually so-called Pre-Plated Leadframe has several different designs around the world. The first PPF(4-layer: nickel-nickel + palladium alloy-nickel-palladium) is innovated and patented by  $H$  many years ago. The main disadvantage of this design is the price, due to the necessary license charge of the supplier, and only Shinko has gotten the manufacturing license. However it is reported that the 2-layer(nickel-palladium) design is comparable to 4-layer design in terms of manufacture capability but no license is needed. So most of  $\beta$  manufacturing sites start with this 2-layer PPF. The third dominant design is 3-layer structure(nickel-palladium-gold flash), which is preferred by some Japanese customers.

Now 3-layer nickel palladium leadframes will probably be selected instead of 2/4-layer design for PPF production according to the strategy of FMO PPF team. METL has reported significantly improved bonding quality with 3-layer PPF. We are going to start the evaluation, too.

#### (2) Gold wire

All gold wires we are using now has 99.99% gold. Test-bonding with different types of gold wire finds no difference in terms of bonding quality. So we believe gold wire is not a key point in optimizing PPF wire bonding.

### (3) Die Attachment

Through evaluation, CRM-1064MA epoxy was adopted for PPF by sector. It's reported as a low outgassing and high die shear attachment material. But low die shear strength problem was found for the combination of 1064MA and PPF in MCEL. This brings much difficulty to W/B process. Much effort has been involved to solve this problem.

Besides snap cure process has shortcoming for epoxy cure, epoxy thickness was found taking an important role to solve die shear problem. By adjusting the thickness, die shear strength of PPF was proved improving much.

## 2. Process

### (1) Bond Parameters

The main issue PPF bring to wire bond process is the quite different second bond characteristic. When using the Ni-Pd player instead of silver plating, more energy is needed to form good intermetallic compound when gold wire is bonded to the L/F. So bonding parameters are adjusted specially. Bonding time, power and force are all set at a higher level than usual copper L/F, the TCM form can be referred to for the details. Below is an example for it:

Example: Parameter contrast for PPF vs silver plated copper L/F:

	PPF	Copper
Lead Bond Time (ms)	6-15	15-25
Lead Bond Power (mW)	100-130	170-200
Lead Bond Force (g)	100-130	140-170
Lead S_Force (g)	110-160	160-180
SPC. 1	0-2	1-2

This reference comparison is for Shinkawa UTC-105 wire bonder, other wire bond machines are as the same.



quality if L/F or the bonder is in unacceptable conditions. In other words, the bonding parameters can be easily optimized through experiment design once all other factors are good enough.

(2) Lead Tilt Problem

Besides parameter optimization, L/F inner lead design was found having big impact on assembly quality.

Although PPF has same physical dimensions with the copper leadframe, flatness of inner leads turns to be a important property for PPF. Wire peel strength was found to be very low for PPF during evaluation. After much effort to optimize wire bonding quality of stamped, we find that L/F manufactured with current  $\beta$  specification can not meet the flatness requirement needed for normal PPF production.

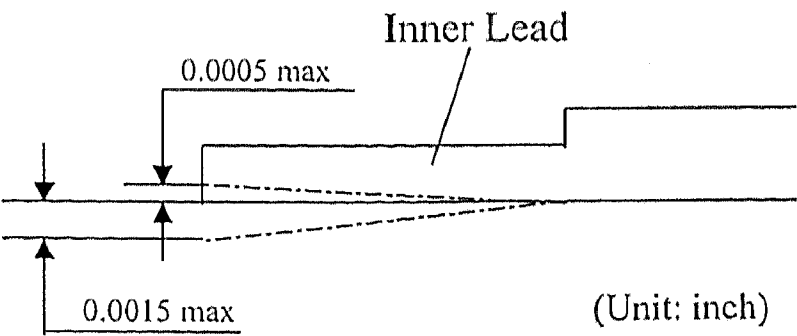


Figure 1. Before Modification

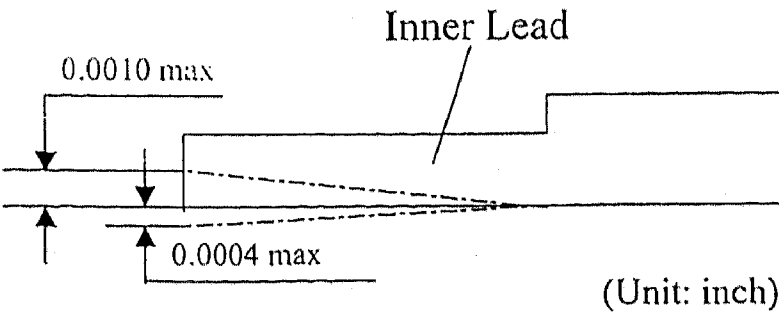


Figure 2. After Modification

The inner lead dimension on L/F drawing document is show in figure1. This design show a bad bondarability for PPF. Below lists some wire peel data of PPF using this “unproper” SPEC.

Leadframe Part No.: H00980A706

Package: SOIC 16LD

Lot No.	Date	M/C No.	Max	Min
P4SVEH0007	23/May/98	SWB-19	9.3	2.0
P4SVEH0010	24/May/98	SWB-29	9.3	2.3
P4SVEH0049	25/May/98	SWB-27	10.5	2.0
P4SVEH0059	26/May/98	SWB-35	9.0	2.3
P4SVEH0221	30/May/98	SWB-29	10.3	2.0
P4SWEH0047	31/May/98	SWB-29	9.0	3.0

From the data above, we can see that wire peel is a difficult problem to assembly line.

Through experiment and analysis, the “angled coining” inner lead design was proved to be the root cause of the bad peel strength. The modified inner lead drawing is as figure2. A downward “angled coining” for the lead tip of inner lead before modification is changed to a “flat coining” ( no downward angle).

After modification of lead tilt design, this problem never occur online. All peel strength collected is above 4.0g. METL confirmed the modification is effective.

Amendment on the flatness spec has been suggested to FMO test bonding on the new samples turns out to be positive. However, SPEC modification lead to new stamping tools and new measuring equipment which is very expensive. So, the new spec has not been published as a new issue so far. It's decided that stamping tools would only be modified on an “as needed” basis.

The “flat coining” stamping tools available by now we know include:

- H00980A704 (SOIC 16LD)
- H00980A706 (SOIC 16LD)
- H00978A704 (SOIC 14LD)

Not only wire bonding process, but also the solderability performance are very sensitive to surface contamination and/or damage of PPF, so finger coat is a must when handling PPF products once direct contact with L/F surface is necessary. It must be emphasized that palladium layer will also be oxidized when exposed to high temperature circumstance such as epoxy curing tunnel or bond site, so N2 should not be eliminated from these places. This has been verified by actual practice stated in a few documents provided by the suppliers and friend assembly sites. This oxidation will probably degrade bonding quality to unacceptable level. A study has been initialized by FMO PPF team and been in progress to evaluate the storage time of finished units up to 5 years in normal warehouse condition.

#### (4) Capillary

Capillary with smaller face angle is supposed to be better for wire bonding, the capillary we are using for PPF has a face angle of 4 degrees, which is also used in METL for the same products.

Capillary usage limit is changed to 600k points from 1,200k of copper L/F. This limit is transferred from METL. Experiment show that the lifespan can be expected longer if lower bond parameters be used.

#### (5) Quality verification

Ball shear and wire pull strength will not be affected(at least, not so significantly) as long as the bonding temperature is kept the same. Only a few of part No. of PPF was modified lead tilt SPEC, so the wire peel inspection during assembly should also be of much importance.

Wire peel test is introduced for PPF production control in our process, though it is not applied for PPF production in METL. From engineering standpoint, this is absolutely necessary before our engineers and technician get more knowledge on PPF production. The acceptance criteria of wire peel test is decided on a consensus between process, production and QA people.

### 3.Equipment:

#### (1) Conversion kits

must be stored in the dedicated conversion kit rack when it is idle. The window clamp-heat block system must be adjusted so that all inner leads of PPF are firmly clamped. The heat block with protrusion is preferred for SOIC 8/14/16/28 LD PPF, it can make the clamping condition more robust. But flat heat block is better for QFP or other high lead count PPF, the reason lies in the improved flatness of coin area when the lead count increases.

## (2) Bonding temperature

Higher temperature is better for PPF bonding, but will also degrade ball bond performance due to the poor high temperature property of die adhesive. So 200c or 205c is commonly used in  $\beta$  for PPF bonding. Temperature is so important for PPF bonding that calibration must be done regularly to see that bonding site temperature is in line with the key-board setting. There are a few other reasons why higher bonding temperature is not set in the production, e.g., higher temperature accelerates oxidation on L/F surface, higher temperature leads to significant parameter adjustment for first bonds

## (3) Contamination

Because L/F will be conveyed by the indexing system of wire bonder and stay there for more than ten minutes, the workholder of wire bonder must be kept clean enough to avoid possible contamination. This includes the heat block surface, supply pipe of  $N_2$  gas,

# 28ld SOIC Kobold Assembly Characterization

Baking process for MSL3 experiment

C5

# 28ld SOIC Kobold Assembly Characterization

## Baking process for MSL3 experiment

### Problem Description:

Current Tianjin's soic28ld MSL data can only support level 3 (with elevated reflow temp 125degC), as requested by Bosch, we need to bake and drypack all its product before shipping it out.

Ideally, we should bake the tested good product before tape&reel process for soic28ld, but the plastic tube can not withstand high temp 125degC 6hrs, our production people had to unload them from metal(copper) tubes, it is not practical for mass production, as it requires manual work and is easy to cause handling induced defect(include ESD issue).

A series experiments had been made to find the alternative solutions, we need verify following question:

- what is the moisture absorption rate and package weight increase in production environment?
- how long the package could be stayed in production floor after baking without any significant weight increase?
- need a method to simulate the moisture absorption checking done by our customer, how could we pass their incoming inspection on package weight increase.

### experiment :

There are a series of experiment were performed to verify the above questions:

#### experiment 1 Condition:

choose 10 units of soic28ld device is J31D to go through baking oven and weight every 6hrs.

#### experiment 2 Condition:

Choose 10 units of soic28ld, device is J31D. baking for unit1 to unit5 when 168hrs.

##### Test flow:

Weight after T/F, weight after suction 2 hrs, weight after B/I 6 hrs 125degC, weight each 24hrs.

Unit1---unit5: Trim Form---->Weight----->Soaking(2hrs,room temp)---->Weight---->Baking (6hrs, 125degC) Weight----->Weight after every 24hrs----->Baking after 168hrs staging.

Unit6---unit10: weight after suction 2 hrs, weight after B/I 6 hrs 125degC, weight each 24hrs.

Unit1---unit5: Trim Form---->Weight----->Soaking(2hrs,room temp)---->Weight---->Baking (6hrs, 125degC) Weight----->Weight after every 24hrs----->till 216hrs.

#### experiment 3 Condition of MSL3:

Choose 20 units of soic28ld, device is J31D.

##### Test flow:

Choose 20 units----->weight----->baking(125degC, 6hrs)---->T/H(30degC/60%rh, 240hrs)----->weight ----->IR(245degC, 3cycles)---->weight----->check delamination&crack

(note: MSL3 stands for moisture absorption level3)

# 28ld SOIC Kobold Assembly Characterization

Experiment 4 Condition:

Use 10 units of soic28ld, device is J31D.

Flow:

Age the strip for 125degC 6hrs before T/F and go through the remaining process ---->stored in  
vacuum floor for 168hrs---->weight the package again----->baking the package 125degC 6hrs—  
weight these units.

## Experiment 1:

Get the min baking time under 125degC.

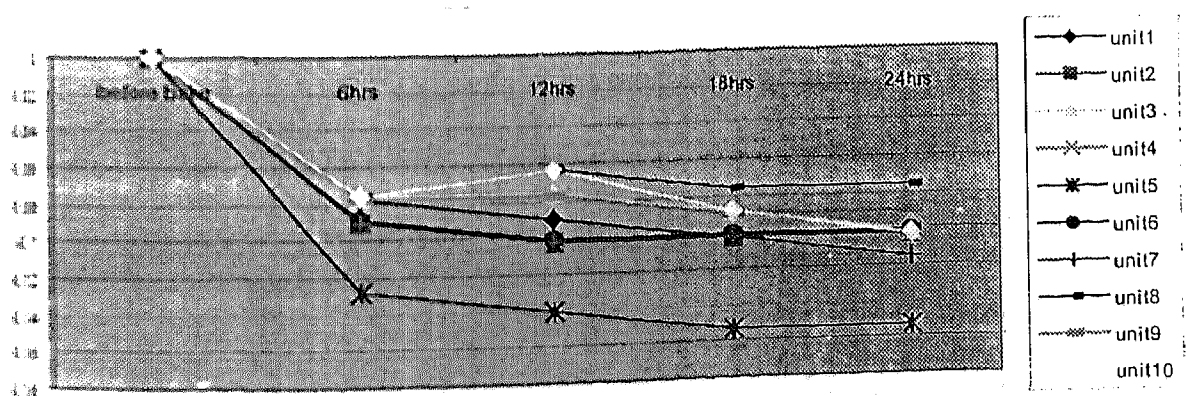
Units were selected to go through baking oven and their weight loss was recorded every 6hrs.

Before absorption weight increase:

	unit1	2	3	4	5	6	7	8	9	10
Before	0.7831	0.7823	0.786	0.7865	0.7849	0.7859	0.7795	0.7847	0.78	0.7852
1	0.7825	0.7816	0.7854	0.7856	0.7839	0.7852	0.7788	0.7841	0.7794	0.7846
2	0.7824	0.7815	0.7854	0.7857	0.7838	0.7851	0.7787	0.7842	0.7794	0.7847
3	0.7823	0.7815	0.7853	0.7856	0.7837	0.7851	0.7787	0.7841	0.7793	0.7845
4	0.7823	0.7815	0.7852	0.7856	0.7837	0.7851	0.7786	0.7841	0.7793	0.7844

After absorption relative weight increase:

Unit	unit1	unit2	unit3	unit4	unit5	unit6	unit7	unit8	unit9	unit10
Before	0	0	0	0	0	0	0	0	0	0
1	-0.07662	-0.08948	-0.07634	-0.11443	-0.1274	-0.08907	-0.0898	-0.07646	-0.07692	-0.07641
2	-0.08939	-0.10226	-0.07634	-0.10172	-0.14015	-0.10179	-0.10263	-0.06372	-0.07692	-0.06368
3	-0.10216	-0.10226	-0.08906	-0.11443	-0.15289	-0.10179	-0.10263	-0.07646	-0.08974	-0.08915
4	-0.10216	-0.10226	-0.10178	-0.11443	-0.15289	-0.10179	-0.11546	-0.07646	-0.08974	-0.10188



# 28ld SOIC Kobold Assembly Characterization

Conclusion:

Baking can effectively remove moisture built inside the package.  
The longer baking time (than 6 hrs), the moisture remove is not significant. 80% more of the moisture inside the package are removed by the first 6hrs of baking.  
(See the attachment for the detail data of experiment 1)

Experiment 2:

Make out moisture absorption rate test:  
Use 10 units of soic28ld, device is J31D. baking for unit 1 to unit 5 when 168hrs.

Test flow:  
Weight after T/F, weight after suction 2 hrs, weight after B/I 6 hrs 125degC, weight each 24hrs.  
Unit 1---unit 5: Trim Form---->Weight----->Soaking(2hrs, room temp)---->Weight---->Baking  
(24hrs, 125degC) Weight----->Weight after every 24hrs----->Baking after 168hrs staging.

Unit 6---unit 10: weight after suction 2 hrs, weight after B/I 6 hrs 125degC, weight each 24hrs.  
Unit 1---unit 5: Trim Form---->Weight----->Soaking(2hrs, room temp)---->Weight---->Baking  
(24hrs, 125degC) Weight----->Weight after every 24hrs----->till 216hrs.

Moisture absorption weight increase:

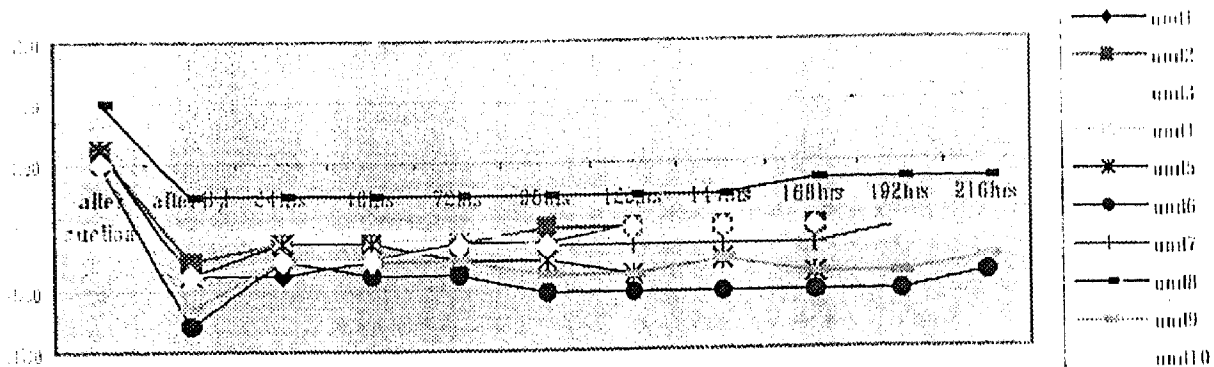
before suction	after suction	after B/I	24hrs	48hrs	72hrs	96hrs	120hrs	144hrs	168hrs	192hrs	216hrs
0.7837	0.7837	0.783	0.783	0.7831	0.7832	0.7832	0.7833	0.7833	0.7833		
0.7849	0.785	0.7843	0.7844	0.7844	0.7844	0.7845	0.7845	0.7845	0.7845		
0.7858	0.7858	0.7851	0.7853	0.7853	0.7853	0.7852	0.7852	0.7852	0.7851		
0.7819	0.7821	0.7815	0.7814	0.7816	0.7815	0.7814	0.7815	0.7815	0.7814		
0.7867	0.7868	0.786	0.7862	0.7862	0.7861	0.7861	0.786	0.7861	0.786		
0.7811	0.7811	0.7801	0.7805	0.7804	0.7804	0.7803	0.7803	0.7803	0.7803	0.7803	0.780
0.781	0.781	0.7803	0.7804	0.7804	0.7805	0.7805	0.7805	0.7805	0.7805	0.7805	0.780
0.7806	0.781	0.7804	0.7804	0.7804	0.7804	0.7804	0.7804	0.7804	0.7805	0.7805	0.780
0.7816	0.7816	0.7807	0.781	0.781	0.781	0.7809	0.7809	0.781	0.7809	0.7809	0.78
0.7818	0.7818	0.7811	0.7812	0.7812	0.7813	0.7813	0.7814	0.7814	0.7814	0.7814	0.781

Moisture absorption relative weight increase:

before suction	after suction	after B/I	24hrs	48hrs	72hrs	96hrs	120hrs	144hrs	168hrs	192hrs	216hrs
0.7837	0.0000	-0.0893	-0.0893	-0.0766	-0.0638	-0.0638	-0.0510	-0.0510	-0.0510		
0.7849	0.0127	-0.0764	-0.0637	-0.0637	-0.0637	-0.0510	-0.0510	-0.0510	-0.0510		
0.7858	0.0000	-0.0891	-0.0636	-0.0636	-0.0636	-0.0764	-0.0764	-0.0764	-0.0891		
0.7819	0.0256	-0.0512	-0.0639	-0.0384	-0.0512	-0.0639	-0.0512	-0.0512	-0.0639		
0.7867	0.0127	-0.0890	-0.0636	-0.0636	-0.0763	-0.0763	-0.0890	-0.0763	-0.0890		
0.7811	0.0000	-0.1280	-0.0768	-0.0896	-0.0896	-0.1024	-0.1024	-0.1024	-0.1024	-0.1024	-0.0896
0.781	0.0000	-0.0896	-0.0768	-0.0768	-0.0640	-0.0640	-0.0640	-0.0640	-0.0640	-0.0512	-0.0512
0.7806	0.0512	-0.0256	-0.0256	-0.0256	-0.0256	-0.0256	-0.0256	-0.0256	-0.0128	-0.0128	-0.0128
0.7816	0.0000	-0.1151	-0.0768	-0.0768	-0.0768	-0.0896	-0.0896	-0.0768	-0.0896	-0.0896	-0.0768
0.7818	0.0000	-0.0895	-0.0767	-0.0767	-0.0640	-0.0640	-0.0512	-0.0512	-0.0512	-0.0512	-0.0512



# 28ld SOIC Kobold Assembly Characterization



Summary:

Soaking for 2hrs does not cause any significant weight increase, as soaking is done in room temp, considering that a relative large amount of water is removed after baking.

For unit 1 to unit 5, they are baked after 168hrs baking, it is found that there is weight increase after 7 days staging, this can guarantee that when our customer unpack the drypack and perform similar incoming inspection of moisture absorption by ways of baking, they will not find any weight loss, implying package is dry. So there is impact on moisture absorption between our recommended baking process with conventional baking process.

There is no significant change/increase in terms of package moisture absorption among different staging hours within 6 days after 125degC baking. The max moisture absorption rate is less than 0.04%. (see the attachment for the detail data of experiment 2)

We recommend that the cycle time between T/F and drypack could be controlled within 72 hrs.

## Experiment 3:

Experiment 2 Condition of MSL3:

For MSL3 the stress condition is 30degC/60%RH for 192hrs. This represents a production environment where the condition during transportation is protected by dry pack. This means that for package with MSL3 rating, the shelf life (under production condition) is 192hrs. So adopt the following process for test the max moisture absorption after MSL3 precondition which could be set as guarding band.

Choose 20 units of soic28ld, device is J31D.

Test flow:

Choose 20 units ----> weight ----> baking(125degC, 6hrs) ----> T/H(30degC/60%RH, 240hrs) ----> weight ----> IR(245degC, 3cycles) ----> weight ----> check delamination & crack

# 28ld SOIC Kobold Assembly Characterization

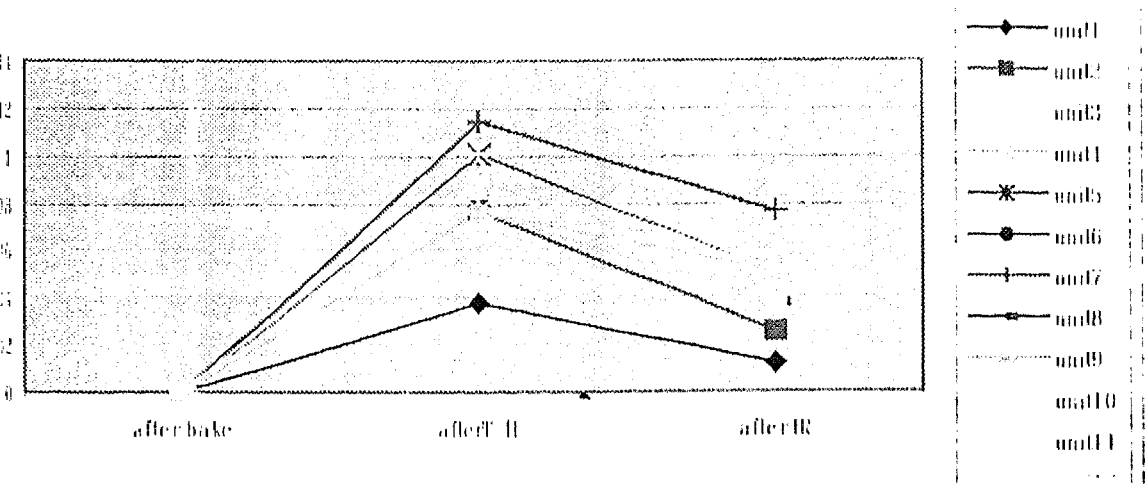
ure absorption weight increase

	before bake	after bake	afterT/H	after IR
	0.7875	0.7871	0.7874	0.7872
	0.7829	0.7826	0.7832	0.7828
	0.7856	0.7852	0.7858	0.7856
	0.7859	0.7854	0.7861	0.7858
	0.7895	0.7891	0.7899	0.7895
	0.7861	0.7858	0.7865	0.7861
	0.7872	0.7869	0.7878	0.7875
	0.7869	0.7866	0.7872	0.7869
	0.7824	0.782	0.7827	0.7823
	0.7883	0.7879	0.7885	0.7882
	0.7858	0.7853	0.786	0.7856
	0.7848	0.7843	0.785	0.7847
	0.7845	0.7842	0.7848	0.7845
	0.7851	0.7847	0.7855	0.7851
	0.7856	0.7853	0.786	0.7857
	0.7837	0.7833	0.7839	0.7836
	0.7878	0.7873	0.7879	0.7876
	0.7867	0.7862	0.7868	0.7866
	0.787	0.7864	0.787	0.7867
	0.7859	0.7855	0.7862	0.7858

ture absorption relative weight increase:

	before bake	after bake	afterT/H	after IR
	0.7875	0	0.038115	0.012705
	0.7829	0	0.076668	0.025556
	0.7856	0	0.076414	0.050942
	0.7859	0	0.089127	0.050929
	0.7895	0	0.101381	0.050691
	0.7861	0	0.089081	0.038178
	0.7872	0	0.114373	0.076249
	0.7869	0	0.076278	0.038139
	0.7824	0	0.089514	0.038363
0	0.7883	0	0.076152	0.038076
1	0.7858	0	0.089138	0.038202
2	0.7848	0	0.089252	0.051001
3	0.7845	0	0.076511	0.038256
4	0.7851	0	0.10195	0.050975
5	0.7856	0	0.089138	0.050936
6	0.7837	0	0.076599	0.0383
7	0.7878	0	0.07621	0.038105
8	0.7867	0	0.076316	0.050878
9	0.787	0	0.076297	0.038149

# 28ld SOIC Kobold Assembly Characterization



Summary:  
The moisture absorption after IR(245degC,3cycles) is 0.076%.  
Inspection the package under SAT/SAM, the result is normal, and is the same status of one before MSL3 test. The package can be withstood 240hrs T/H until we ensure that there is no crack, no delamination within the package.  
From the data of experiment 3, we can see that max moisture absorption after MSL3 test is 0.076%, which could be set as guarding band.  
(see the attachment for the detail data of experiment 3)

## Experiment 4:

Use 10 units of soic28ld, device is J31D.  
Flow:  
Baking the strip for 125degC 6hrs before T/F and go through the remaining process ---->stored in production floor for 168hrs---->weight the package again---->baking the package 125degC 6hrs---->weight these units.

Following process for testing the moisture absorption rate after baking.  
Finish---->baking on strip---->T/F ----->staging 24hrs----->weight----->weight after every 24hrs staging.

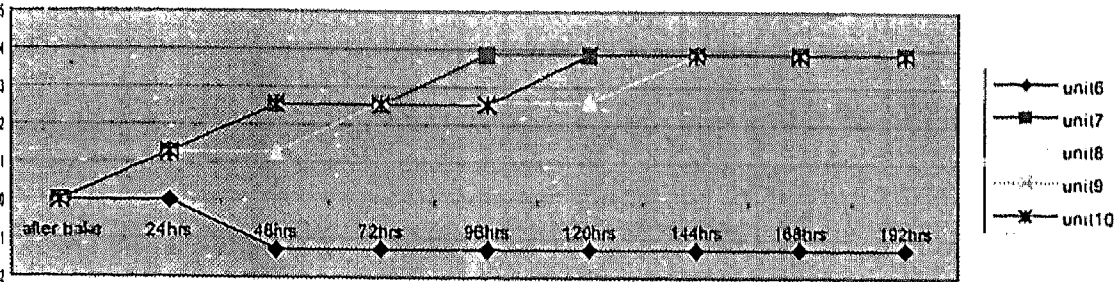
# 28ld SOIC Kobold Assembly Characterization

ure absorption weight increase

after bake	24hrs	48hrs	72hrs	96hrs	120hrs	144hrs	168hrs	192hrs
0.7809	0.7809	0.7808	0.7808	0.7808	0.7808	0.7808	0.7808	0.7808
0.7796	0.7797	0.7798	0.7798	0.7799	0.7799	0.7799	0.7799	0.7799
0.779	0.7791	0.7791	0.7792	0.7792	0.7792	0.7793	0.7793	0.7793
0.7778	0.7779	0.778	0.778	0.778	0.7781	0.7781	0.7781	0.7781
0.782	0.7821	0.7822	0.7822	0.7822	0.7823	0.7823	0.7823	0.7823

ure absorption relative weight increase:

after bake	24hrs	48hrs	72hrs	96hrs	120hrs	144hrs	168hrs	192hrs
0	0	-0.01281	-0.01281	-0.01281	-0.01281	-0.01281	-0.01281	-0.01281
0	0.01283	0.02565	0.02565	0.03848	0.03848	0.03848	0.03848	0.03848
0	0.01284	0.01284	0.02567	0.02567	0.02567	0.03851	0.03851	0.03851
0	0.01286	0.02571	0.02571	0.02571	0.03857	0.03857	0.03857	0.03857
0	0.01279	0.02558	0.02558	0.02558	0.03836	0.03836	0.03836	0.03836



mary:

There are no significant change/increase in terms of package moisture absorption over different staging hours with 6 days after baking. The max moisture absorption is less than 0.04%.

cycle time between T/F and drypack could be controlled within 72hrs, then the max moisture absorption is within 0.03%.

(see the attachment for the detail data of experiment4)

Finally, the factory environment does not contribute significantly to package water absorption within 6 days after baking at prior trim & form process.

# 28ld SOIC Kobold Assembly Characterization

## 3. Conclusion:

Thus it proves that our approach of “baking before trim and form” can reach the same effectiveness of moisture removal as that of normal baking process if we can control the production cycle time from trim and form to tape & reel within 3 to 6 days, which is easy to be met.

Again, baking process position is not a key factor affecting moisture removal effectiveness under normal production environment and cycle time compared with drypacking process while later is a key factor as severe transportation condition and longer staging time (half year to one year) under unknown temperature and humidity may be the fatal to moisture absorption.

## **APPENDIX B**

### **MALAYSIAN TECHNICAL REPORTS**

**Note:** Throughout the Malaysian Technical Reports, **B** stands for the multinational organization that this study chose. **A** stands for one of the rival companies of this multinational organization. **C**, **D**, **E**, and **F** stand for some of the engineers of this multinational organization.

## STACKING PREBAKE AND VACUUM SEALING FOR PBGA SUBSTRATES

M1

### Abstract

Parts received from suppliers may have different moisture content level. If those moisture is not dry out, the moisture within the substrate creates blistering effect between the interface of die attach and die, also interface of soldermask to die attach. Thus, substrate prebake in magazines has been a practice in KLM PBGA assembly. The limitation of this method is the capacity of each oven load is only 6 to 10K units. Prebake using substrate stacking and vacuum seal method has been studied in this paper. For this method, each oven load can be 16 to 27k units. Initially, substrates were prebaked in stack for 3 hrs 10 min minimum at 125°C. Substrates were then vacuum sealed for 50 strips/packet. The packet was staged for 16, 35, 44 and 56 days. Response taken was CSAM Tzero after diebond cure. The results conclude that the vacuum seal method can last up to 56 days and the effect of stacking prebake is as effective as prebake in magazine. Substrates after MSL3+ soaking and stack prebake also showed no blister delamination. Total staging time in open air is found to be 10 hrs from prebake out to diebond cure in. Monitoring result for stacking prebake implementation shows zero delamination.

### Phenomena of Blister Delamination

There are several aspects need to be addressed in order to understand the moisture characteristic within the substrate. Fig. 5 shows the moisture penetrate into substrate through solder resist and BT resin results of the relative humidity (RH) of a working environment. As the package reflow at 220 C, the stresses that causing the blister is exactly equivalent to the vapor pressure generated from transformation of water to vapor pressure. Fig. 6 indicates the vapor pressure increase exponentially as the temperature go beyond 200 C. Assuming that the unit reflow at 240 C, the water vapor pressure is 33 times of the atmospheric pressure, which is a very high stress for the interfaces with the PBGA unit. Definitely, this stress will create delamination.

H<sub>2</sub>O from Ambient (60% RH) will be absorbed by the solder mask and BT-laminate (organic)

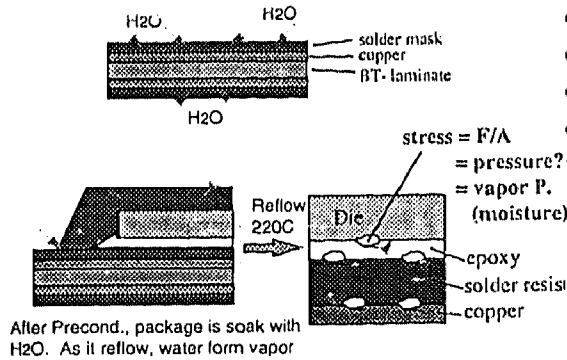


Fig. 5. Organic substrate with moisture reaction during reflow

PT-Diagram of Vapor-pressure Curve for Pure H<sub>2</sub>O

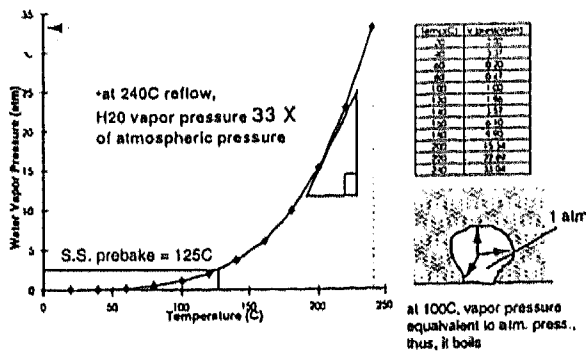


Fig. 6. The effect of temperature on the water vapor pressure.

In the aspect of the moisture or vapor volume as an effect of pressure, Fig. 7 shows the Pressure-Volume (PV) diagram for one mol of pure water. Water can exhibit as liquid, gas and mixture (gas/vapor) phases depending on the pressure and water volume/mol. In order to further understand PV of water in effect of temperature, the Van der Waals equation of state is used (see Fig. 8). Fig. 9 indicates the volume of the water (moisture absorbed within substrate) expands 49 times / mol H<sub>2</sub>O as the unit reflow at 240 C. This volume

expansion generate a sudden shock to the interfaces thus creating delamination. Inversely, as the unit cool down after reflow, the vapor condensation is -49 times. This also create sudden shock to interfaces and worsen the delamination further.

Pressure-Volume Diagram for H<sub>2</sub>O Fluid

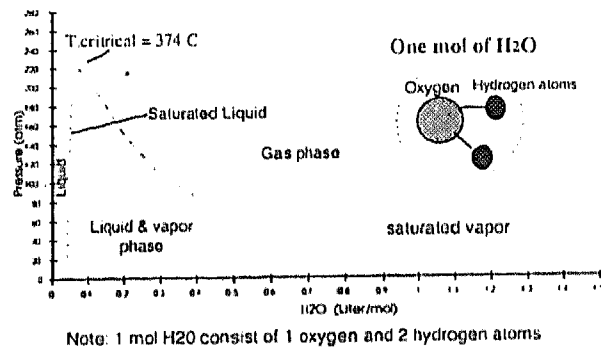


Fig. 7. PT diagram of one mol pure water

PVT Behaviour of Pure Fluid (H<sub>2</sub>O)

The Van der Waals Equation of State:

$$P = \frac{RT}{V_m - b} - \frac{a}{V_m^2}$$

where, P = pressure (atm)  
 R = universal gas constant (L.atm/(K.mol))  
 T = temperature (K)  
 V<sub>m</sub> = molar volume (L/mol)  
 a & b = Van der Waals constants

Note: At high pressure, most fluid will not behave as an Ideal Gas or Perfect Gas. (Ideal Gas is  $PV = nRT$ )

Fig. 8 PVT by Van der Waals Equation of State



## Pressure-Volume Diagram for H<sub>2</sub>O Fluid

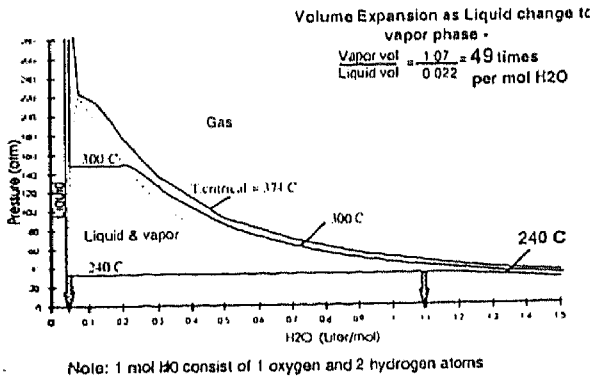


Fig. 9. PVT diagram for pure water

### Problem Description

Current magazine prebake method has many constraints :

1. Capacity and equipment constraint  
Capacity of Magazine Prebake for one full load is only 6K of 40mm substrates or 10K of 30mm substrates. In Dec 99, the demand at Die Bond per shift is 15K of 40mm substrates and 8K of 30mm substrates. Thus, 4 Prebake Oven is needed to fulfill the demand at Die Bond.

Problem : From Q1'00 onwards, runrate ramps up nearly 2x causing Die Bond demand to increase to 24K for 40mm and 10K for 30mm. If prebake method remain unchanged, at least 2 more ovens have to be added for substrate prebake and many more in future as the runrate continues to ramp up rapidly.

### 2. Production Inflexibility

Staging time in N<sub>2</sub>/open air between prebake out and epoxy cure in has been controlled as stated below in order to avoid black spots/blistering due to moisture absorption.

30mm substrates ==> 12 hrs

40mm substrates ==> 8 hrs

Problem : Die bond can not finish the substrates before expiry time. Thus expired substrates need to be prebake again.

### Solution Proposal and Expected Benefits

1. Stacking prebake for higher output.  
Condition : 50 strips/stack and 54 stacks per load. See illustrations below :

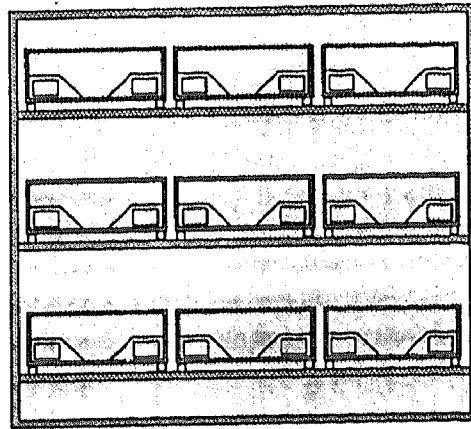


Fig. 10. Front view of oven with trays for stacking prebake.

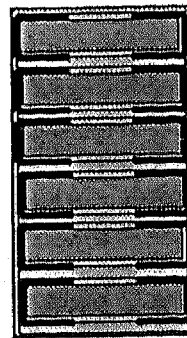


Fig. 11. Top view of a tray which is designed to hold 6 stacks of substrates per tray.

Output of stacking prebake is 2.7x higher than magazine prebake.

Substrate Type	Magazine Prebake	Stacking Prebake
30 mm	10 K	27 K
40 mm	6 K	16.2 K

Table 1. Output comparison.

With higher output, only 2 ovens are required for stacking prebake to supply for diebond's demand in Q1'00. Therefore the other 2 ovens can be freed up for epoxy curing and PMC (for 119PBGA and 240 recipe).

2. Vacuum Sealing shortly after prebake to provide better production flexibility. Substrates with vacuum sealing will be allowed to stage up to 7 days as in ASE-CL.

3. To convert  $N_2$  substrate storage cabinet to open air to reduce  $N_2$  usage.

### Experiments and Results

All data is collected at T-zero/T3 Csam.

1. Stacking prebake vs Magazine prebake with vacuum sealing using 272 PBGA S23835W003 substrates (0.56 mm thickness) with magazine prebake oven settings

2. Stacking prebake with full load (6 x 9 stacks on new trays) using 357 PBGA W011 substrates (0.36 mm thickness) with magazine prebake oven settings

3. To obtain oven profile with full load (6 x 9 stacks on new trays) through optimization of oven settings

4. Stacking prebake with new oven settings and full load (6 x 9 stacks on new trays) using 272 PBGA S23835W003 substrates (0.56 mm thickness)

5 (a). After soaking in MSL3+ precondition, stacking prebake with new oven settings and full load (6 x 9 stacks on new trays) using 0.56mm thickness substrates : 272 PBGA S23875W002 (4 layers) and S23835W003 (2 layers)

5 (b). Vacuum sealing for center strips after prebake and die bond after 14 days with 10 hrs staging in air

6. To obtain oven profile with new oven settings and full load in 2nd prebake oven.

Constants : Ablestick 8360 die attach epoxy, 357PBGA 860 device ink dice.

### Experiment 1

Stacking prebake vs Magazine prebake with vacuum sealing using 272 PBGA S23835W003 substrates (0.56 mm thickness) with magazine prebake oven settings

#### Experimental method :

1. Prebake : Stacking prebake (50 strips/stack) & Magazine prebake was done in one oven (with magazine prebake oven settings) with stacking prebake on top shelf (20 stacks, 6K substrates) and magazine prebake on bottom shelf (20 slotted magazines, 3K substrates). Total substrate quantity is 9K

2. After prebake, substrates were vacuum sealed with 50 strips per packet within 2 hrs. In that 50 strips, half were stacking prebaked and half were magazine prebaked. Moisture indicators were placed in each packet.

3. After vacuum sealed, packets of substrates were staged in air for a period

of time before they were opened up for die bond. After opening, substrates were staged in open air in magazines for 4 hrs, 6 hrs, 8 hrs and 10 hrs.

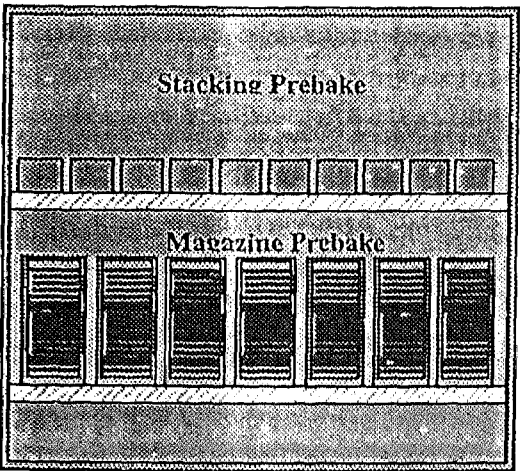


Fig. 12. Illustration of material arrangement in prebake oven (front view).

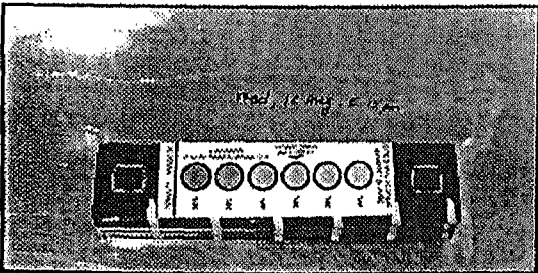


Fig. 13. Substrates after vacuum sealed (50 strips/packet) with moisture indicator.

T-zero Csam Result

No. of days vacuum sealed	Moisture Ind. color change?	Staging time b/w vacuum seal opening and epoxy cure in		CSAM T-zero	
		Planned	Actual	Stacking	Nonstacking
16 days	No	0 hrs	1 hr	0/18	0/18
		2 hrs	6 hrs	0/18	0/18
		4 hrs	6 hrs	0/18	0/18
36 days	No	4, 6, 8 hrs	7 hrs 30 mins	0/54	0/54
44 days	No	4 hrs	3 hrs 25 mins	0/18	0/18
		6 hrs	5 hrs 45 mins	0/18	0/18
56 days	No	8 hrs	7 hrs 50 mins	0/18	0/12
		10 hrs	10 hrs	3/18 (<10%)	4/18 (<10%)

After 56 days of vacuum sealed, substrates (both stack prebake and magazine prebake) can be staged in open

air for 8 hrs without any black spots. However at 10 hrs of staging time, black spots (<10%) are seen in both stack and magazine prebake substrates.

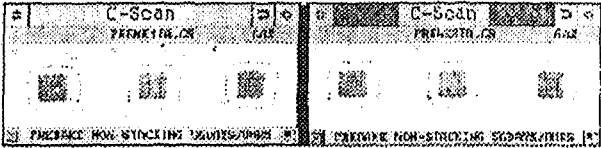


Fig. 13. Magazine prebake and 8 hrs staging in air before epoxy cure. No black spots are seen.

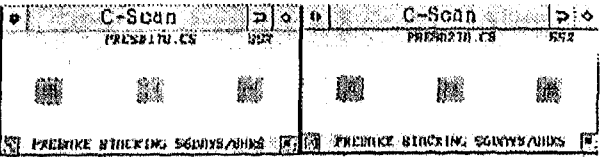


Fig. 14. Stack prebake and 8 hrs staging in air before epoxy cure. No black spots are seen.

Total staging time in open air = 10 hrs.

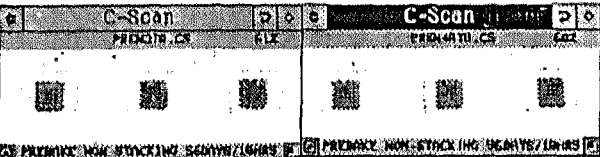


Fig. 15. Magazine prebake and 10 hrs staging in air before epoxy cure has black spots (<10%).

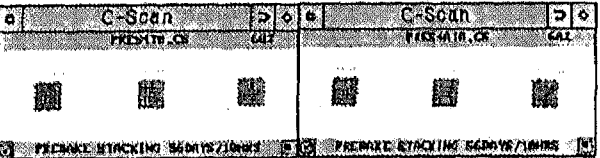


Fig. 16. Stack prebake and 10 hrs staging in air before epoxy cure has black spots (<10%).

Total staging time in open air = 12 hrs.

Experiment 2

Stacking prebake with full load (6 x 9 stacks on new trays) using 357 PBGA

W011 substrates (0.36 mm thickness)  
with magazine prebake oven settings

Substrates are placed in stacks on the  
trays as illustrated below :

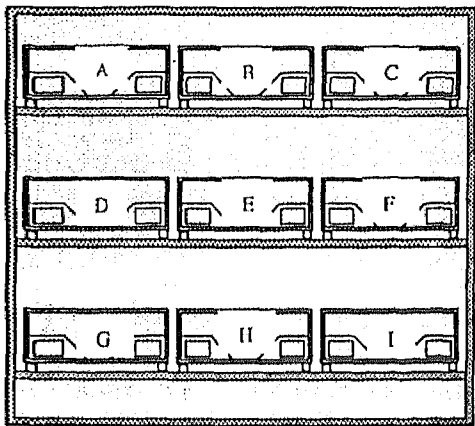


Fig. 17. Tray position in prebake oven.

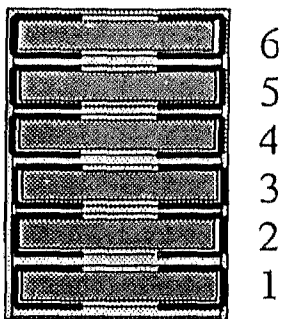


Fig. 18. Stack position in each tray.

After stacking prebake, substrates were  
loaded into magazines and staged in  
open air for die bond. Staging time  
between prebake out to epoxy cure is 10  
hrs 45 mins.

**Result**

T-zero Csam Result shows no black  
spots/blistering. 20 strips were sent for  
MSL3 at 220°C VP reflow and all of  
them pass.

Tray Position	Stack Position	Strip Position in Stack		
		Top	Center	Bottom
A	1	0/6	0/6	0/6
	2	0/6	0/6	0/6

Table 2. T-zero Csam result.

Table 2. T-zero Csam result.

Some units have grey epoxy edges due  
to epoxy settling. No delamination after  
MSL3/220°C VP for units with such  
grey epoxy edges.

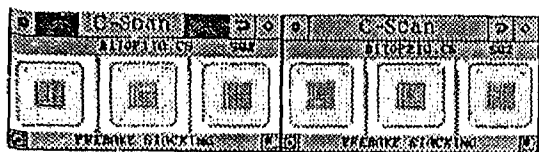


Fig. 19. T-zero Csam for units with grey epoxy edges.

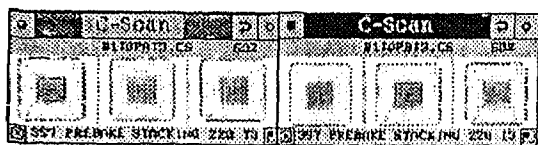


Fig. 20. T-3 Csam for units with grey epoxy edges. No delamination is found.

Control samples with magazine prebake were also built in the same oven with full load (40 slotted magazines). Staging time between prebake out to epoxy cure in is 10 hrs 20 mins. T-zero result shows no black spots.

This experiment has proven the effect of of stacking prebake to be as effective as the current magazine prebake.

### Experiment 3

To obtain oven profile with full load (6 x 9 stacks on new trays) through optimization of oven settings

Temperature profile of prebake oven is consist of 4 segments :

- N2 purging time
- Ramping up time
- Hold/Cure Time
- Cooling Time

Total process time = A+B+C+D

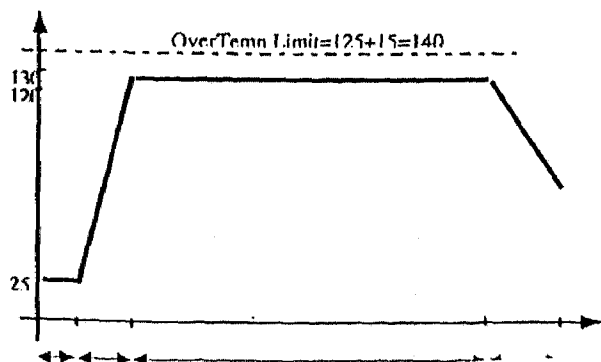


Fig. 21. Temperature profile of prebake oven.

The purpose of this experiment is to obtain stacking prebake profile within Prebake Profile Spec : hold time at 125°C +/- 5°C for 3 to 4 hrs.

The first profile for stacking prebake with full load was run with magazine prebake settings. The hold time was found to be 2 hrs 53 mins only, 7 mins below spec. After some settings adjustment and optimization, profile was obtained within spec.

	current setting	new setting
purging	20 mins	20 mins
ramping up	30 mins	1 hr
hold time at 125°C +/- 5°C	3 hrs 10 mins	3 hrs 30 mins
cooling	40 mins	40 mins
total process time	4 hrs 40 mins	5 hrs 30 mins

Fig. 22. Oven settings adjustment and optimization for stacking prebake.

With the optimized oven settings, 3 profiles were run, with one profile for each shelf. There were 27 points in each profile : 9 points on each tray (front, center, back stacks) and 3 points on each stack (top, center, bottom position).

### Result

Hold time at 125°C +/- 5°C for the 3 profiles are all within Spec. Peak temperature is 127.2°C.

	minimum	maximum
Top Shelf	3 hrs 12 mins	3 hrs 45 mins
Center Shelf	3 hrs 15 mins	3 hrs 50 mins
Bottom Shelf	3 hrs 10 mins	3 hrs 50 mins

Table 3. Hold time at 125°C +/- 5°C.

This result is compatible with the average hold time of 3 hrs 10 mins for conventional magazine prebake which is obtained with current settings during oven profiling after PM.

With the new settings, profile is also run with magazine prebake to check out the hold time. The result is within spec at 3 hrs 25 mins minimum. Therefore the new settings is proven to be flexible for both stacking prebake and magazine prebake.

#### Experiment 4

Stacking prebake with new oven settings and full load (6 x 9 stacks on new trays) using 272 PBGA S23835W003 substrates (0.56 mm thickness)

The purpose of this experiment is to confirm the effectiveness of the new settings, which logically should be better than the magazine prebake settings.

Substrates were placed in the oven with the arrangement similar to Experiment 2. After prebake, substrates were loaded in to magazines and staged in open air for die bond. Staging time between prebake out to epoxy cure in was 10 hrs 30 mins.

#### T-zero Csam Result

Good result was obtained with no black spots/blistering.

Table 4. T-zero Csam result for new oven settings check out.

Tray Position	Stack Position	Strip Position in Stack		
		Top	Center	Bottom
A	1	0/6	0/6	0/6
	2	0/6	0/6	0/6
	3	0/6	0/6	0/6
	4	0/6	0/6	0/6
	5	0/6	0/6	0/6
	6	0/6	0/6	0/6

#### Experiment 5 (a)

After soaking in MSL3+ precondition, stacking prebake with new oven settings and full load (6 x 9 stacks on new trays)

using 0.56mm thickness substrates : 272 PBGA S23875W002 (4 layers) and S23835W003 (2 layers)

Substrates were pre-soak in MSL3+ precondition (30°C/60%RH for 9 days). The purpose of soaking is to simulate the condition of incoming substrates in the worst case of wetness to test out the effectiveness of stacking prebake in handling the wettest substrates.

After soaking, substrates were placed in the oven with the arrangement similar to Experiment 2. After prebake, substrates were loaded in to magazines and staged in open air for die bond. Staging time between prebake out to epoxy cure in was 10 hrs 30 mins.

#### T-zero Csam Result

Even after soaking and with 10.5 hrs of staging, no black spots/blistering was found. This further proves the effectiveness of stacking prebake in drying up moisture in wet substrates.

Tray Position	Stack Position	Strip Position in Stack		
		Top	Center	Bottom
A	1	0/6	0/6	0/5
	2	0/6	0/6	0/6
	3	0/6	0/6	0/6
	4	0/6	0/6	0/6
	5	0/6	0/6	0/6
	6	0/6	0/6	0/6
B	1	0/6	0/6	0/6
	2	0/6	0/6	0/6
	3	0/6	0/6	0/6
	4	0/6	0/6	0/6
	5	0/6	0/6	0/6
	6	0/6	0/6	0/6
C	1	0/6	0/6	0/6
	2	0/6	0/6	0/6
	3	0/6	0/6	0/6
	4	0/6	0/6	0/6
	5	0/6	0/6	0/6
	6	0/6	0/6	0/6

Table 5. T-zero Csam result for stacking prebake after MSL3+ precon. soaking.

#### Experiment 5 (b)

Vacuum sealing for center strips after MSL3+ soaking and stacking prebake

After MSL3+ soaking and stacking prebake, center strips of each stack were vacuum sealed into one packet within 2 hrs. Moisture indicator was placed in the packet of 54 strips. It was then staged in open air at frontend for 14 days. After 14 days, substrates were loaded into magazines and staged in open air for die bond. Staging time between prebake out to epoxy cure in was 10 hrs 5 mins. This gave a total staging time of 12 hrs 5 mins.

#### T-zero Csam Result

Result for 9 center strips with one from each tray showed no black spots. However, black spots (<10%) were

found on 4 strips which was blistering caused by moisture absorption due to long hours of staging time. This confirmed the result in Experiment 1 where substrates staged in open air for 8 hrs had no black spots but at 10 hrs of staging time, black spots (<10%) were seen in both stack and magazine prebake substrates.

Tray Position	Stack Position	Center Strip 1-zero CSAM Result
A	1	0/6
B	3	0/6
C	5	4/6 (<10%)
D	2	2/6 (<10%)
E	4	0/6
F	6	4/6 (<10%)
G	6	0/5
H	1	0/6
I	3	3/6 (<10%)

Table 6. T-zero Csam Result for strips with vacuum seal after MSL3+ precon. soaking and stacking prebake.

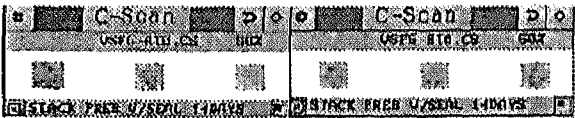
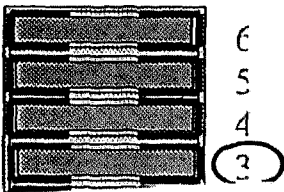


Fig. 23. T-zero Csam of strip with black spots.

Experiment 6

To obtain oven profile with new oven settings and full load in 2nd prebake oven

Temperature profile check out for 2<sup>nd</sup> stacking prebake oven with full load was done with 9 TC wires : one at each tray, at the center of stack no. 3.



Oven Door

Fig. 24. Top view of tray with placement of TC wire at the center of stack no. 3.

Result

Temperature profile for 2<sup>nd</sup> prebake oven is within spec. Peak temperature is 126.9°C.

Hold time at 125°C +/- 5°C is shown below :

minimum	maximum
3 hrs 22 mins	3 hrs 40 mins

Discussion and Conclusion

- Experiment 1 and 2 have proven that Stacking Prebake is as effective as Magazine Prebake. No black spots with up to 10 hrs 45 mins of staging time. Black spots of <10% are seen at 12 hrs staging.
- Experiment 3 shows that as the load increases, longer prebake time is needed to dry up the moisture in substrates. Therefore stacking prebake cycle time is 5.5 hrs, which is 50 mins longer than magazine prebake cycle time.
- Experiment 4 confirms the effectiveness of new oven settings for stacking prebake. No black spots are seen at 10.5 hrs of staging time.
- Substrates prebaked after MSL3+ soaking show no black spots after 10.5 hrs of staging. However after 14 days of vacuum sealed and with 12 hrs 5 mins of staging time, black spots (<10%) are



found in 4/9 strips which confirms the result in Experiment 1.

- Therefore, total staging time is to be controlled at 10 hrs.

- Vacuum seal after stacking prebake :

- Stops the clock of moisture absorption even up to 56 days (2 months).

- Practical production control will be 7 days as in ASE-CL.

- Substrates after stacking prebake have to be sealed within 2 hrs.

- Staging time between vacuum seal opening and epoxy cure in will be controlled at 8 hrs to fulfill the 10 hrs of total staging time.

- In this studies, ALL staging data is established in OPEN AIR. This proves that  $N_2$  environment is NOT required for substrate staging. Thus  $N_2$  kaman will be converted to OPEN AIR to reduce  $N_2$  usage.

## Correlation and Validation of Stacking Method

Comparison of the stacking staging time from substrate prebake out to die bond cure in has been observed.

## ASE-CL Stacking Prebake Method

ASE-CL has performed a stacking prebake study by moisture weight gain. Eight Daisho and WWEI substrates each were prebake in stack at 125C. Then the strip were placed in 30C/60%RH chamber. Substrate weight was taken at 30, 60, 120, 180 and 3600 minutes. Fig. 26 shows the stacking method use with a weight on top.

## ASE-CL stacking prebake

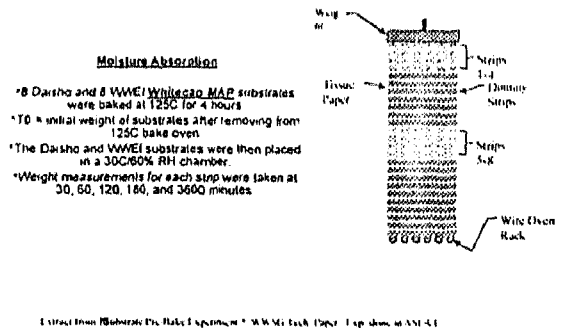


Fig. 26 Stacking prebake method by ASE-CL

Fig. 27 shows the final weight % of the Daisho moisture gain after a given time. The slope from 30 to 180 hours is steep which translate a greater moisture absorption. This is a typical trend moisture absorption curve for substrate. In the case of current production environment which is 25°C/45%RH, the slope gradient is expected to be lower. Thus, there is a significant difference between 10 and 12 hours of staging time as they fall within the slope region.

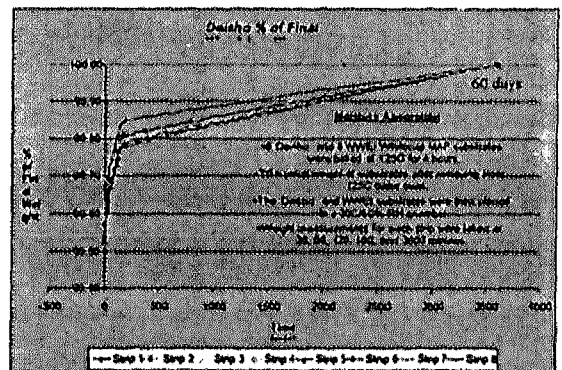


Fig. 27 Daisho %moisture weight gain

## Implementation of Stacking Prebake

- Stacking Prebake was implemented in ww48'99 after training was conducted for operators and supervisors. Staging time is guard band to 8 hrs.

- Only 2 prebake ovens are required to supply for die bond demand based on the runrate in Q1'00. The other 2 ovens are freed up for epoxy cure and PMC.

- T-zero monitoring is done for the first few loads by random sampling from production lots after epoxy cure (one inked strip/AO). No blistering or black spots are observed so far.

- MSL3/220VP monitoring for 3 production lots (5-10 units/lot) shows no blistering delamination.

See Appendix A & B for Csam pictures.

#### Vacuum Seal Implementation Plan

- Original plan was to implement together with stacking prebake in ww48'99. However it was delayed due to dry-pack machine constraint : only one m/c is available at PBGA backend FOI for dry-packing of engineering lots (NPI).

- In ww52'99, Engineering group has managed to obtain approval from ATX for not doing dry-packing for NPI engineering lots. This allows the dry-pack m/c to be relocated to frontend (substrate prebake area). Due to manpower constraint, relocation will only be done in ww03'00.

- Training for operators will be in ww03'00 after dry-pack m/c relocation. Substrates will be sealed in plastic containers from substrates supplier to prevent warping.

- Vacuum seal implementation is planned in ww04'00.

- T-zero and T3/220VP monitoring will be done upon implementation.

#### Advantages

- Cost avoidance of buying at least 2 prebake oven to support the Q1'00 runrate (2 x USD22K/oven = 44K).

- Increase of output by 2.7x per loading.

- Reduce no. of oven required → Save energy and floorspace.

- Converting N<sub>2</sub> (at 80scfh flow rate) to open air gives an annual saving of USD1.3K

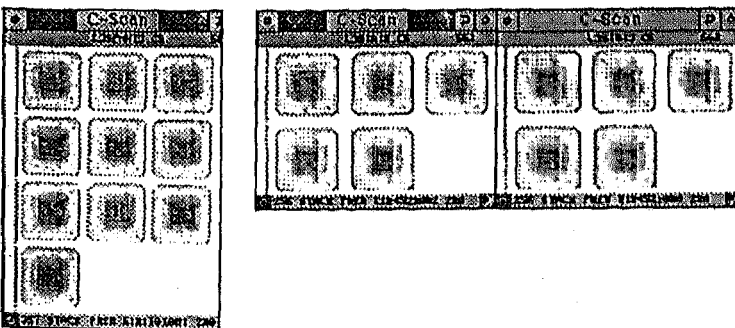
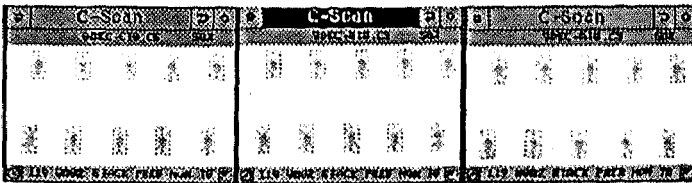
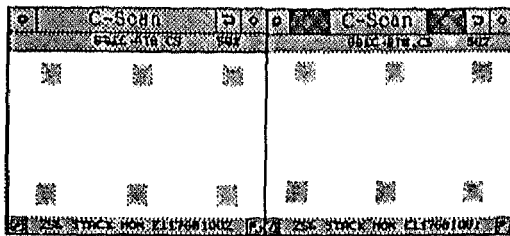
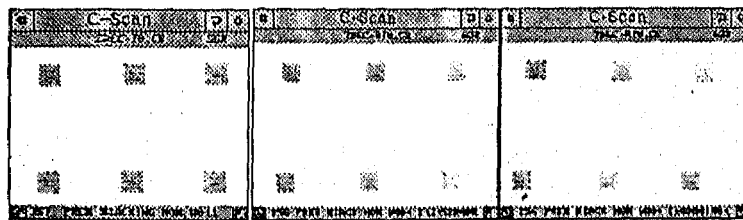
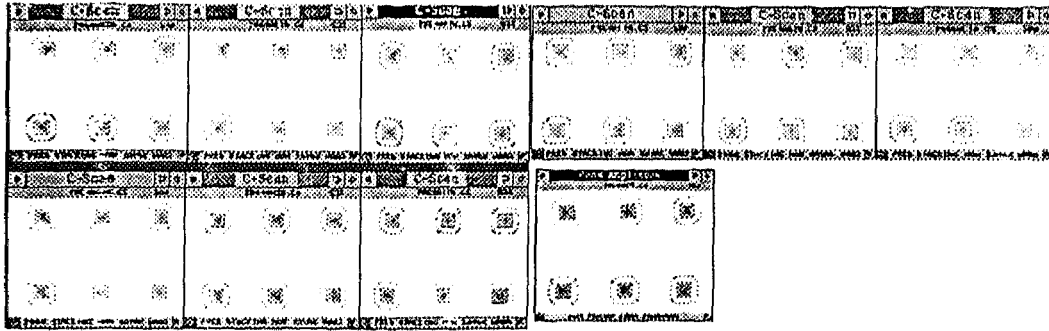
- Vacuum sealing improves production flexibility and provides easy production planning and minimizes changes of substrate rebake.

#### REFERENCES

1. BY Low, CL Lai, LJ Koh, CC Leong, Challenges of PBGA Assembly and Understanding of Moisture within Organic Substrate during reflow at 240 Deg.C, *SEMICON Singapore 99*
2. ASE-CL, Substrate Pre-Bake Experiment, *WWSG Tech. Paper*.

#### Appendix A

Production monitoring Csam pictures  
(T-zero & T3)



## Failure Analysis: Signal Conditioner Key Off Timer Issue

**ABSTRACT (Helvetica 10 Bold)** - This report details the failure analysis (FA) procedures conducted in response to a wafer probe yield loss of about 5% at MOS8 for the past one year. The estimated cost impact is about US\$250K/year. Microprobing has narrowed the failure site down to faulty flip flop in the Key Off Timer Circuitry. Electrical characterization leads to the discovery of open metal 2 to metal 1 via. Using advanced FIB tungsten deposition, detailed verification of failure can be reconfirmed. Specific defect information was relayed back to the fab so that corrective actions could be pursued.

**KEY WORDS** - KOT, Open Via, FIB

### INTRODUCTION

Mos 8 five inch wafer probe test was having about 5% yield loss due to Key Off Timer (KOT) failure for the past one year. The estimated cost impact is about US\$250K/year. Wafer mapping performed revealed, positional fallout at the bottom of the wafer. The probe failure samples were assembled and tested, confirming the KOT failure. Three units from probe failure samples were submitted for analysis. A thorough and systematic analytical approach leads to the identification of the root cause was due to open metal 2 to metal 1 via. The use of advanced Focus Ion Beam (FIB) tungsten deposition tool enabled detailed verification of the failure. Specific defect information was relayed back to the fab for corrective action.

### ANALYSIS

Curve tracing on all units showed no anomaly. X-ray analysis did not show any wirebond anomaly. Three units were verified to fail Key Off Timer tests using the bench test setup. The setup involves sending a sequence of commands to the KOT register address and then reading the return data. The failing units have the data always at \$00 to \$03. A correlation good unit has the data changing with each read ranging from \$00 to \$FF.

All units were decapsulated, visual inspection did not reveal any anomaly. Light emission analysis was performed on all units but no light emission spot was detected. Liquid crystal analysis was unable to be performed because the liquid crystal changed state during device powerup.

S/n 1 and 2 were depassivated using Reactive Ion Etching (RIE) for microprobing. Microprobing has narrowed down the defective area to a toggle flip flop in the KOT circuitry whereby the output was stuck low instead of a clock signal. Figures 1&2 show the KOT circuitry schematic and identify the failing flip flop.

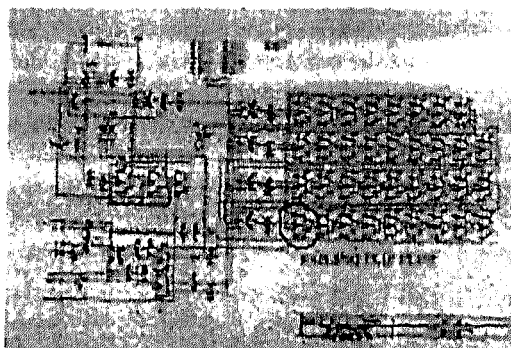


Figure 1: Key Off Timer (KOT) circuitry schematic identifying failing flip flop.

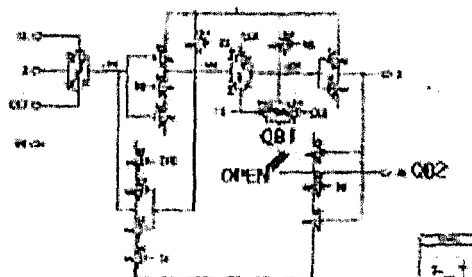


Figure 2: Detailed of the failing flip flop schematic.

Figures 3 & 4 show the partial layout of the flip flop and the probe points. Figure 5 shows the various probed signals on this flip flop. All the clock input signals to the flip flop were present. Powered curve trace was carried out at the input and output circuits of the flip flop but no anomaly was observed. Next, similar routed signals were probed and it was noted that the QB (Q Bar) output signals probed at QB1 and QB2 points were in the opposite state (see Figure 5). These two signals should be the same as QB1 and QB2 are connected through metal 2 to metal 1 via. This indicates possible open via between the two points.

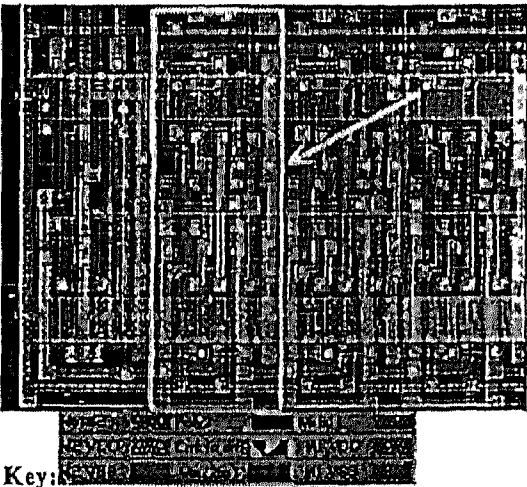


Figure 3: Partial layout of the failing flip flop - marked in red box.

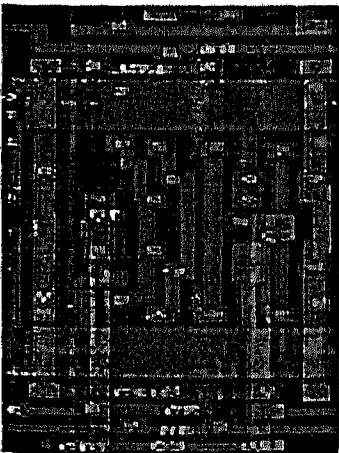


Figure 4: Layout of the failing flip flop shows the various signals. "X" indicates some of the signals that were probed. Further probing confirmed open via at QB1.

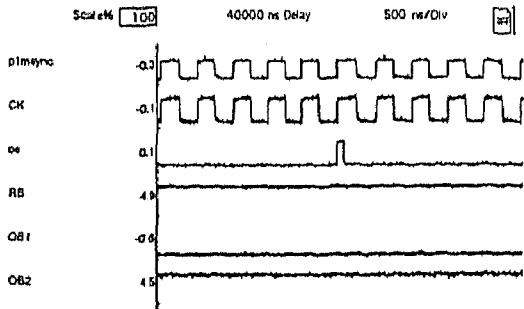


Figure 5: The various probed signals from the failing flip flop.

Focus Ion Beam (FIB) was used to open a small window down at metal 1 for probing. Curve trace confirmed an open metal 2 to metal 1 via at QB1. FIB cross sectioning was performed at the center of the open via. Voltage contrast imaging confirms that the via is open (Figure 6).

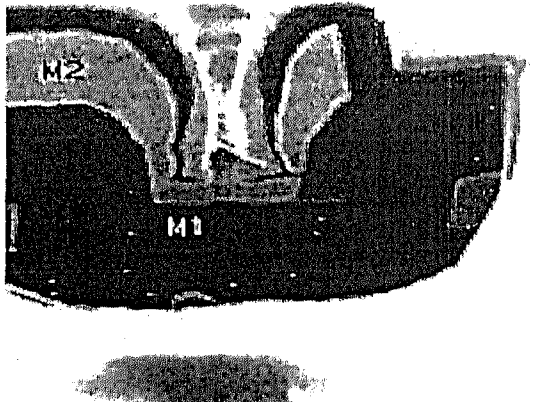


Figure 6: Voltage contrast imaging of the open via.

Figure 7 shows a correlation voltage contrast imaging on a good via. Wright etch was used to stain the sample for better imaging. Scanning Electron Microscopy (SEM) showed what was believed to be an interlevel oxide layer above the metal 1 layer blocking the via connection to it (Figure 8 and 9). Figure 10 shows a correlation good via. Both s/n1 and 2 were found with similar failure mechanism.

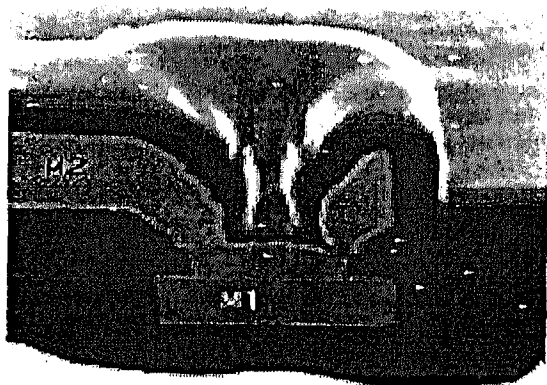


Figure 7: Voltage contrast imaging on good via.



Figure 8: SEM imaging on s/n1 shows that an interlevel oxide layer was above the metal 1 layer blocking the via forming a connection.

Note: Passivation layer removed.

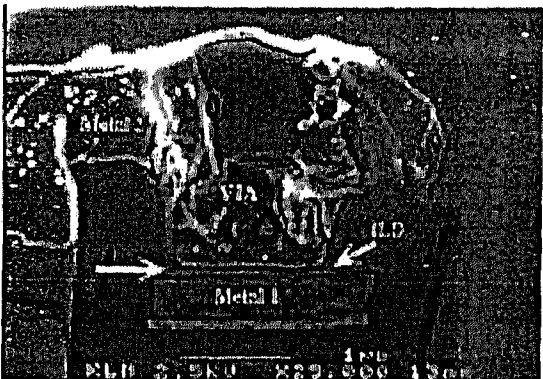


Figure 9: SEM imaging on s/n2 shows that an interlevel oxide layer was above the metal 1 layer blocking the via forming a connection.

Note: Passivation layer has been removed.

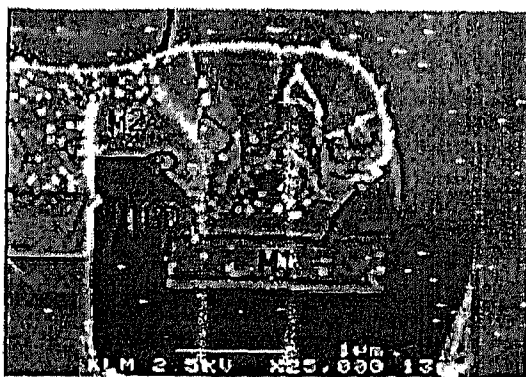


Figure 10: SEM imaging on a correlation good via.

To reconfirm the open via, FIB was used on s/n 3 to reconnect the QB signal at the failing flip flop. A verification on the bench setup showed that the unit has partially recovered. The returned read data was changing from \$00 to \$07. Hence, the next stage flip flop QB signal was suspected to be in opposite state as well. FIB was used to open probe windows on the QB signal and probing confirming another open via. FIB reconnection of the QB was performed. Verification on the bench has return read data changing from \$00 to \$0F. The unit still did not recover. The next successive stages of the flip flop were probed and reconnected until the fifth stage flip flop (Figure 11). The unit has finally recovered with the return read data changing with each read. FIB cross sectioning confirmed that all the vias were open at all five successive flip flop.

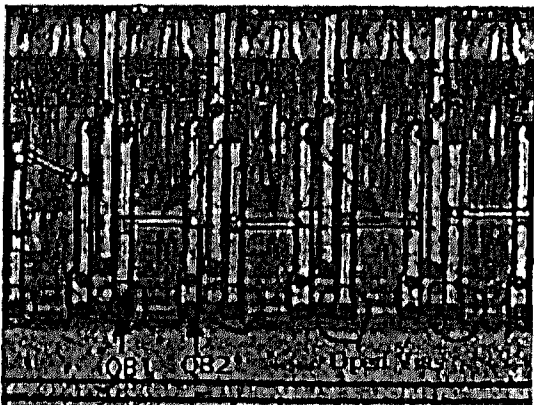


Figure 11: Image shows FIB reconnection of the QB signal on five successive stages of the flip flops. Unit has recovered. The open vias were circled in the picture.

Metal etch was done on s/n 1 to determine the presence of the interlevel oxide between metal 1 and 2 via. The results indicated that the bad via has a layer between the metal 1 and 2 via. SEM picture

clearly indicates that there has a layer separating metal 1 and 2 via (Figures 12 and 13).

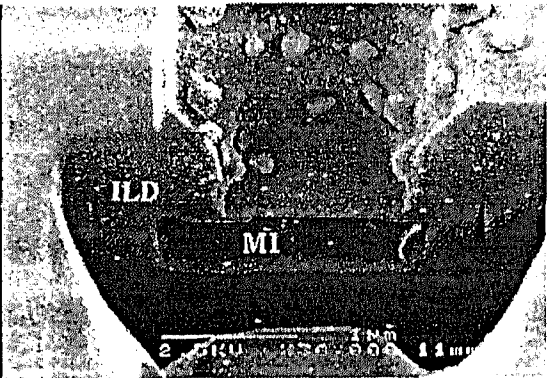


Figure 12: After metal etch, SEM image indicates that there is a layer (believed to be ILD) separating M1 and M2.



Figure 13: After metal etch, SEM image on a good via.

#### CONCLUSION

This report detailed a thorough failure analysis procedure for identifying the root cause and understanding of the fail mechanism of the KOT circuitry on the signal conditioner IC. All units failed with positional open metal 2 to metal 1 via at QB signal on the flip flop in the Key Off Timer (KOT) circuitry. The cause of the open via is due to insufficient anisotropic metal 2 to metal 1 via etch. Specific defect location on die has been relayed back to the fab for corrective action. The findings has resolved a year of problem and estimated cost savings of US\$250K/year. Mos8 will be increasing the etch time after a series of DOEs on control wafers. Further investigation on the fab process is recommended.

## Abstract

With the rapid advancement in wire bonding technology, ultra fine pitch (UFP) bonding with 60 $\mu$ m bond pad pitch (BPP) and below has fast become a reality. While the standard capillary design meets many current industrial needs from their proven reliability, demands for small ball size formation with large wire size in UFP bonding application requires a different tool design and configuration to contain the amount of gold squashed out during bonding. Using an unconventional approach in bonding tool design, a small hole to wire clearance for larger wire size with adequate chamfer diameter (CD) have been achieved.

Research and development on special tool design for UFP bonding on QFP and BGA material has been carried out to address the issue of small ball formation with large wire size. This paper discusses the bonding tool design aspects to control the desired MBD with the use of 25 $\mu$ m Au wire on a 60 $\mu$ m BPP platform. The intent is to establish the design feasibility to be used on the 50 and 40 $\mu$ m BPP at a later stage. Comparison of various bonding responses between standard and new bonding tool design obtained in both laboratory and manufacturing environment was also demonstrated.

## 2.0 Introduction:

In UFP bonding, the most difficult tasks are the small ball consistency with a reliable stitch formation. In most cases, the eventual mashed ball diameter (MBD) is only 5 to 8 $\mu$ m smaller than the bond pad opening (BPO). Such tight constraint on the ball bonds would require a consistent small ball formation, high PRS

control on the bonding tool dimensions. In addition, the use of large wire diameter (23 or 25 $\mu$ m) requires the hole diameter to be at least 30 $\mu$ m for a consistent looping. These constraints, together with those problems like open wire, bond lift off, looping performance, surface contamination, etc, have now become a critical process control requirement to achieve a stable wire bond process yield.

## 3.0 Objective

The main intent of this study is to establish and demonstrate the actual bonding response capability of the UFP capillary with the new design concept on a 60 $\mu$ m BPP platform. Reliability performance of the bonded wires is analysed through etching test and cross-sectioning after the temperature cycle test.

## 4.0 Experimental Setup

The evaluation was performed on a high frequency wire bonder, using test chip die attached on BGA 256 substrate and QFP 208 copper lead frame with silver coating.

Special capillary for 60 $\mu$ m BPP was used based on the capillary design consideration (See next section). SPT capillary, DFXE-332B-AZM-1/16XL was used for the BGA device and DFXE-30ZQ-AZM-1/16XL for QFP device.

A 25 $\mu$ m diameter gold wire was used for this purpose.

For the optical inspection and measurement, a high power microscope of 0.5 $\mu$ m resolution was used for ball height, ball size, and loop height measurement.



Ball shear strength and stitch pull test was performed on the shear tester. For the ball shear test, the shear height was set at 3µm.

All responses and measurements were taken with a sample size of 25 readings.

Temperature cycling was performed at -150°C to +150°C for the BGA device. Ball shear and wirepull reading were taken at 100, 500, 1000, and 2000 cycles.

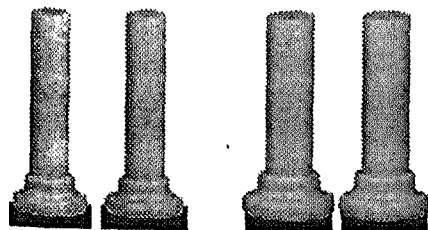
4.1 Capillary Design Considerations

For the ultra-fine pitch bonding, the given BPP and BPO requires a much smaller wire diameter (WD) of 20µm and below. Although this offers an advantage in cost reduction and a simple and straight forward capillary design, the problem takes place in wire sweeping during wire bonding, and molding process. The solution has reverted back to use larger wires ranging from 23µm to 25µm. However, various problems rises on using larger WD on a smaller BPO as explained below.

Firstly, for a WD of 23µm, the minimum hole size need to be at least 28µm. Considering a tolerance of +2/-0 µm, the minimum CD need to be at least 34µm for a reliable stitch bond. Such a CD size will almost be impossible to achieve an average ball size of 38µm for a 50µm BPP bonding.

Secondly, considering that the smallest Free Air Ball (FAB) size at 1.4 times the wire diameter (WD) that the current bonders can attained consistently, the deformed ball size cannot be further reduced as shown in Figure 1.

Figure 1: Ball sizes comparison for larger wire size



To address the above-mentioned issues, a unique capillary configuration know as DFX capillary has been designed to contain the amount of gold squashed out during bonding

control on the bonder, such design has proven to be able to control the desired mashed ball and hence reduce the ball size to a smaller dimension. The effect of such capillary design is illustrated in Figure 2.

In addition to the special capillary design configuration, consistent ultrasonic transfer is crucial for the ball size formation. This can be achieved by using the slimline bottleneck capillary with higher tip breakage resistant and consistent dimension repeatability.

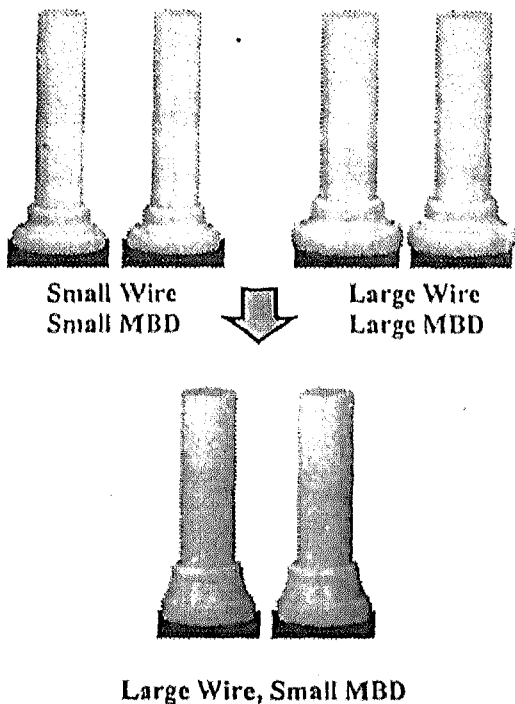


Figure 2: Special capillary configuration for small ball/ large wire capability

4.2 Results & Discussion:

A comparison study was carried out to check on the the performance of both the Standard and the new DFX capillary . Results were then discussed based on the bonding responses performance as well as the intermetallic coverage.

4.2.1 Bonding Response

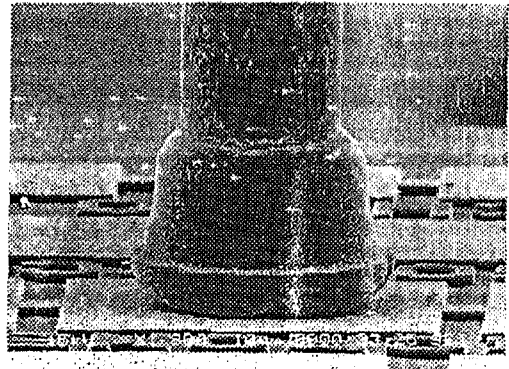
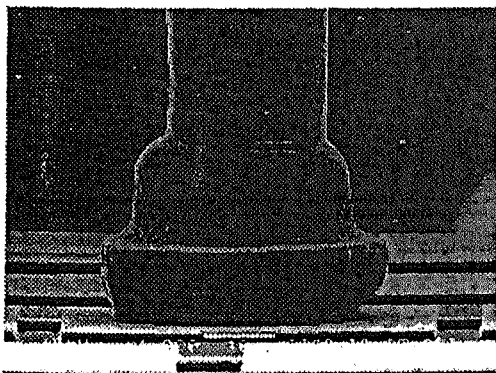
A design of experiments (DOE) was conducted to determine the

capillary on a QFP platform. A selected single point parameters was used for bonding response comparison with the result as shown in Figure 3 and 4.

Capillary Design	Standard Design	DFX Design
Device	QFP 208	QFP 208
Capillary Type	SBNE-30ZA	DFXE-30ZA
Wire Diameter $\mu\text{m}$	23	23
Ball Dmtr $\mu\text{m}$		
Average	42.6	39.2
Std Dev.	0.59	0.56
Ball Shear Strength, gm		
Average	15.4	11.9
Std Dev.	1.04	0.66
Ball Shear Stress $\text{N/mm}^2$		
Average	106.4	96.8
Std Dev.	5.3	3.9
Wirepull Strength, gm		
Average	5.8	5.7
Std Dev.	0.2	0.2

Figure 3: Bonding response comparison for standard and DFX design capillary

Standard Design



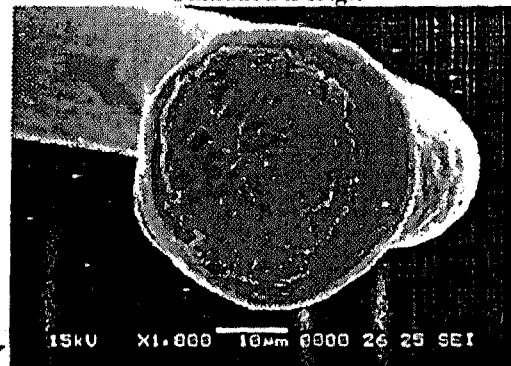
DFX Design Capillary

Figure 4: SEM picture for standard and DFX design capillary

#### 4.22 Inter-metallic Analysis

Inter-metallic analysis was analyzed through the etching test to further understand the effect of the new capillary design on the inter-metallic formation. From the pictures shown in Figure 5, no significant difference was observed between the standard and DFX capillary.

Standard Design



DFX Design Capillary



Figure 5: Intermetallic analysis for standard and DFX design capillary

from the bonding response and inter-metallic analysis, it can be seen that the DFX design capillary is capable of producing a smaller ball size as compared to the standard design with a minimum ball shear stress of 90 N/mm<sup>2</sup> (6g/mil<sup>2</sup>). Hole and CD dimensions remain the same for both capillary designs.

Having validated such design concept, a similar experiment was conducted with the new DFX design but with a larger hole and CD dimensions. The main purpose is to investigate the possibility of using a bigger hole diameter for larger wire application while maintaining the average bonded ball size at 42µm.

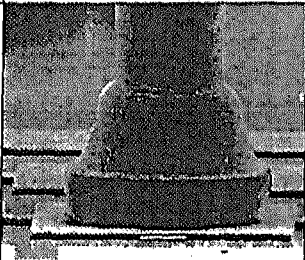
Capillary Design	DFX Design
Capillary Type	DFXE-33ZQ
Wire Diameter µm	23
Ball Dmtr µm	
Average	41.9
Std Dev.	0.62
Ball Shear Strength,gm	
Average	15.8
Std Dev.	0.75
Ball Shear Stress N/mm <sup>2</sup>	
Average	112.5
Std Dev.	4.2
Wirepull Strength,gm	
Average	5.6
Std Dev.	0.3
SEM Picture	

Figure 6: Bonding response for DFXE-33ZQ

Results from the various bonding responses have indicated that a similar ball size can be achieved with a larger CD and hole diameter with acceptable bond quality. Therefore, a larger wire size can be used with such a design feature for UFP application with controlled ball size.

4.3 Reliability Analysis

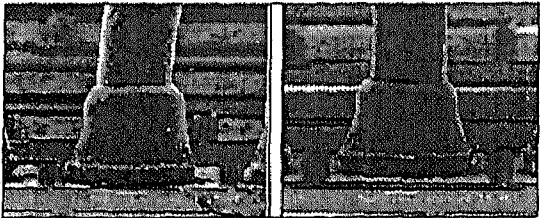
Having understood the bonding behavior of the DFX design, reliability study was conducted with temperature cycling at condition -150°C to +150°C for a standard 256 BGA device on various bonded ball thickness. Again, Esec3018 with 125KHz was used for this purpose.

Since the evaluation is mainly to check on the realibility of the different ball thickness resulted from the new capillary design, important parameters such as Bond Force, Bond Power and Bond Time were kept constant whilst three different Free Air Ball (FAB) parameters were used. Details of the evaluation parameters is as in Figure 7.

	Eval #1	Eval #2	Eval #3
1 <sup>st</sup> Force	280mN	280mN	280mN
1 <sup>st</sup> Time	15ms	15ms	15ms
1 <sup>st</sup> Power	23.1%	23.1%	23.1%
2 <sup>nd</sup> Force	530mN	530mN	530mN
2 <sup>nd</sup> Time	15ms	15ms	15ms
2 <sup>nd</sup> Power	25.50%	25.50%	25.50%
Auto FAB	40	42	44

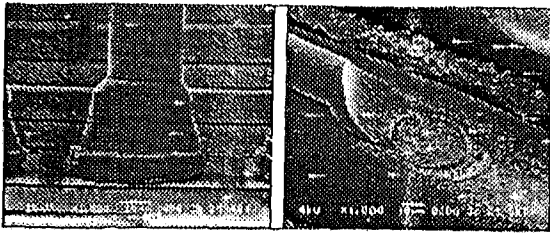
Figure 7: Evaluation layout

All samples were then subjected to the temperature cycling at condition -150°C to +150°C for 100, 500, 1000 and 2000 cycles. Responses were taken both after wirebonding process as well as after each cycle.



Eval #1

Eval #2



Eval #3

Stitch bond

Process	Response	Auto Free Air Ball (FAB)		
		40.00	42.00	44.00
After WB	Ball Dmtr (μm)	Av:46.33 SD:2.17	Av:49.21 SD:1.49	Av:50.62 SD:1.78
	Ball Hgt (μm)	Av:5.50 SD:1.76	Av:11.35 SD:2.25	Av:15.80 SD:1.94
	Wirepull (gm)	Av:8.45 SD:0.24	Av:8.27 SD:0.19	Av:8.45 SD:0.22
	Wirepeel (gm)	Av:6.21 SD:0.35	Av:5.68 SD:0.42	Av:5.88 SD:0.55

Figure 8: Bonding responses after wire bond

Note: Data was based on average value

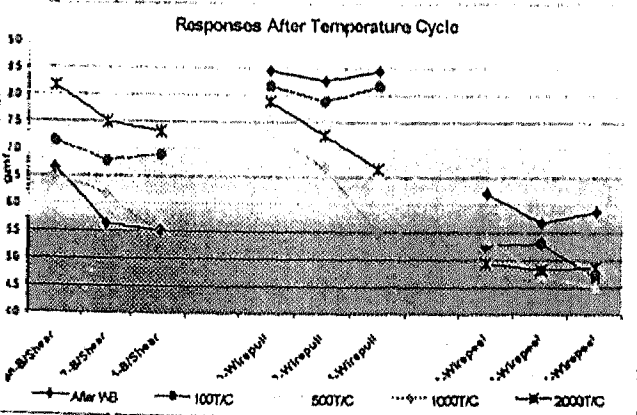
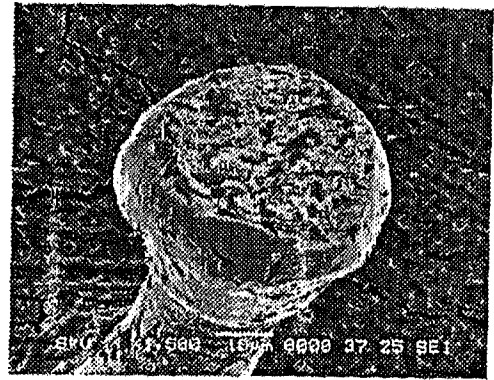
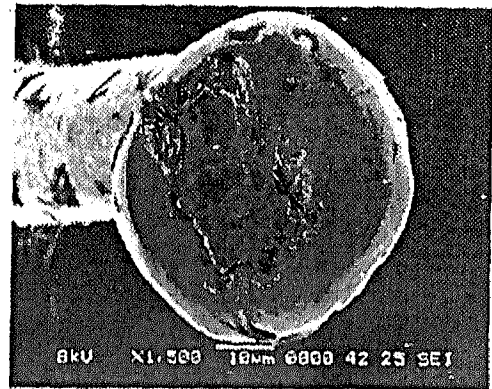


Figure 9: Responses after temperature Cycle

With the same bonding parameters, a smaller FAB setting result in a lower ball height but with a higher ball shear reading. This may be due to the efficient transfer of the ultrasonic energy through the capillary to the smaller amount of squashed gold that helps to develop the intermetallic formation between the Al pad and the Au ball. This observation was verified with an etching test on those units with different ball height readings as shown in Figure 10.



Ball Height = 6μm



Ball Height = 16μm

Figure 10: Intermetallic analysis for different ball heights

Result indicates that the inter-metallic coverage for the thinner gold ball is approximately 15% more than for the thicker ball. A sufficient coverage of inter-metallic is very crucial in the UFP bonding that requires small and thin bonded ball to cater for the narrow pitch requirement and at the same time did not sacrifice on the bonding performance.

In addition, the degradation of the interface between the bonded ball and the Al pad during temperature cycle was also studied by monitoring the ball shear strength. Fluctuation in the ball shear stress was observed at each read out with the highest reading recorded at 2000T/C. No interface degradation was observed for all units. In fact, there was an increase in the ball shear stress at certain read out.

On the other hand, wirepull and wirepeel strength using the new capillary design concept were comparable to the standard design before temperature cycle test. However, a gradual decrease in the pull and peel strength was observed in most cases but still beyond the above the 4gm minimum limit. Such observation has little impact on the FAB setting since the stitch quality was basically controlled by the FA, OR and T dimensions of the capillary.

In addition to the various bonding responses, a cross section on the ball bond was performed on units for eval#1 with the results as shown below Figure 11.

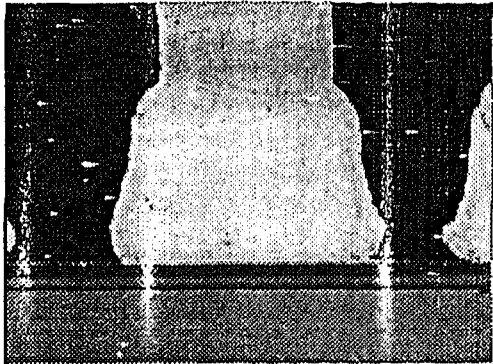


Figure 11: Cross section analysis

Measurement for the inter-metallic thickness revealed that compound thickness varies from 1.5 $\mu$ m to 3 $\mu$ m with no significant difference between 0 and 2000T/C.

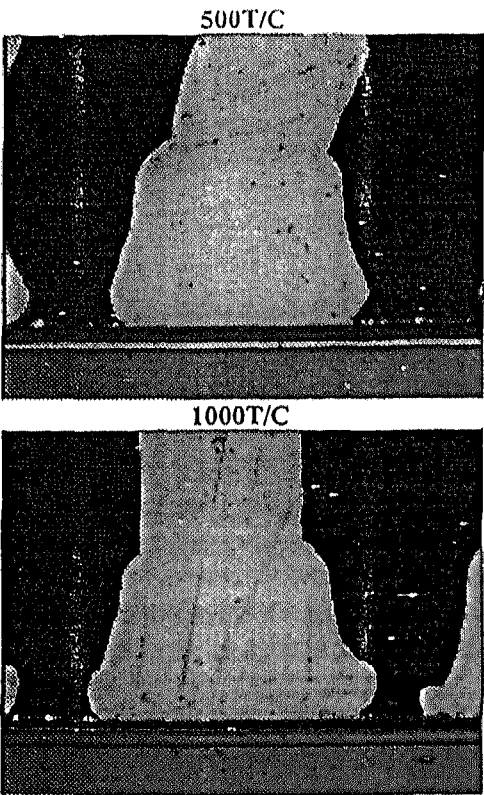
On the overall, temperature cycling effect did not have significant impact on ball height variation. Likewise, stitch performance remains within the acceptable quality after temperature cycling.

5.0 Conclusion

Wire bonding experiment with the new capillary design concept for ultra fine pitch bonding has shown that the ball and stitch bonds can be bonded with equivalent quality as compared to the standard design. The bondability and reliability tests have confirmed that the new capillary design can be introduced for volume production, without any bonding reliability issue. Results from the bonding test have also demonstrated that a minimum ball size of 10% larger than the CD dimension can be achieved in a production environment for a 25 $\mu$ m wire size on a 60 $\mu$ m BPP. The findings and reliability data provide a useful platform for such design to be used on even smaller pitch bonding application, which required a small ball size formation with large wire size.

6.0 Future Development

With the development and verification of the new capillary design on a 60 $\mu$ m BPP, the emphasis by the assembly houses is to incorporated with ...



2000T/C

testing has demonstrated that such design is capable of bonding on a 50 $\mu$ m BPP platform with a 23 $\mu$ m wire size with acceptable bond quality.

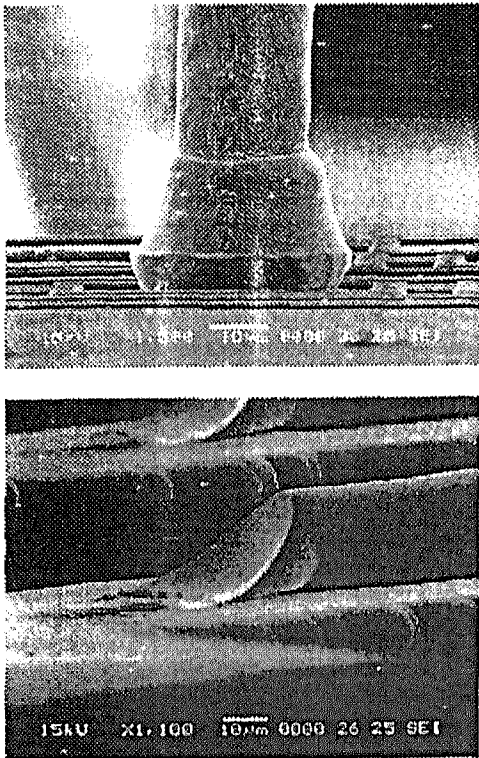


Figure 12: 50 $\mu$ m BPP capability

#### References:

1. Jimmy Castaneda, Winston Bautista, and Goh Kay Soon – The 50 $\mu$ m Bond Pad Pitch AZ Capillary (A Feasibility Study on its Design & Capability), pp123, Semicon Taiwan Packaging Seminar 1998.
2. Souad Aarsalane and Victor P. Jaecklin – The Fine Pitch Road Map (Challenges from 80 to 50 $\mu$ m Pad Pitch), pp107, Semicon Taiwan Packaging Seminar 1998.
3. Jimmy Castaneda, Winston Bautista, and Goh Kay Soon – Capillary & Process Optimization For 50 $\mu$ m Bond Pad Pitch, Semicon Singapore Packaging Seminar 1999.

## Radio Frequency Strip Oppose Emitter(RFSOE) Competitive Constructional Analysis

**ABSTRACT** - *A and B's competitor device was analyzed for constructional analysis. Conventional techniques and tools such as visual inspection and optical microscope together with advance failure analysis tools such as scanning electrons microscope(SEM), Energy Dispersive X-ray(EDX) and Focus Ion Beam(FIB) were utilized to reveal competitor package and die constructional features. For comparison purposes, only the die and elemental material identification from A 10035 device were compared to B MRF19030 as both devices are housed in a different package but similar application. Analysis findings on A and B devices package and die indicates differences in numbers of MOSCAPS used, wire material, wire bonding quality, die constructional pad layout, die thickness, passivation layers, number of metal layer scheme, gate length and gate thickness.*

**KEY WORDS** - *A 10035 device, B MRF19030 device, Focus Ion Beam, Scanning Electron Microscope(SEM), Energy Dispersive X-ray(EDX) Analysis.*

### 1.0 INTRODUCTION

One A 10035 device in Radio Frequency Strip Opposed Emitter(RFSOE) platform was submitted to B Product Analysis Laboratory for constructional analysis. This request was submitted by Wireless Infrastructure System Division(WISD) Packaging Benchmarking Team. The intention of this analysis is to perform a package and die level analysis on a A competitor part.

This A 10035 is a 30W, 1.9 - 2.0 Ghz device housed in a A A1164 package. This A1164 is similar to B NI600 package. However B does not have a

similar device in application that is housed in this package. On the other hand, B MRF19030 device share the similar application to A 10035 device but housed in a Micro400 package that have a different package case outline.

For comparison purposes, both the die and elemental analysis from A 10035 and B MRF19030 will only be compared as both device are housed in a different package case outline.

Below are the outline on how the constructional analysis was conducted on the A 10035 and B MRF19030 device:-

1. Package Measurements
2. Package Decapsulation
3. Visual inspection
4. Package and Die Material Identification
5. Die Cross-Sectioning and Chemical Staining

### 2.0 PACKAGE MEASUREMENTS

Tool maker microscope was used for package outline and wire loop measurements for both A and B device. These measurements includes the die size, wirebond pad size, Flange dimension, Lead dimension, wire diameter, lid dimension, window frame thickness, internal cavity dimension and individual MOSCAPS dimension and thickness. Table 1 summarizes the measurements dimension for both A and B devices. In addition, material analysis results for both A 10035 and A 10035 package and die is also included in table 1.

The wire loop dimension and post to pad or pad to pad wire length were also measured and shown in figure 18 for better visualization. This measurements is only documented for A 10035 device due to different wirebonding scheme.



Comparison to **B** MRF19030 might not be comparable.

Item Information	A	B	Remarks
Die Size (L x W x T) mils	208.37 x 45.35 x 4.46	208.17 x 27.26 x 5.03	
Top metal	NA	NA	
Base metal	NA	NA	
Die Attached Material	Sr and Gold Eutectic	Sr and Gold Eutectic	
Active Area Size	37.80	7.47	
Active Area Shape (L x W) mils	2.64 x 7.48	4.79 x 6.97	
Die Attachment Material	Solder and Nitrogen	Solder and Nitrogen	
Range			
Frame Dimensions (L x W x T) mils	103.17 x 39.5 x 6.01	79.96 x 36.20 x 4.33	
Flange Material	NA	NA	
Flange Plating	Cu/Ni	Cu/Ni	
Flange Thickness (to distal end)	NA	NA	
Plating the back of flange	NA	NA	
Coating of Thermal Interface	Yes	No	
Leads			
Plating the leads	NA	NA	
Lead Dimensions (L x W x T)	431.50 x 154.75 x 6.20	281.54 x 150.17 x 5.35	
Lead Material	Cu/Ni	Gold	
Lead Attachment Material	NA	NA	
Wirebonds			
Wire Diameter (mil)	2 mils / Cu/Ni	2 mils / Aluminum	
Wire Length	4.68	11.92	
Lead			
Lead Compression	NA	NA	
Gray Flashed	Yes	Yes	
Lead Dimensions (L x W x T)	598.05 x 395.02 x 37.04	309.72 x 395.26 x 86.81	
Window Frame			
Window Frame Material	Aluminum and Cu/Ni	Aluminum and Cu/Ni	
Window Frame Thickness	27.62 mils	21 mils	
Window Frame Attach Method			
Internal Cavity Dimensions (mm)	473.53 x 231.43	270.64 x 209.92	
MOSCAPS	2 MOSCAPS	3 MOSCAPS	
Dimensions (L x W x T)	332.82 x 124.97 x 4.77	217.82 x 114.78 x 3.17	MOSCAP 1
		217.83 x 26.81 x 3.19	MOSCAP 2
		219.08 x 7.17 x 5.67	MOSCAP 3

Table 1. Compilation of **A** versus **B** device measurements. The table also include the package and die material identification inclusive of DIE and MOSCAP quantity and dimensions.

3.0 PACKAGE DECAPSULATION

The ceramic lid for both **A** and **B** was removed by using a tweezer from the window frame after heating the unit header at 250C on a heater block for a minute. This is done prior to some of the internal package measurements. Figure 2-5 shows **A** 10035 and **B** MRF19030 devices before and after the ceramic lid removal.

Figure 1 : Optical view showing **A** 10035 device prior to ceramic lid removal. This device is housed in **A** A1164 package

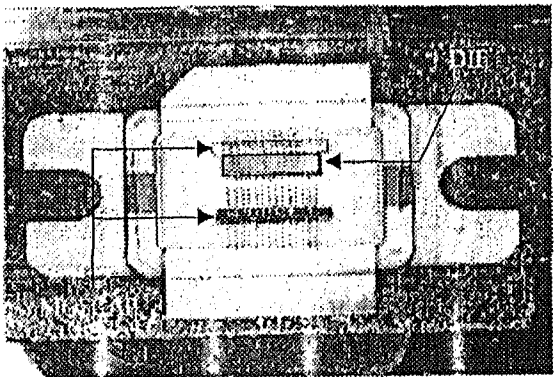


Figure 2 : Optical view showing the **A** 10035 device after ceramic lid removal. Photo also shows that the device of a single die diebonded on a header placed in between two MOSCAPS.

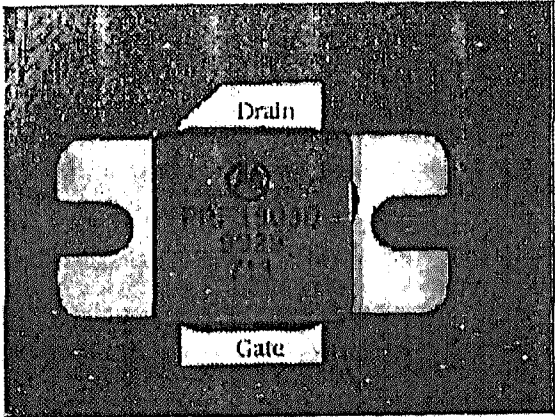


Figure 3 : Optical view showing **B** MRF19030 device prior to ceramic lid removal. This devices is housed in a micro400 package that have a smaller package case outline as compared to **A** 10035 device

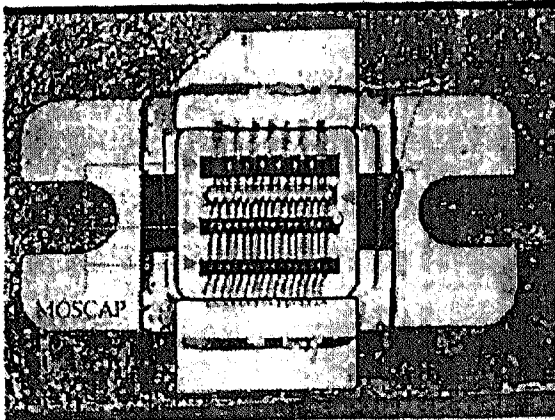


Figure 4 : Optical view of **B**. MRF19030 device after ceramic lid removal. This device consist of three MOSCAP as compared to two for **A** 10035 device.



#### 4.0 VISUAL INSPECTION

Low power and high power microscope were used to inspect for both *A* 10035 and *B* MRF19030 devices for any unique features. Optical inspection revealed that *A* 10035 device is constructed with 2 MOSCAPs(Figure 5) compared to 3 MOSCAPs for *B* MRF19030 device(Figure 6). Both device, is only constructed with a single die( Figure 5 and Figure 6).

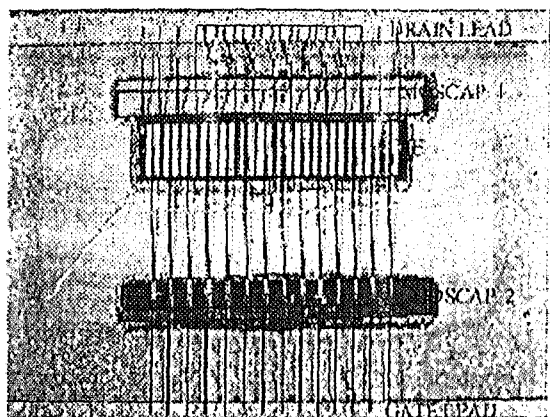


Figure 5 : Optical view focusing on the wirebonding scheme between the LEADS, MOSCAP and DIE for *A* 10035 device

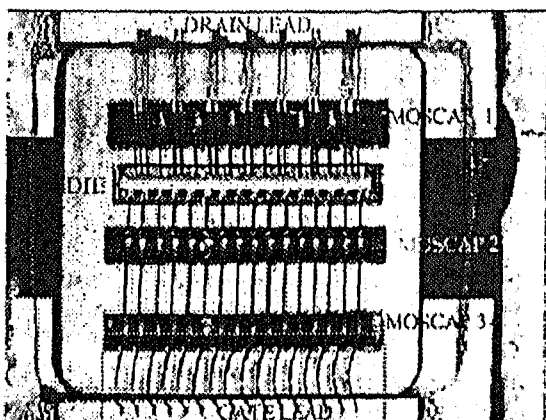


Figure 6 : Optical view focusing on the wirebonding scheme between the LEADS, MOSCAP and DIE for *B* MRF19030 device. This optical view also reveal that the wirebond between MOSCAP3 to gate lead is skewed evenly to the left.

Optical inspection on the wirebonding of *A* 10035 device revealed that the drain wire connection from DRAIN post to MOSCAP1 is skewed to the right and almost touches the DRAIN wire connection from DRAIN post to DRAIN pad on the die( Figure 7 ).

*B* device on the other hand, shows no abnormalities on the wire connection except for MOSCAP3 to GATE post connection where the wires were skewed evenly to the left( Figure 6).

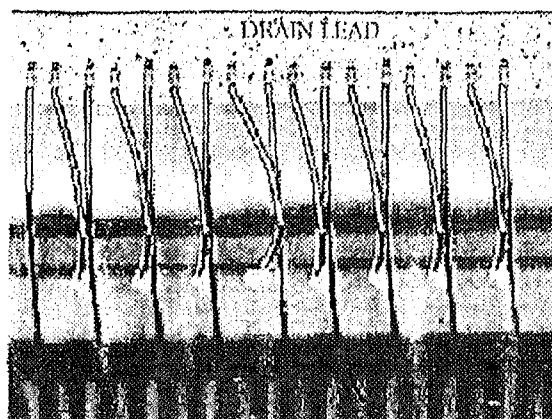


Figure 7 : Enlarged optical view of the red box depicted from figure 5 on *A* 10035 device. The higher wire loop is skewed to the right. Close examination indicated that the higher wire loop does not touches the lower wire loop.

Further optical inspection on the die revealed that the pad layout for both *A* 10035(Figure 8) and *B* MRF19030 device( Figure 9) are different. *A* 10035 drain pad is smaller in comparison to *B* MRF19030. Furthermore *A* 10035 have individual drain bond pad as compared to *B* MRF19030, that share a common bigger drain bond pad.

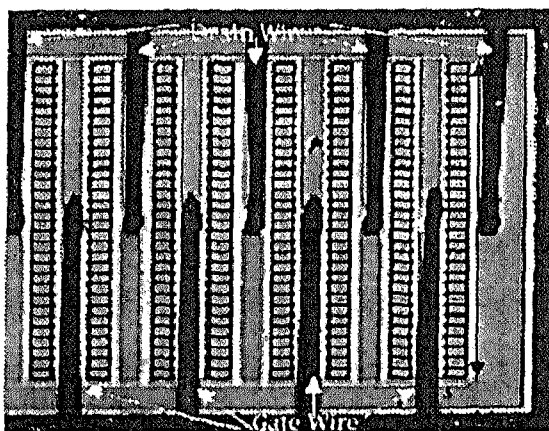


Figure 8 : Optical view showing *A* 10035 die with wirebonding intact. Red arrow shows the active area measurements. No evidence of ESD protective circuit was located on the die.

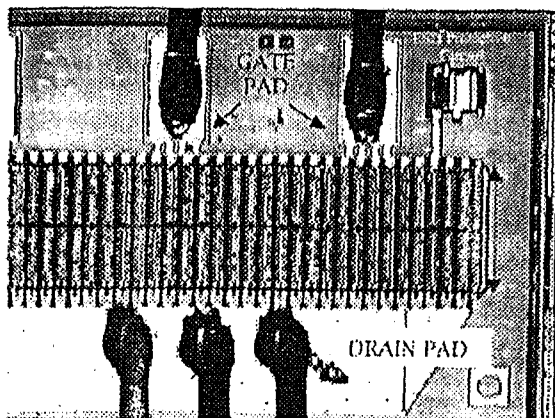


Figure 9 : Optical view showing *B* MRF19030 die with wirebonding intact. Red arrow shows the active area. ESD protective circuit is indicated by the green box. This die have two ESD protective circuit tied to the gate at both ends of the die.

No ESD protective circuit was visible for *A* 10035 device as compared to *B* device that utilizes 2 ESD protective circuit tied to both ends of the gate pad. Figure 9 shows one of the ESD protective circuit on *B* part depicts by the green box.

In addition, scanning electron microscope(SEM) was used to show the details of the feature observed on *A*. 10035 and *B* MRF19030 devices.

Figure 10-18 shows the SEM wirebonding micrograph between Drain post, on the die and on the MOSCAP for *A* device. No comparison were made to MRF19030 due to the package differences.

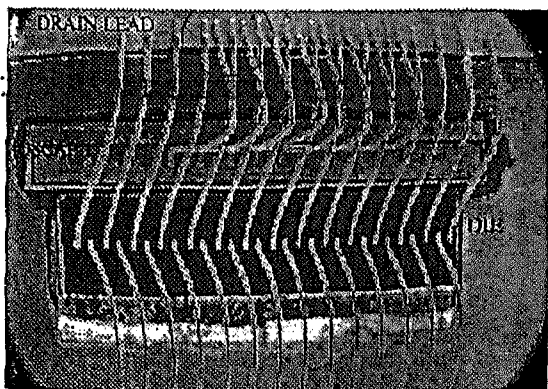


Figure 10 : SEM micrograph showing the MOSCAP1 wire connection to DRAIN LEAD( have 8 high loop wires) and DRAIN LEAD to DIE( have 15 wires). Fourteen(14) wirebonding connection from DIE to MOSCAP2 to GATE LEAD(not visible here in this micrograph)

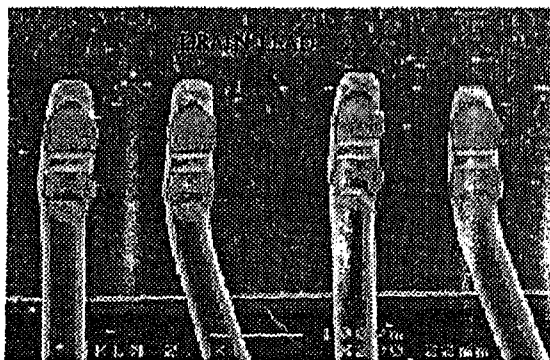


Figure 11 : SEM micrograph of *A* . 10035 device at the DRAIN LEAD post indicated by the red circle in figure 5 on *A* 10035 device. Wedge wirebonding was used.

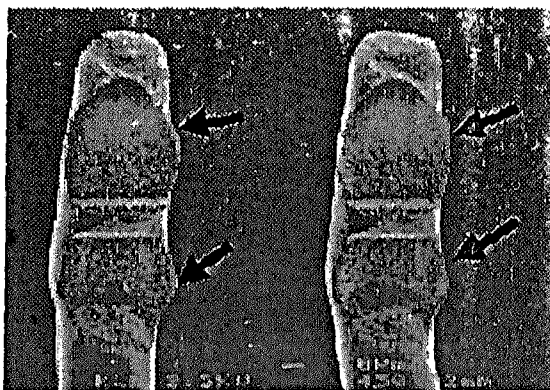


Figure 12 : SEM wirebonding micrograph at the DRAIN LEAD post for *A* . 10035 device with magnification of 400X. No pad tail was visible from the wedge wirebonding. The wirebonding impression on the DRAIN LEAD post is pressed in between as shown by the arrows.

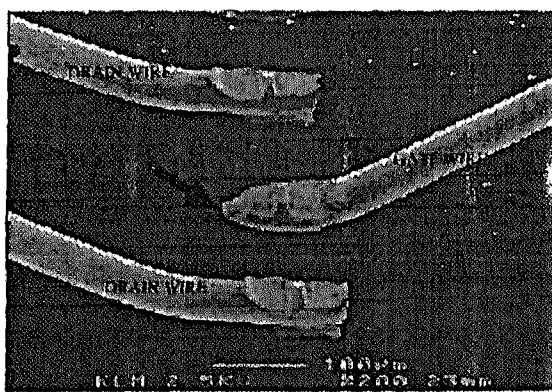


Figure 13: SEM die wirebonding micrograph for *A* 10035 tilted at 10 degree. It is observed that the wire connection from DRAIN LEAD post to die( DRAIN wire) has a blunt edge, indicated by the red arrow. Wirebonding from DIE to MOSCAP2 to GATE LEAD(GATE wire) post has a narrow look edge, pointed by the blue arrow

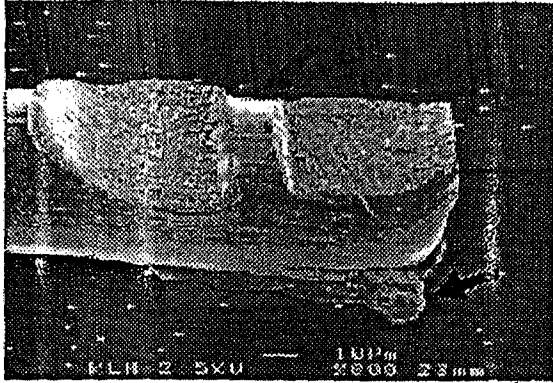


Figure 14 : SEM micrograph showing the details of *A* 10035 device single DRAIN wire tilted at 10 degree. The quality of wirebonding is not good. There seems to be an access wire impression on the bond pad as shown by the arrow. Side view also shows that the wire bond tool does not pressed the wire evenly as visible by the middle bump, pointed by the blue arrow.

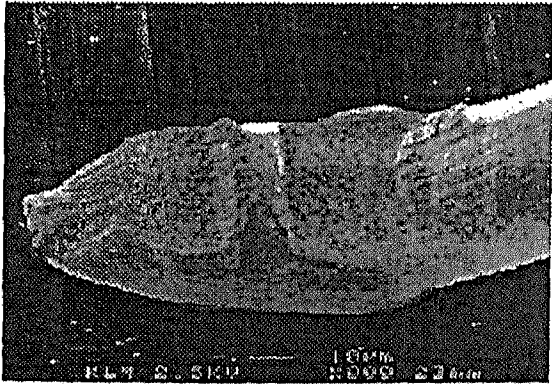


Figure 15: SEM micrograph showing the details of *A* 10035 device single GATE wire tilted at 10 degree on the die bond pad.

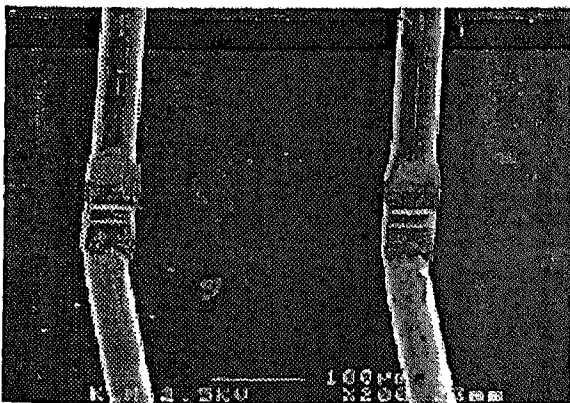


Figure 16 : SEM micrograph of *A* 10035 device wirebonding on MOSCAP2. The wire connection is from GATE pad to MOSCAP2 to GATE LEAD post.

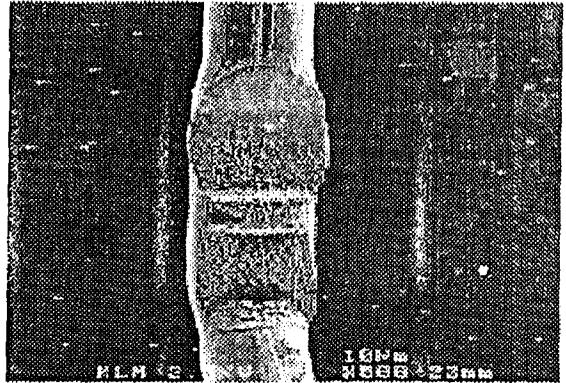


Figure 17 : SEM micrograph showing the details of *A* 10035 device single GATE wire connection on MOSCAP2. Similar unpressed middle bump feature is observed for this wedge wirebonding.

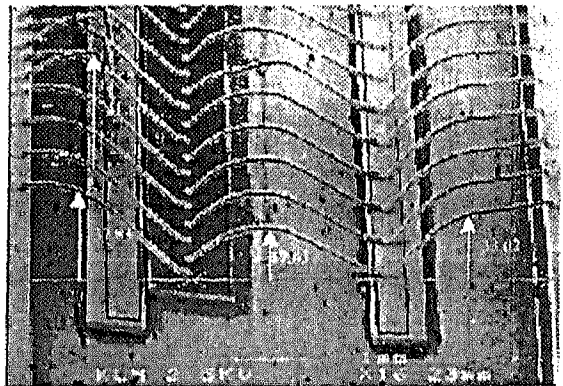


Figure 18 : SEM micrograph of *A* - 10035 device tilted at 40 degree showing the wire loop. The wire length and wire loop dimension was also included in this micrograph All the dimensions are in mils.

## 5.0 PACKAGE AND DIE MATERIAL IDENTIFICATION

Energy Dispersive X-ray(EDX) analysis at 15kV and SEM were used together during the analysis to determine the elemental identification qualitatively.

All the elemental identification for die passivation, die attached material, Flange plating, Lead material and window frame material were summarized in Table 1.

## 6.0 DIE CROSS-SECTIONING

Much advance equipment such as Focus Ion Beam(FIB) was used to cross-section both the *A* and *B* die. The cross-section area were depicted on figure 19 for *A* die and Figure 20 for *B* die.

Both of the cross-section area were selected in between the drain and gate pad. Prior to milling,

tungsten was deposited on the top portion of the area for cross-section. This tungsten layer is to protect the top part of the passivation layer from collapse when milling was conducted.

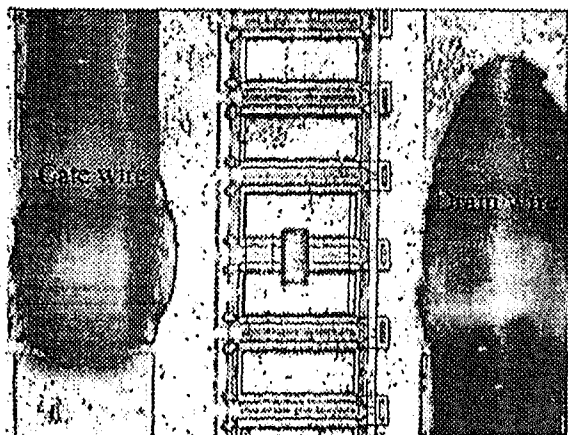


Figure 19 : Optical view of *A* 10035 die finger where the cross-sectioning was conducted utilizing FIB to understand the die cross-section structure. The cross-sectioned finger is conducted between the GATE wire and DRAIN wire as indicated by the red box

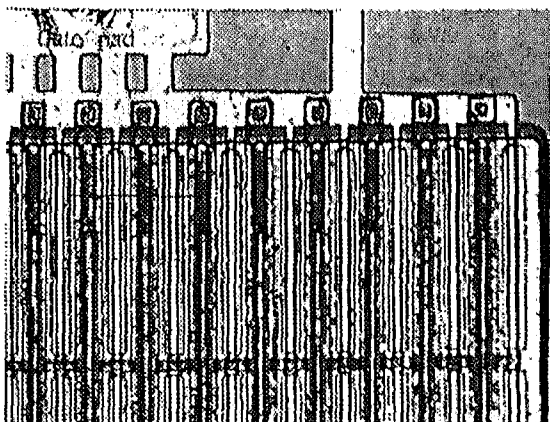


Figure 20 : Optical view of *B* MRF19030 die finger where the cross-sectioning was conducted utilizing FIB to understand the die cross-section structure. The cross-sectioned finger is conducted between the GATE wire and DRAIN wire as indicated by the red box

SEM were later conducted on the cross-section area of both *A* ( Figure 21 ) and *B* die (Figure 22) to observed the details of the die. Prior to that both the cross-sectioned die were chemically stained for a few seconds using Wright etch to highlight the die boundaries.

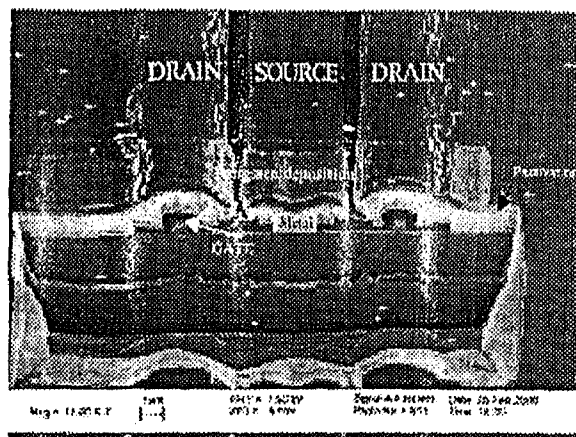


Figure 21 : SEM micrograph of *A* 10035 cross-sectioned die magnified at 12000X showing the junction details. Take note that tungsten was deposited on top of the passivation layer for edge protection during FIB cross-sectioning. This die uses only 1 metal scheme.

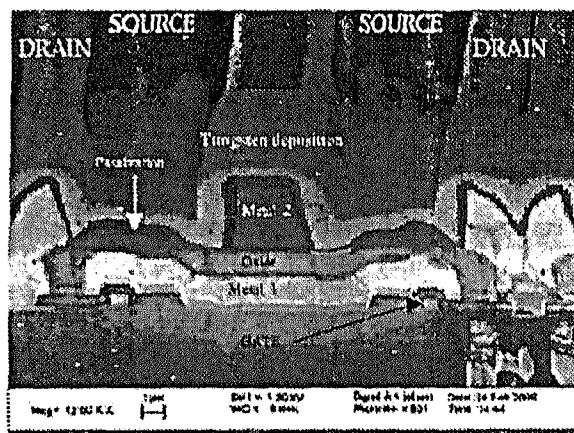


Figure 22 : SEM micrograph of *B* MRF19030 cross-sectioned die magnified at 12000X showing the junction details. Take note that tungsten was deposited on top of the passivation layer for edge protection during FIB cross-sectioning. This die uses 2 metal scheme

Some measurements were also done on the metal thickness, gate length thickness and width. Figure 23 depicts the *A* die cross-section measurements and Figure 24 depicts the *B* die cross-section measurements.

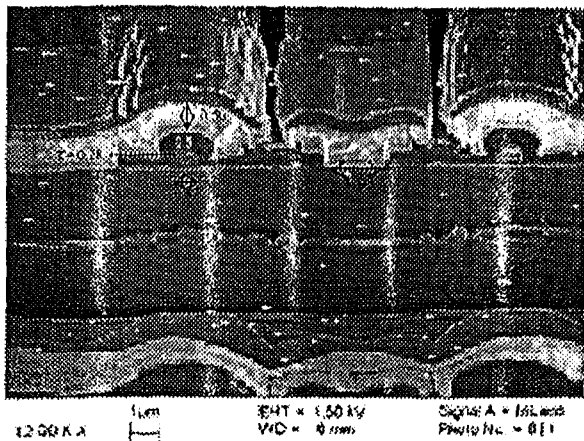


Figure 23 : SEM micrograph of *A* 10035 cross-sectioned die magnified at 12000X showing the junction details with dimension included. All dimensions are in microns. This die passivation layer thickness is 0.37 microns

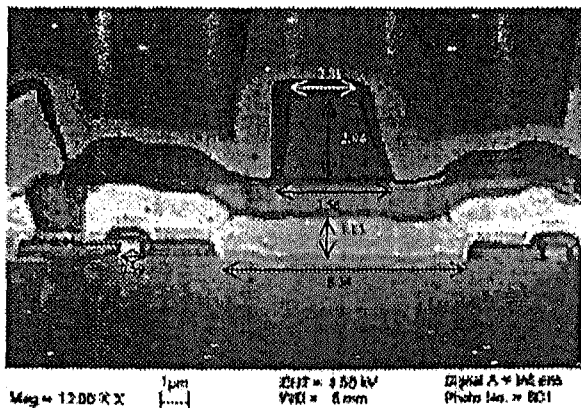


Figure 24 : SEM micrograph of *B* MRF19030 cross-sectioned die magnified at 12000X showing the junction details. All dimensions are in microns. This die passivation layer thickness is 0.47 microns

## 6.0 CONCLUSION

The constructional failure analysis has successfully identified several features incorporated in *A* 10035 device as compared to *B* MRF19030 device. Those differences are outlined as below:-

1. The numbers of MOSCAP, where *A* utilizes only a single MOSCAP as compared to three for *B* device
2. *A* device uses gold wire as compared to aluminum wire for *B* device
3. There were differences in *A* and *B* device construction pad layout where *A* have a smaller and individual bond pad for gate and drain wire as compared

to *B* that requires bigger bond pad size and each drain pad shares the same drain bonding pad

4. *A* die thickness thinner(4.46 mils) as compared to *B* having a thickness of 5.93 mils
5. *A* have a bigger die active area(37.80 mils) as compared to *B* die having a thickness of 7.47 mils.
6. *A* die does not have any ESD protective circuit as compared to *B* die.
7. EDX analysis on *A* die passivation indicated that it is passivated with silicon nitride while *B* die is passivated with silicon oxide.
8. From the die cross-sectioning it is noted that *A* die uses only one metal layer scheme as compared to two metal layer scheme for *B* die
9. From the die cross-sectioning, it is noted that the gate length for *A* die is shorter (0.50 microns) as compared to 0.59 microns for *B* die. *A* gate thickness is also thinner(0.28 microns) in comparison to *B* gate thickness of 0.44 microns.

These form of analysis helps package and die benchmarking team to improve our existing device. The paper is published in Quality Labs Quarterly Knowledge Presentation Web Site and circulated to *B* operation. and Wireless Infrastructure System Division(WISD) Packaging Benchmarking Team.

## ACKNOWLEDGMENTS

Special thank you to *C* for SEM and EDX training. *D* and *E* for FIB operation training and assistance. Thank you also to all Failure Analysis personnel for assisting in the successfulness of this analysis.

## REFERENCES

- [1] Failure and Yield Analysis Handbook - Technology Associates.
- [2] Failure Analysis Report number I-TR000401H-ERICSSON10035, *F*



## 01 (Active) Bridging Defect Found on 87.5% UDR2 Technology

**ABSTRACT** - Sub-lots of SSP26311GC80 DSP device exhibited 10% pin leakage failure at hot and room tests. Failure analysis on the failed device showed that the source of the pin leakage failure was 01 (active) bridging defect found on ESD thick field transistor. Further analysis revealed that the leakage occurred from source to drain of the thick field device because of the 01 bridging. The 01 bridging happened due to the difficulty in patterning or etching the long and narrow field region between the two active areas at the wafer fabrication site, MOS11. The findings have led to a recent process improvement change in MOS11 where P01 resist process of J22A mask set with 87.5% UDR2 TLM 0.42 $\mu$ m technology has been changed. Erratic results can be seen on their class probe structure that is similar to the bridged structure in this report. The resist thickness has been reduced to help resolve the narrow spaces such as this. The change, subsequently, affects other UDR2 and CDR designs in MOS11. No 01 bridging defect has been reported since then. This paper outlines a systemic and thorough failure analysis approach in identifying the failure mechanism and describes efforts taken to help resolve the issue.

**KEY WORDS** - Digital Signal Processor (DSP) Unified Design Rules 2 (UDR2), Semi In Len Scanning Electron Microscope (SEM), Communication Design Rule (CDR), Focused Ion Beam (FIB), Electro Static Discharge (ESD), 01 Bridging.

### 1. INTRODUCTION

Six sub-lots from wafer lot, E115070 exhibited 10% leakage at hot and room tests. Ten units with pin leakage failures had been analyzed. Failure analysis done on the units revealed that the leakage failure was due to 01 bridging defect found on ESD thick

field transistor. The defect was induced during wafer fabrication process.

### 2. FAILURE VERIFICATION

The units were verified in the product analysis laboratory using a curve tracer. Curve trace results showed that leakage could be found at various pins on all of the units. Figure 1 showed a typical IV curve of leakage pin. It was noted that the leakage pins were from pins 134 to 144 (Table 1). Leakage pins that were unable to be detected by the ATE were also verified and the result revealed an early breakdown during Vdd power up process (Figure 2).

Unit	Leakage Pin
1	139 (TIX)
2	134 (IROD)
3	139 (TIX)
4	135 (IROC)
5	134 (IROD)
6	144 (SC11)
7	141 (TCK)
8	143 (SC12)
9	143 (SC12)
10	143 (SC12)

Table 1. Details of leakage pins.

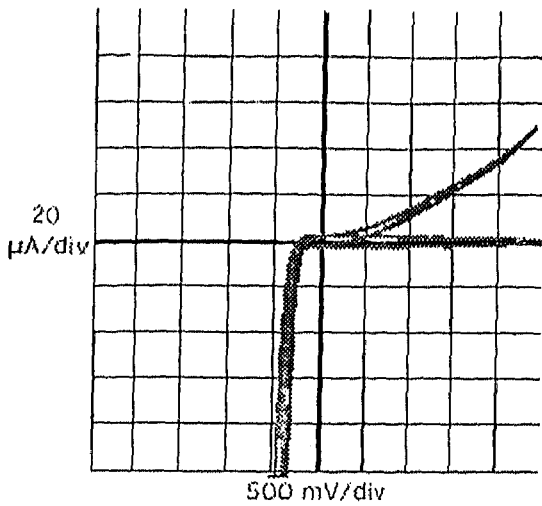


Figure 1. A typical IV curve revealed leakage on pin 139 (TDO). Similar leakage was observed on the respective failing pins. Green Curve: good unit. Red Curve: bad unit.

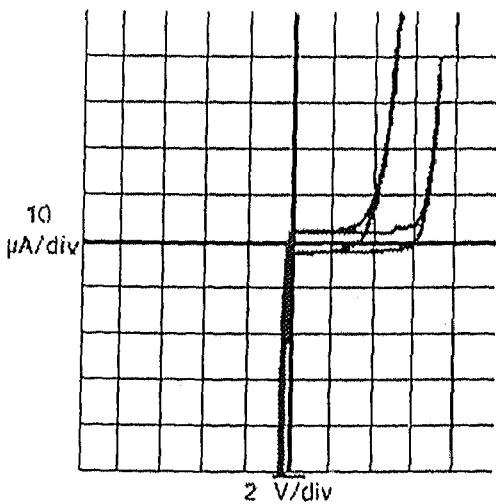


Figure 2. A typical IV curve revealed an early breakdown on pin 143 (SC12) when powered up to 3.3V. Green curve: good unit. Red curve: bad unit.

### 3. DECAPSULATION

The BGA Glob Top package was de-capsulated using the B&G Decapsulator. The package mold compound requires a mixture of fuming nitric acid and sulfuric acid to dissolve them with no residual mold compound left around the bond pads. The package was then cleaned with acetone.

### 4. VISUAL INSPECTION

The units were inspected using X-ray. No defects were observed on the die surface.

### 5. FAILURE ISOLATION- NON DESTRUCTIVE TECHNIQUES

#### 5.1 LIGHT EMISSION ANALYSIS

Light emission analysis revealed a light spot on the respective leakage pins (Figures 3 and 4).

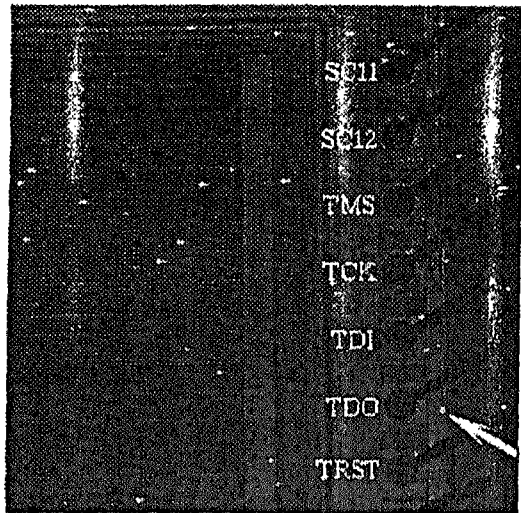


Figure 3. Light emission analysis revealed a typical light spot on leakage pin (139 - TDO) as indicated by a white arrow. Similar light emission was observed on the respective failing pins.

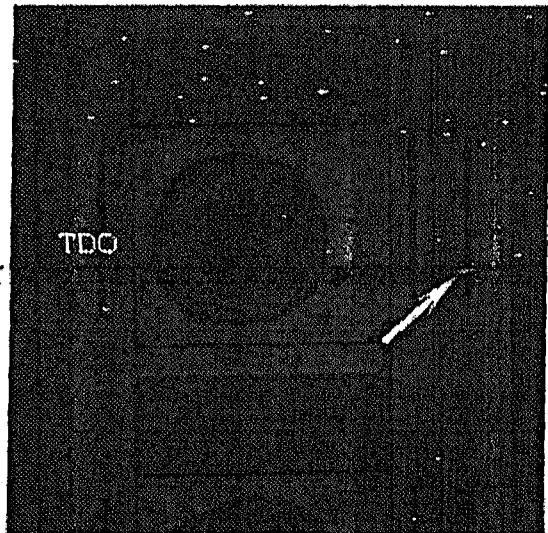


Figure 4. A close up view of the light spot on the leakage pin (pin 139 - TDO) as indicated by a white arrow. Similar light emission was observed on the respective failing pins.

#### 5.2 LAYER DEPROCESSING

Units 1, 2, 3 and 4 were de-processed and inspected layer by layer. An anomaly was found on the ESD thick field transistor of the respective failing pins (Figures 5 to 8). It was observed the defect could also be found from pins 134 to 144.

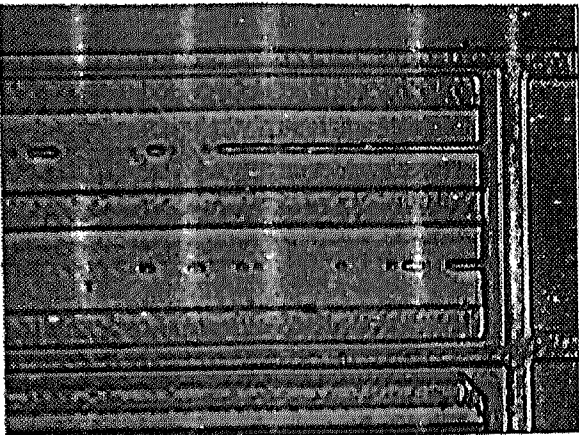


Figure 5. Optical micrograph revealed a typical anomaly on ESD protection diode where the light emitted (pin 139 - TDO). This anomaly was observed on all pins, from pins 134 to 144.

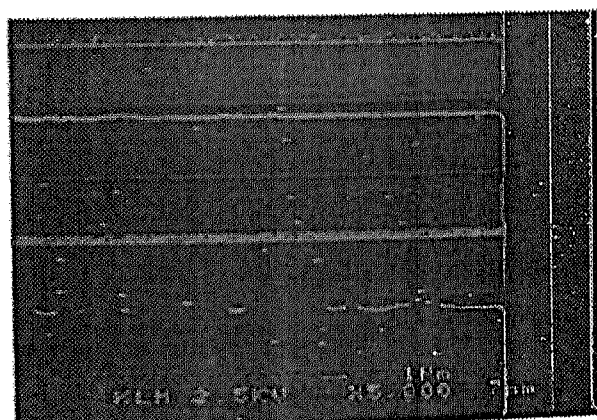


Figure 6. SEM micrograph revealed a typical anomaly on ESD protection diode where the light emitted (pin 139 - TDO). This anomaly was observed on all the pins from pins 134 to 144.

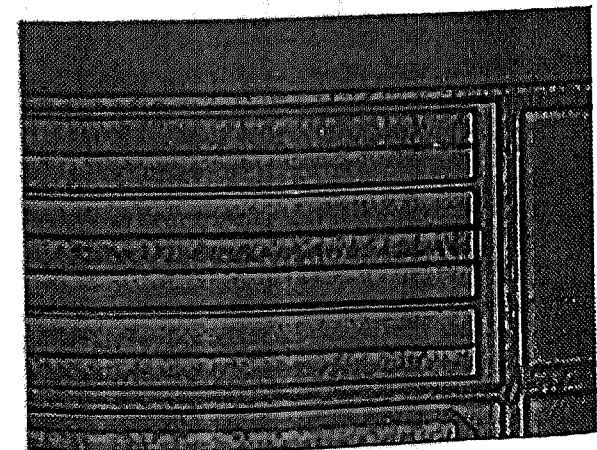


Figure 7. Optical micrograph revealed no anomaly on ESD protection diode of a correlation unit (Trace Code - XQAB9945).

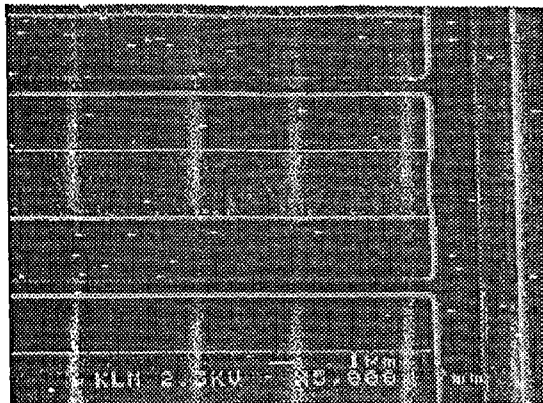


Figure 8. SEM micrograph revealed no anomaly on ESD protection diode of a correlation unit (Trace Code - XQAB9945).

## 6. FAILURE ISOLATION -- DESTRUCTIVE TECHNIQUES

### 6.1 FOCUS ION BEAM (FIB)

FIB cross-section revealed there was no groove underneath the poly lines on unit 5 as compared with good units (Figures 9 to 14). The groove in fact is the presence of field oxide. When the active areas are bridged, only gate oxide is present. Therefore, there is no field oxide, so the "groove" is not there.

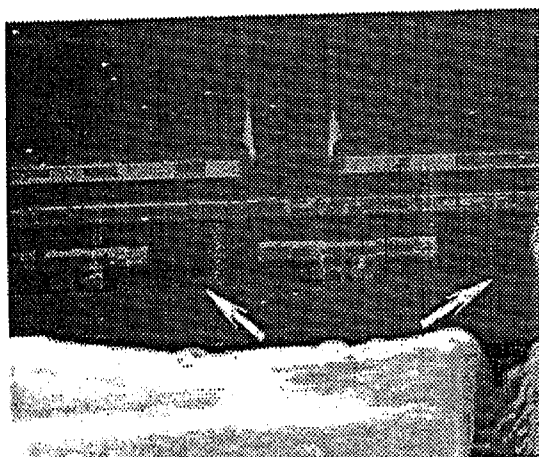


Figure 9. FIB micrograph revealed no groove underneath both poly lines as indicated by white arrows (pin 134 - IRQD).



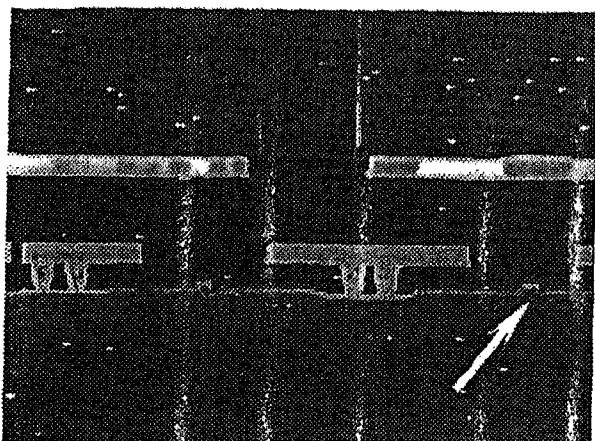


Figure 10. FIB micrograph revealed a groove underneath the left poly line but not on the right poly line as indicated by a white arrow (pin 134 -IRQD).

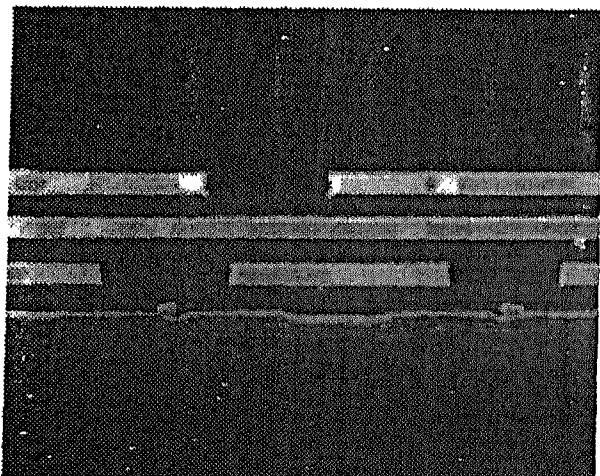


Figure 11. FIB micrograph revealed a groove underneath the poly lines on ESD protection diode of a correlation unit (Trace Code - XQAB9945).

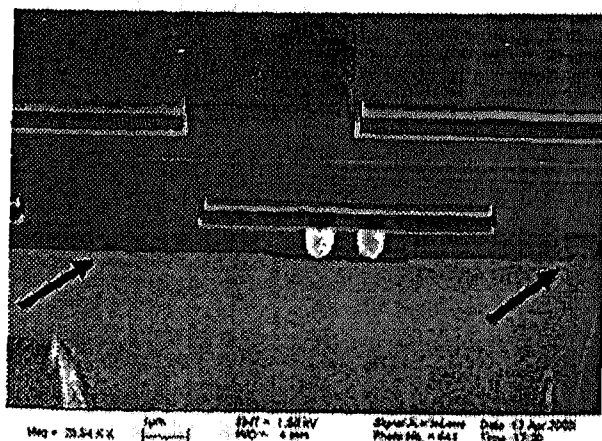


Figure 12. SEM micrograph revealed there was no field oxide underneath both poly lines as indicated by black arrows.

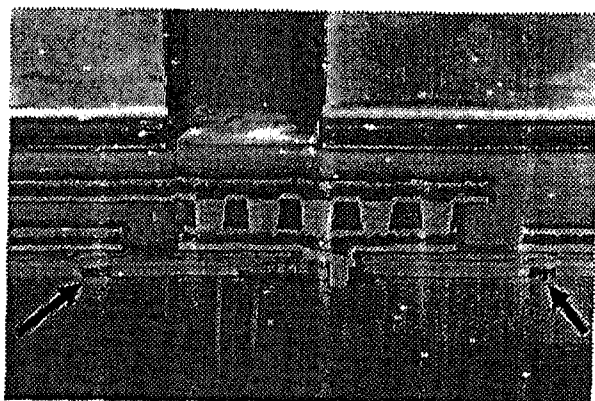


Figure 13. SEM micrograph revealed there was a field oxide underneath the poly of a correlation unit (Trace Code - XQAB9945).

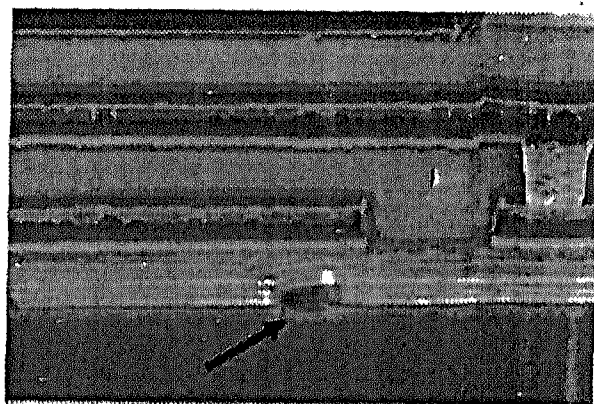


Figure 14. A close up SEM micrograph revealed there was a field oxide underneath the poly of a correlation unit (Trace Code - XQAB9945).

## 7. LAYOUT ANALYSIS

Layout analysis showed that pins 134 to 144 were from J22\_MQ\_IUP1 module. The defect site was at each of the IO01PTD5V circuit. (Figures 15 and 16).

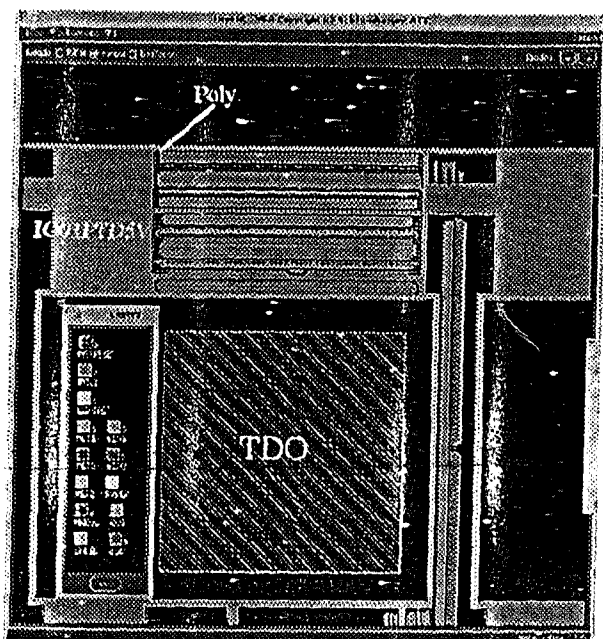


Figure 15. Die layout showed a typical pin (pin 139 - TDO) from J22\_MG\_IUP1 module where an anomaly was found on ESD thick field transistor (IO01PTD5V).

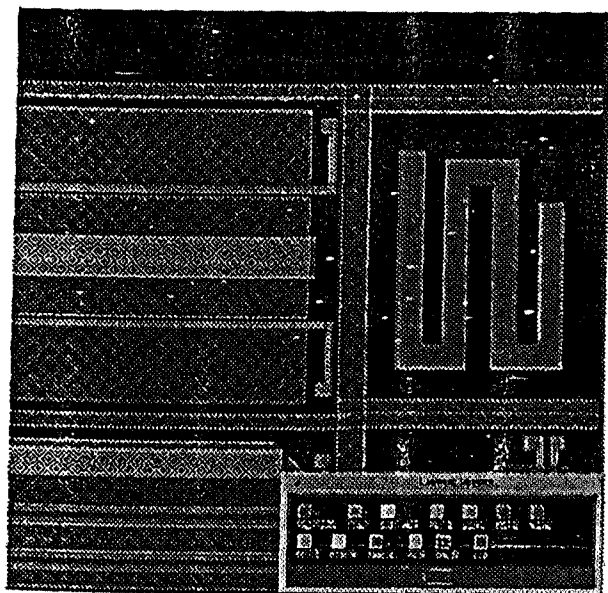


Figure 16. A close up die layout showed a typical pin (pin 139 - TDO) from J22\_MG\_IUP1 module where an anomaly was found on ESD thick field transistor (IO01PTD5V).

## 8. FACE LAPPING

In order to further examine the failure, unit 6 was face lapped close to the poly. Optical microscope revealed that the defect found on the ESD thick field appeared to be poly patterning defect (Figures 17 to 19). The poly looks like it was mis-patterned because some parts of the poly are higher than others. The poly is lowered where the bridging occurs. Two tested good units from the same wafer

lot were sampled for inspection. It was observed that one of the tested good units had similar poly patterning defect but in a lesser extent (Figure 20).

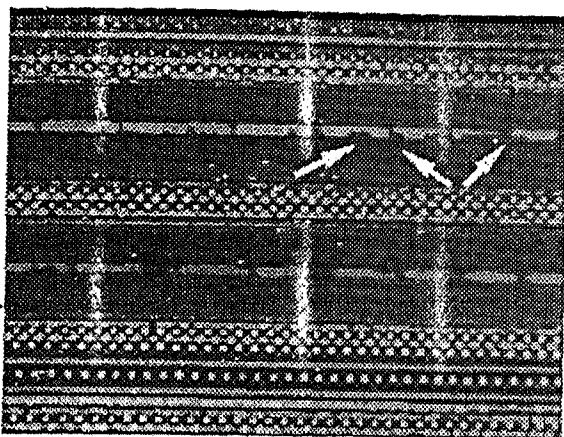


Figure 17. Optical micrograph shows the defect found on ESD thick field transistor appeared to be appeared to be poly patterning defect (pin 144 - SC11).

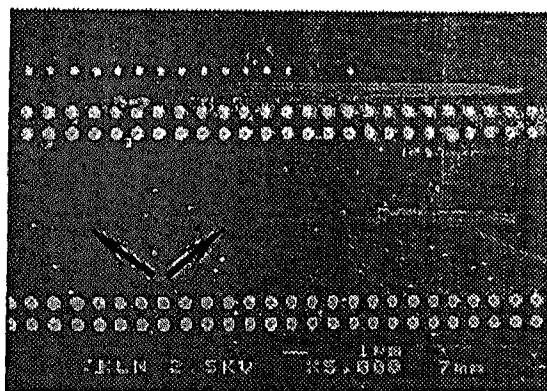


Figure 18. SEM micrograph revealed a poly patterning defect on ESD protection circuit (pin 144 - SC11).

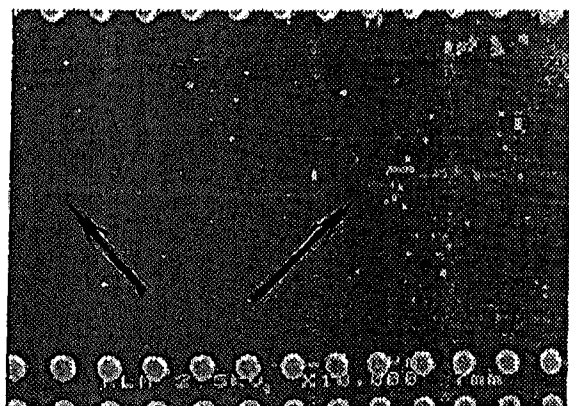


Figure 19. A close up view of the poly patterning defect on ESD protection circuit (pin 144 - SC11).

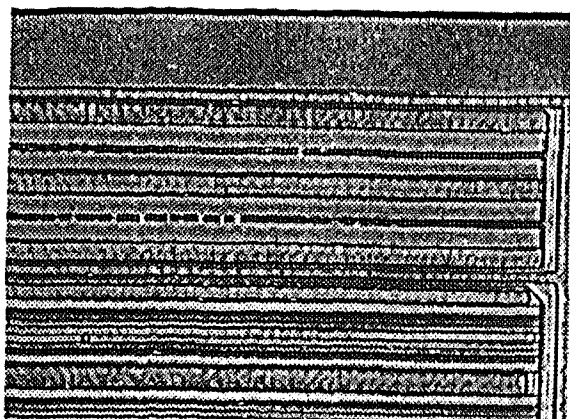


Figure 20. Optical micrograph revealed an anomaly in a lesser extent on ESD protection diode on a good unit from the same wafer lot, E115070. This anomaly was observed on most of the pins from 134 through 144.

## 9. FURTHER DISCOVERIES

Extra effort was taken to further understand the defect from MOS11. The defect found is termed as O1 (active) bridging. The O1 bridging occurs due to the difficulty in patterning or etching the long and thin field region between the two active areas. Small variations in the lithography tool focus or resist thickness can cause the problem to appear. In order to resolve the issue, the resist thickness was reduced.

## 10. RESULTS

This is a successful product analysis to directly determine the cause of this high leakage failure. Key to this finding is O1 bridging defect. The method was formulated in KLM product analysis lab. This showed the O1 bridging defect clearly. The product analysis findings have led to several process improvements especially in helping MOS11 to identify the defect due to patterning or etching issues. No failure of the same nature was reported since then. The method used during the analysis to remove the residual mold compound left around the bond pads on BGA Glob Top packages was fan out to IES, WSSG and NCSG Failure Analysis Groups in Oak Hill and Toulouse. The documentation is available on the compass web site as part of the knowledge sharing process.

## 11. CONCLUSION

The methodological product analysis approach has successfully identified the O1 (active) bridging failure. The use of an innovative method to de-capsulate BGA Glob Top package enables light emission analysis to be performed to identify the leakage spot. The key finding which relates to the

O1 (active) patterning process has led to several process improvements. The two main areas identified that need improvements are probe test and wafer fabrication processes. It was discovered that the probe program for mask set 4J22A was having a test coverage issue. A discussion on updating the test program has taken place. It was concluded that with the advent of the new mask set OK36A, mask set 4J22A was to be eliminated and a more robust probe test program is envisioned. A new type of resist which will have an increased depth of focus from current process of 0.8 - 1.0 $\mu$ m to 1.2 - 1.5 $\mu$ m is to be implemented. This increased depth of focus will result in increased resolution capability.

## **APPENDIX C**

### **THE QUESTIONS OF INTERVIEWS WITH THE SENIOR PROCESS ENGINEERING MANAGER**

1. Do the Chinese and Malaysian engineers communicate in English with superiors, colleagues, and subordinates?
2. What post are the Chinese and Malaysian engineers holding and what departments are they attached to?
3. How long have the Chinese and Malaysian engineers been working for this multinational organization?
4. How many engineers among the Chinese and Malaysian engineers studied overseas?
5. How often do the Chinese and Malaysian engineers write technical reports?
6. For what purposes do the Chinese and Malaysian engineers write technical reports?

C2

## **No PMC Study on SOIC28WB Package with Fast Cure Molding Compound**

## Background

As we know, PMC process has much contribution to our assembly cycle time as well as it to the quality of our products. Many investigations are being performed aiming to eliminate this process. TJ plant had passed the BOM standardization qualification with No PMC process on 08/14/16 last year and no additional process was required. Molding compound used in the material is MP8000 series and EME6600CS series which are both categorized in fast cure. For SOIC28WB, same project will be launched. Before this, we have to determine if we can eliminate PMC or how many hours it can be shortened through study on compound properties based on current process.

In the industry, we must go through the validation test for major process/material change. In other words, we must pass reliability test. The reliability performance has close relation to the mechanical interaction between the plastic package and the silicon device it surrounds. Thermal expansion, dynamic modulus and adhesion studies are used to describe this interaction. So, our investigation was divided into two stages, one is compound properties comparison between PMC and No PMC, another is the reliability test.

## Performance of Molding Compound Before and After Postcure

Due to the high glass filler content of the IC encapsulant compound are very stiff, high modulus, brittle material. Although the coefficient of expansion for this type of material is low, the combination of high curing temperature and high modulus can lead to serious thermally induced stress that can damage the silicon device or result in cracking of the epoxy package during temperature cycling. Any fissure in the IC package can provide a path for the ingress of moisture contaminants that can cause failure of the device. Thermally induced stress can also cause adhesive bond failure between the epoxy and the copper lead frame, which allows another means for moisture to reach the device. Therefore, the heat history is very important in order to get elements with high reliability. Economics is the driving force behind industry interest in no postcure epoxy packages. At the same time, microelectronic performance requirements remain high. Thus, these key characteristics need special scrutiny regarding to no-postcure and postcure.

The study is mainly on comparing the performance of molding compound before and after postcure. Four types of commercial molding compound were selected for evaluation and categorized as A, B, C, M. A, C and M are all belong to fast cure family.

and analysis (I) - effect on Tg

es epoxy chemistry, its heat history is an important crosslink factor. Up to 95% of al crosslinks may be established during molding of integrated circuits. Additional link occurs during postcuring of molded parts in an oven for 4-16 hours. Mold and ure temperature may vary form 160 - 190degree. Most often, postcure conditions of 2-8 at 170degree are employed.

e 1 and Fig. 1 presents Tg data versus postcure time. It is always significantly higher postcure. Therefore, high Tg-specification generally can not be served without postcure.

Table 1 postcure effect on Tg

Table 1 Postcure effect on Tg

cure condition	Tg degree			
	A	B	C	M
NPMC	103	129	130	111
170@2 hrs	127	154	142	132
170@4hrs	149	167	149	155

ark: Tg is measured by DMA which is defined the temperature at the peak of the tan delta.

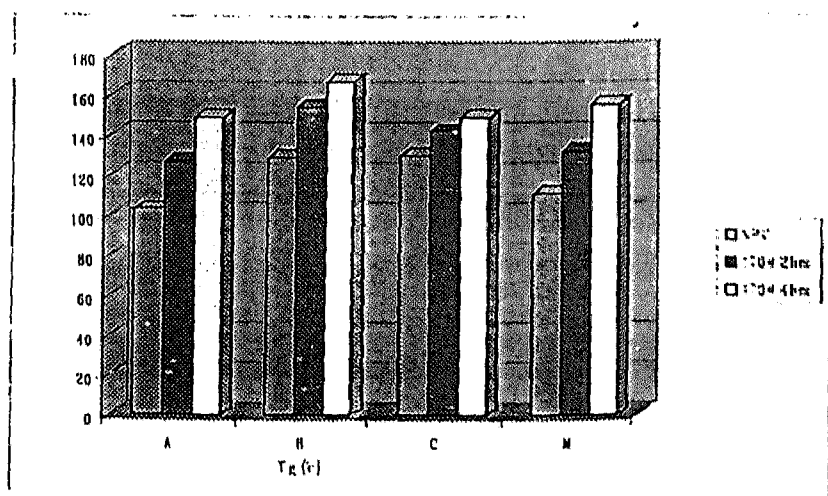


Fig. 1 The postcure effect on Tg



## and analysis (2) - effect on adhesion properties

Importance of good adhesion of the epoxy to the silicon device for excellent package crack was discovered as the result of a special test design to simulate the stress concentrations at chip corners to observe epoxy cracking. If there is good epoxy-silicon adhesion, the thermal stress that develops at low temperature in the element of epoxy will couple into the silicon. However, if there is poor adhesion over the surface leading up to the corner, the stress in the element no longer couples into the silicon but will cause an increase in the stress at the corner.

As shown in table 2 and Fig. 2, the effect of postcure on adhesion to metal lead frames is dependent on the compound type. The adhesion of Molding compound A with postcure to copper leadframe was found lower than that of no-postcure, while Molding compound C had higher adhesion to copper leadframe after postcure.

Table 2 Postcure effect on adhesion to Copper lead frame

Table 2 Postcure effect on adhesion to cu lead frame

cure condition	adhesion(kgf)	
	A	C
NPMC	129	111
170@2hrs	167	155

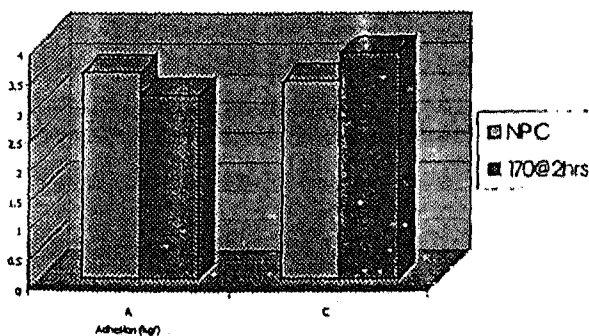


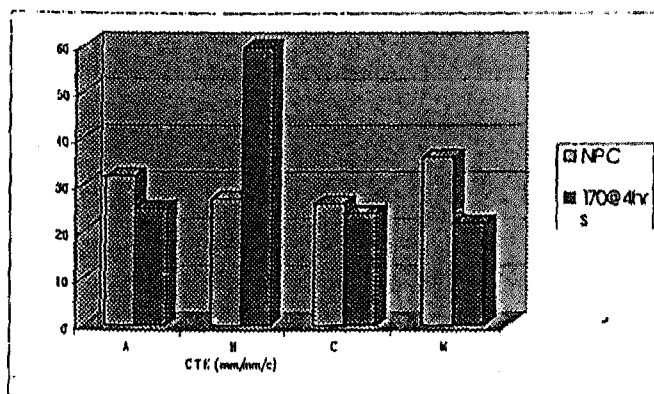
Fig. 2 Adhesion to cu lead frame

### and analysis (3) - effect on CTE

coefficient of expansion (CTE) are generally governed by filler type and level, not by postcure conditions. As displayed in Table 3 and Fig. 3, however lower CTE after postcure have been noticed except B.

Table 3 Postcure effect on CTE(25 - Tg)

cure condition	CTE (mm/mm/degree)			
	A	B	C	M
NPMC	32	27	26	36
170@4hrs	25	60	24	22



### 3 Coefficient of thermal expansion of no-postcure versus postcure

### and analysis (4) - effect on moisture absorption

fully cured by various mechanical measurements, there remains, in fact, a measurement of unreacted epoxy groups. This phenomenon, we believe, has its origin in the physical constraints in highly crosslinked networks that render inaccessible to a fraction

groups during the final stages of cure. The postcure step in the stoichiometric and rich formulations caused an additional crosslink.

Effect of postcure on moisture absorption depends on its moisture condition. Moisture uptake in Fig. 4 and table 4 showed that postcure increase moisture absorption. The phenomenon has been explained an increase in free volume with postcure.

Table 4 Postcure effect on moisture absorption

(dipped in deion water at room temperature for 10 days)

cure condition	Moisture Absorption(%)			
	A	B	C	M
NPMC	0.66	0.13	0.16	0.55
170@4hrs	1	0.18	0.28	0.68

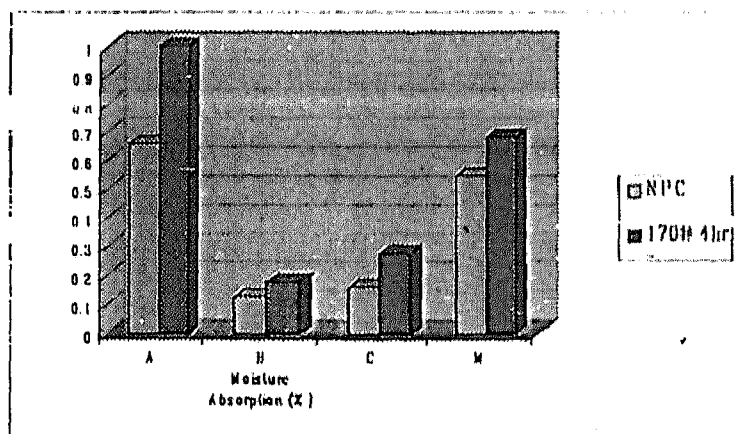


Fig. 4 Moisture absorption of no-postcure versus postcure

Table 5 Postcure effect on moisture absorption

(Exposure to hast 85degree/85% RH)

cure condition	Moisture Absorption(%)	
	A	C
Cured at 180°C /40s	0.33	0.41
Cured at 180°C /60s	0.43	0.56
2hrs PMC 40s	0.39	0.55
4hrs PMC 40s	0.47	N/A

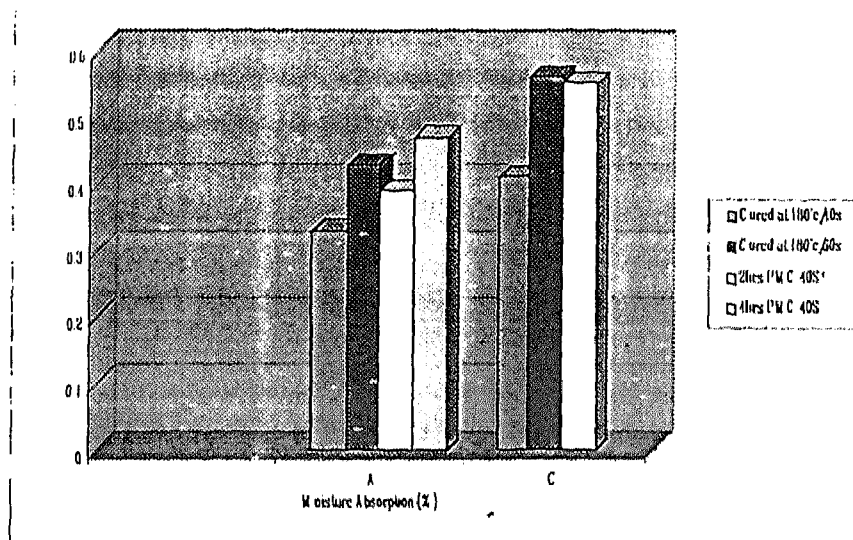


Fig.5 Moisture absorption of no-postcure versus postcure

analysis (5) - effect on modulus

As the CTE, the modulus is governed by the filler content, since filler is the predominant ingredient with a high modulus in the order of 69Gpa(10Mpsi), compared to only 0.5Gpa(0.5Mpsi) for the organic portion of the compound.

Table 6 Postcure effect on storage modulus

cure condition	Storage Modulus(Gpa)			
	A	B	C	M
NPMC	13.5	4.9	12.6	10.5
170@2hrs	12.9	5.4	12.8	12.6
170@4hrs	12.4	4.9	14	11.4

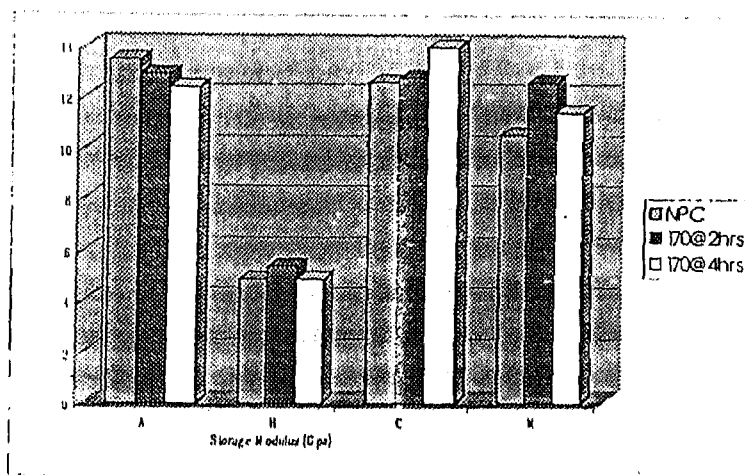


Fig.6 The effect of postcure on storage modulus

Table 7 Postcure effect on flexural strength

cure condition	Flexural Strength(Kgf/mm <sup>2</sup> )			
	A at 140°C	A at 170°C	C at 190°C	C at 240°C
PMC 2 hrs	2.1	1.13	0.82	0.75

### Reliability Performance Evaluation

on above investigation on molding compound, we build 7 lots with different molding condition to compare the impact of no-postcure and postcure process on IC reliability performance. The different molding conditions are as following:

Compound type	in mold cure time	post mold cure time
C	60s	0 hour
	40s	0 hour
	40s	2 hours
A	60s	0 hour
	40s	0 hour
	40s	2 hours
	40s	4 hours

Compound C&A are both fast cure type. Vendors recommended that they have the capability achieve no postcure process but this also depend on molding condition in user's pr

evaluation was aimed to choose appropriate molding condition for further no or less qualification on SOIC28 wide body. One type of micro controller MC68HC705P6 was vehicle for this evaluation.

Reliability is the probability that a semiconductor device will perform its specified function in environment for a specified period of time. In other words, reliability is quality over environmental conditions.  $\beta$  has always stressed reliability and quality considerations in designing any new product and developing new process.

There was no expectation this time. But, how to choose reliability test for this evaluation? It has been found and is not necessary for us to finish a full reliability test table designed for a formal qualification. According to the requirements of AEC-Q100 & MIL-standards, we choose AUTOCLAVE) and HAST(pressure-Temperature-Humidity-Bias) as the test items.

Condition of PTH: 121degree, 15psig, 100% relative humidity, 144hours.

Condition of HAST: 85%RH/121degree/15psig plus abias level which is the nominal rating of device.

For surface mount package, preconditioning process is required before standard environment test is performed. The procedure for preconditioning test is as following:

245 degc; 10cycles) --->Backing (125degc; 24hrs) --->T(85degc/85%RH; 168hrs)  
R(245 degc)

According to AEC-Q100, pre and post stress electrical test must be performed on samples at cold and hot temperature.

Reliability result:

HAST	(245 degc) precondition	precondition	pass
		48hrs	pass
		96hrs	pass
PTH	(245 degc) precondition	precondition	pass
		96hrs	pass
		144hrs	pass

Conclusion

Through above investigation on compound properties, we have further understanding upon the different compound that we are using. To some aspect, we can see there is no significant difference between after and before PMC to fast cure type compound. In the other hand, the compound vendors had their products achieved low stress by rubber type elastomer, achieved reliability by special additive, and so on. This can offset the influence of no-PMC process to some extent. And all lots under different molding condition smoothly went through chosen

ility test with no failure was detected. This gives us more confidence on qualifying no  
process on SOIC WB package.

## Failure Analysis: Signal Conditioner Key Off Timer Issue

**ABSTRACT (Helvetica 10 Bold)** - This report details the failure analysis (FA) procedures conducted in response to a wafer probe yield loss of about 5% at MOS8 for the past one year. The estimated cost impact is about US\$250K/year. Microprobing has narrowed the failure site down to faulty flip flop in the Key Off Timer Circuitry. Electrical characterization leads to the discovery of open metal 2 to metal 1 via. Using advanced FIB tungsten deposition, detailed verification of failure can be reconfirmed. Specific defect information was relayed back to the fab so that corrective actions could be pursued.

**KEY WORDS** - KOT, Open Via, FIB

### INTRODUCTION

Mos 8 five inch wafer probe test was having about 5% yield loss due to Key Off Timer (KOT) failure for the past one year. The estimated cost impact is about US\$250K/year. Wafer mapping performed revealed, positional fallout at the bottom of the wafer. The probe failure samples were assembled and tested, confirming the KOT failure. Three units from probe failure samples were submitted for analysis. A thorough and systematic analytical approach leads to the identification of the root cause was due to open metal 2 to metal 1 via. The use of advanced Focus Ion Beam (FIB) tungsten deposition tool enabled detailed verification of the failure. Specific defect information was relayed back to the fab for corrective action.

### ANALYSIS

Curve tracing on all units showed no anomaly. X-ray analysis did not show any wirebond anomaly. Three units were verified to fail Key Off Timer tests using the bench test setup. The setup involves sending a sequence of commands to the KOT register address and then reading the return data. The failing units have the data always at \$00 to \$03. A correlation good unit has the data changing with each read ranging from \$00 to \$FF.

All units were decapsulated, visual inspection did not reveal any anomaly. Light emission analysis was performed on all units, but no light emission spot was detected. Liquid crystal analysis was unable to be performed because the liquid crystal changed state during device powerup.

S/n 1 and 2 were depassivated using Reactive Ion Etching (RIE) for microprobing. Microprobing has narrowed down the defective area to a toggle flip flop in the KOT circuitry whereby the output was stuck low instead of a clock signal. Figures 1&2 show the KOT circuitry schematic and identify the failing flip flop.

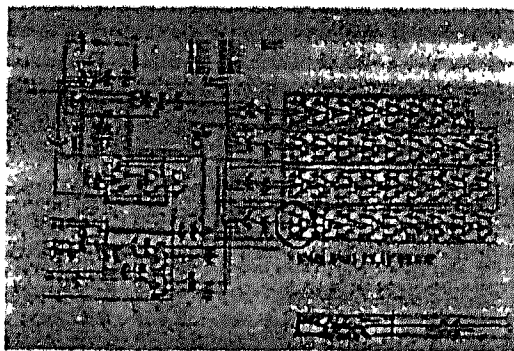


Figure 1: Key Off Timer (KOT) circuitry schematic identifying failing flip flop.

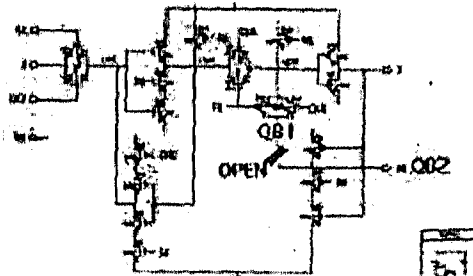
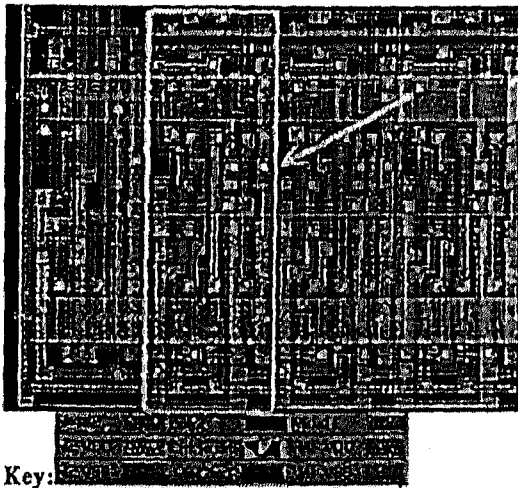




Figure 2: Detailed of the failing flip flop schematic.

Figures 3 & 4 show the partial layout of the flip flop and the probe points. Figure 5 shows the various probed signals on this flip flop. All the clock input signals to the flip flop were present. Powered curve trace was carried out at the input and output circuits of the flip flop but no anomaly was observed. Next, similar routed signals were probed and it was noted that the QB (Q Bar) output signals probed at QB1 and QB2 points were in the opposite state (see Figure 5). These two signals should be the same as QB1 and QB2 are connected through metal 2 to metal 1 via. This indicates possible open via between the two points.



Key:  
Figure 3: Partial layout of the failing flip flop - marked in red box.

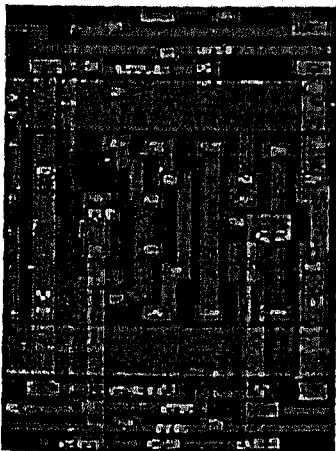


Figure 4: Layout of the failing flip flop shows the various signals. "X" indicates some of the signals that were probed. Further probing confirmed open via at QB1.

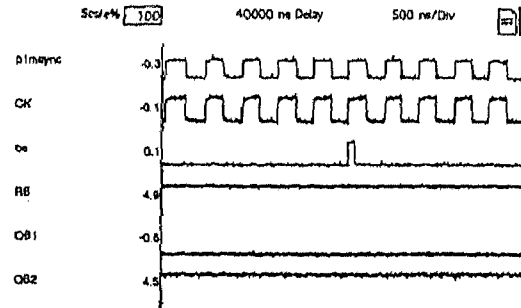


Figure 5: The various probed signals from the failing flip flop.

Focus Ion Beam (FIB) was used to open a small window down at metal 1 for probing. Curve trace confirmed an open metal 2 to metal 1 via at QB1. FIB cross sectioning was performed at the center of the open via. Voltage contrast imaging confirms that the via is open (Figure 6).

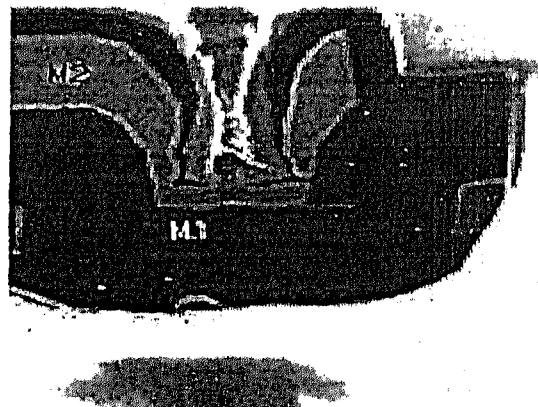


Figure 6: Voltage contrast imaging of the open via.

Figure 7 shows a correlation voltage contrast imaging on a good via. Wright etch was used to stain the sample for better imaging. Scanning Electron Microscopy (SEM) showed what was believed to be an interlevel oxide layer above the metal 1 layer blocking the via connection to it (Figure 8 and 9). Figure 10 shows a correlation good via. Both s/n 1 and 2 were found with similar failure mechanism.

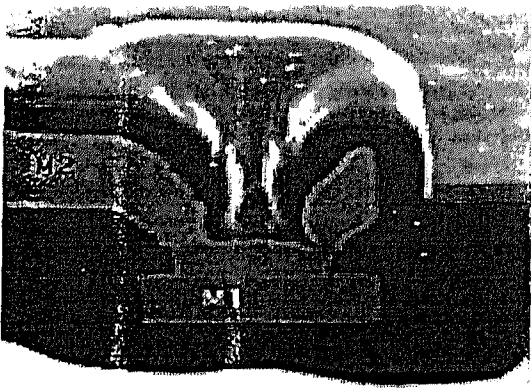


Figure 7: Voltage contrast imaging on good via.



Figure 8: SEM imaging on s/n1 shows that an interlevel oxide layer was above the metal 1 layer blocking the via forming a connection.  
Note: Passivation layer removed.

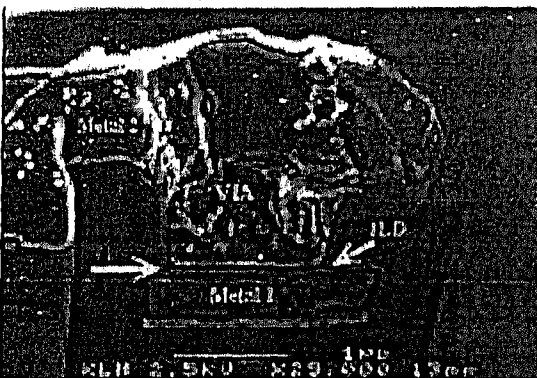


Figure 9: SEM imaging on s/n2 shows that an interlevel oxide layer was above the metal 1 layer blocking the via forming a connection.  
Note: Passivation layer has been removed.

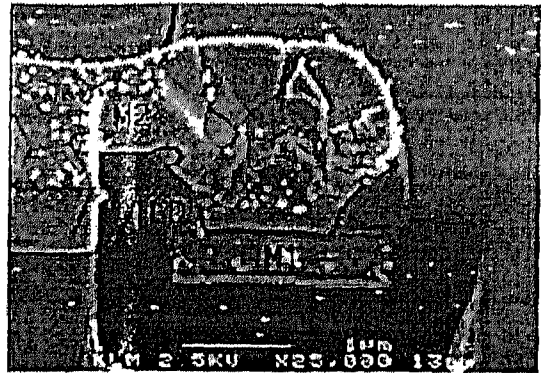


Figure 10: SEM imaging on a correlation good via.

To reconfirm the open via, FIB was used on s/n 3 to reconnect the QB signal at the failing flip flop. A verification on the bench setup showed that the unit has partially recovered. The returned read data was changing from \$00 to \$07. Hence, the next stage flip flop QB signal was suspected to be in opposite state as well. FIB was used to open probe windows on the QB signal and probing confirming another open via. FIB reconnection of the QB was performed. Verification on the bench has return read data changing from \$00 to \$0E. The unit still did not recover. The next successive stages of the flip flop were probed and reconnected until the fifth stage flip flop (Figure 11). The unit has finally recovered with the return read data changing with each read. FIB cross sectioning confirmed that all the vias were open at all five successive flip flop.

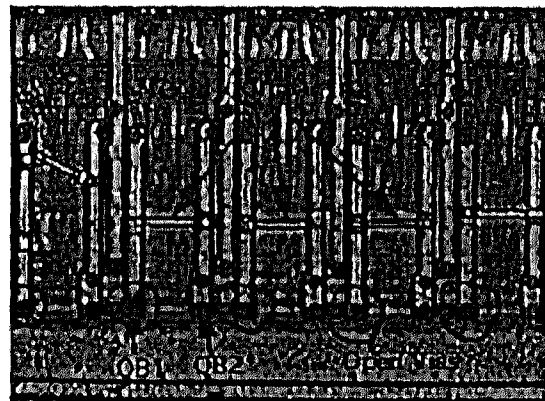


Figure 11: Image shows FIB reconnection of the QB signal on five successive stages of the flip flops. Unit has recovered. The open vias were circled in the picture.

Metal etch was done on s/n 1 to determine the presence of the interlevel oxide between metal 1 and 2 via. The results indicated that the bad via has a layer between the metal 1 and 2 via. SEM picture

clearly indicates that there has a layer separating metal 1 and 2 via (Figures 12 and 13).

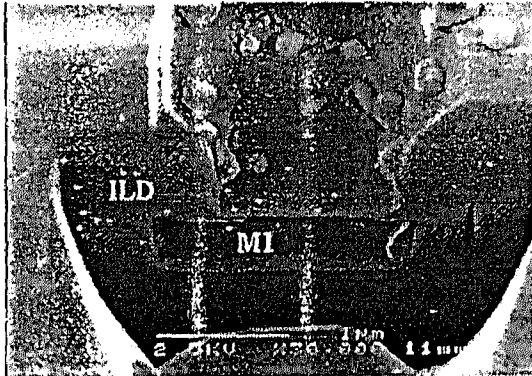


Figure 12: After metal etch, SEM image indicates that there is a layer (believed to be ILD) separating M1 and M2.



Figure 13: After metal etch, SEM image on a good via.

## CONCLUSION

This report detailed a thorough failure analysis procedure for identifying the root cause and understanding of the fail mechanism of the KOT circuitry on the signal conditioner IC. All units failed with positional open metal 2 to metal 1 via at QB signal on the flip flop in the Key Off Timer (KOT) circuitry. The cause of the open via is due to insufficient anisotropic metal 2 to metal 1 via etch. Specific defect location on die has been relayed back to the fab for corrective action. The findings has resolved a year of problem and estimated cost savings of US\$250K/year. Mos8 will be increasing the etch time after a series of DOEs on control wafers. Further investigation on the fab process is recommended.

---

# WIRE BONDING PROCESS

C1

## FINE PITCH WIRE BONDING ON 56L SDIP PRODUCTS

## BACKGROUND:

Shortly after inventing the transistor, Bell Laboratories developed a technique called thermocompression bonding. Bell then began contacting equipment designers to provide the production machines. The year was 1957.

Kulicke & Soffa Company manufactured the first commercially available bonding machines for the infant semiconductor industry. The wire bonding technique became generally applied.

Differently from the original way, today, the thermosonic welding method is the most often used way of wire bonding. It used ultrasonic energy and heat to weld the gold or copper wire from the bondpad of die to the lead of lead frame, thus, the internal connection of electronic circuit formed. Ball bonding takes its names from the shapes of the wire's end just prior to welding.

The requirements of today's high performance products have made fine pitch wire bonding a key semiconductor assembly capability. The introduction of fine pitch not only reduces the cost and raise the output, but also, make the device precision than ever before. It make it possible to bring customer more precious goods with smaller IC.

## EFFECTIVE:

To access the capability of current wirebond models available in MCEL to bond fine pitch devices, an evaluation of fine pitch wire bond on 561 SDIP conducted from Jun/98 to Aug/98. Following is the evaluation reports.

## PRODUCTION:

The evaluation divide into 3 phases, evaluation vehicle by 68H08MQ16, wire bond machine is KNS1488 TURBO and 1488 PLUS. From phase 2, 1488 TURBO is the only tested machine. By the end of phase 3, a Qual lot of XC device was conducted.

## EVALUATION FLOW:

### Phase 1:

To confirm the capability of 1488 wire bonder on handling material on 103 pad pitch, determine the important parameters.

### Phase 2:

Optimize the wire bond machine parameters for better in process responses.

### Phase 3:

Run evaluation lot by shift by operator to determine the possibility of production.

### XC Qual Lot:

Per request of B, a Qual lot was conducted for test the reliability of material.

## EVALUATION INFORMATION:

Wire bond machine:

1488 Turbo & 1488 Plus

1488 Turbo is the continuous improve program version of 1484LXQ, through redesign of the microprocessor architecture, this machine could make long, straight, low loops in 120 milliseconds.

### Evaluation schedule:

PHASE 1	PHASE 2	PHASE 3	XC QUAL
3/JUN/98	3/JUL/98	31/JUL/98	2/AUG/98

Material and lot:

Lead Frame:

H00662A507 pad size 800\*300mil

Epoxy:

SUMITOMO CRM-1078

Gold Wire:

TANAKA FA-100 SUMITOMO NL3

Mold Compound

NITTO MP8000CH

Capillary

MICROSWISS 484FD-2093-R35

Assembly Information:

Die P/N:

D5046000J55G

Die Size:

173.9\*177.9 mil

Min pitch:

103.6 micron

Pass opening:

86.2 micron

Bond Diagram

67ASE04727W

Package:

56L SDIP

EVALUATION:

ASE 1

Evaluation conducted on two model of wirebond machine 1488plus and turbo, W is Sumitomo NL3, the experiment is debugged in two sections:

\*Parameters set for 1488 plus:

	First bond (1488)	Second bond (turbo)
Pre-head time	190 msec	190 msec
Bond site time	200 msec	200 msec
Tip offset	50 tenth-mil	50 tenth-mil
Bond velocity	60 tenth-mil	60 tenth-mil
Bond time	15 msec	15 msec
Bond force	35 g	40 g
Bond power	48 mwatt	40 mwatt
Power profile	1-sqr	1-sqr
USG I/V select	1-volt	1-volt
USG delay	0	0
Warm up	0	0
Warm down	0	0
Initial force	0	0
Initial time	0	0
Force ramp time	0	0



Looping	LF2 worked		
Loop height	60	Wire size	1.0 mil
Loop factor	150 percent	Ball size ratio	1.5
Theta	45	LF4	75
Contact threshold	50	Kink height	55 tenth-mil
Delta loop	0 tenth-mil	Reverse loop	55 tenth-mil
EFO gap	15	Loop trajectory	5
Loop factor 2	10	Contact angle	0
Loop factor 3	0	Toll correction	0
Impact profile	200	Impact time	0

\* Result of 1488 plus: (g)

	MAX	MIN	AVLR	RANGE	S	Cpk
Wire pull	11.0	7.5	9.1	3.5	.8	2.13
Ball wear	46.3	29.7	35.8	16.6	4.0	1.73
Wire wear	8.5	5.5	7.1	3.0	.62	1.67

Other data such as wire sweep and die shear are under spec

\* Parameters set for 1488 turbo:

	First bond (max)	Second bond
Pre head temperature	190 deg C	190 deg C
Bonding temperature	200 deg C	200 deg C
Tip offset	60 tenth-mil	60 tenth-mil
Bond velocity	10 tenth-mil	10 tenth-mil
Bond time	15 msec	20 msec
Bond force	35 g	40 g
Bond power	33 mwatt	40 mwatt
Therm profile	1-sqr	1-sqr
USG IV select	1-volt	1-volt
USG delay	0	0

Looping	LF2 worked		
Loop height	60	Wire size	1.0 mil
Loop factor	150 percent	Ball size ratio	1.5



Theta	23	LF4	35
Contact threshold	50	Kink pitch	55 tenth-mil
Delta loop	-30 tenth-mil	Reverse loop	55 tenth-mil
EFO gap	15	Loop trajectory	5
Loop factor 2	10	Contact angle	0
Loop factor 3	0	Tok correction	0
Impact profile	200	Impact time	2

\* Result of 1488 turbo: (g)

	MAX	MIN	AVER	RANGE	S	Cpk
Wire pull	9.8	7.5	8.7	2.3	0.53	2.95
Ball shear	35.6	24.3	29.1	11.3	2.79	1.68
Wire feed	8.3	5.8	6.9	2.5	0.55	1.76

Result of ball placement: (micron)

Bx	69.95	Sx	1.06	Tx	2.13	Cx	4.42
By	67.95	Sy	1.06	Ty	0.62	Ty	1.59
Cpk(X)	0.52			Cpk(Y)	1.64		

Bx: Ball size (x)

Sx: Ball size std dev (x)

By: Ball size (y)

Sy: Ball size std dev (y)

Tx: Target error

Cx: Target error std dev (x)

Ty: Target error

Cy: Target error std dev (y)

The result shows that: besides the ball placement, other data all above the requirement of spec. Further evaluation needed for improve the ball placement performance.

## ASE 2:

Second phase evaluation emphasized on improving the performance of ball placement, with two kind of wire Tanaka FA type Sumitomo NL3 type.

\* Parameters set for 1488 turbo:

	First bond	Second bond
Pre head temperature	190 deg C	190 deg C
Bond site temperature	200 deg C	200 deg C
Tip offset	70 tenth-mil	70 tenth-mil
Bond velocity	6 tenth-mil	6 tenth-mil
Bond time	20 msec	15 msec
Bond force	35 g	40 g
Bond power	40 mwatt	40 mwatt
Power profile	1-sqr	1-sqr
USG I/V select	1-volt	1-volt
USG delay	0	0

Looping:	LF2 worked		
Loop height	50	Wire size	1.0 mil
Loop factor	140 percent	Bond site	1.85
Theta	23	LF4	50
Contact threshold	40	Kink height	50 tenth-mil
Delta loop	-30 tenth-mil	Reverse loop	55 tenth-mil
EFO gap	10	Loop trajectory	5
Loop factor 2	10	Contact angle	0
Loop factor 3	0	Tol correction	0
Impact profile	80	Impact time	2

Compare with phase 1, the most important parameters of bond force, bond time, and bond power were changed as same with impact profile

\* Result of Sumitomo NL3 (g)

	MAX	MIN	AVER	RANGE	S	Cpk
Wire mil	10.3	7.0	8.5	3.3	0.89	

Ball shear	35.9	26.5	30.5	9.4	1.99	1.76
Wire pier	7.5	5.3	6.4	2.2	0.56	1.42
Loop height(mil)	8.82	7.34	8.25	1.48	0.27	N/A
Ball height(mil)	0.66	0.48	0.55	0.18	0.06	N/A

Result of ball placement: (mil)

Bx	2.69	Sx	0.08	Tx	0.06	Cx	0.04
By	2.63	Sy	0.06	Ty	0.10	Ty	0.10
Cpk(X)	0.52			Cpk(Y)	1.64		

Bx: Ball size(x)

Sx: Ball size std dev(x)

By: Ball size(y)

Sy: Ball size std dev(y)

Tx: Target error

Cx: Target error (mil)(x)

Ty: Target error

Cy: Target error (mil)(y)

\* Result of Sumitomo FA type (g)

	MAX	MIN	AVG	RANGE	S	Cpk
Wire pier	9.5	6.5	8.2	3.0	.71	1.95
Ball shear	38.5	26.7	31.2	11.8	2.65	2.1
Wire pier	6.8	5.0	5.9	1.8	.41	1.55
Loop height(mil)	8.7	7.2	8.0	1.5	.28	N/A
Ball height(mil)	0.6	0.4	0.5	0.1	0.04	N/A

Result of ball placement: (mil)

Bx	2.75	Sx	0.07	Tx	0.06	Cx	0.05
By	2.61	Sy	0.07	Ty	0.13	Ty	0.06
Cpk(X)	1.00			Cpk(Y)	1.09		

Bx: Ball size(x)

Sx: Ball size std dev(x)

By: Ball size (y)  
Tx: Target error  
Ty: Target error

Sy: Ball size (m) (y)  
Cx: Target error (m) (x)  
Cy: Target error (m) (y)

Result shows that the Cpk of ball placement were improved compared with phase 1, the difference between were reduced.

### PHASE 3 and XC Qualification lot

With the same parameters set as phase 2, the third evaluation lot was released to production line besides F/E process, the assembly data tests were taken also

The operation of the lot was conducted by production line operators instead of engineers in phase 1 and 2, the purpose is to examine the capability of process.

Since the Gold wire of FA type shows the same performance with NL3 type, and FA type is the qualified G/W in TianJin plant, we used only FA type in phases 3 and qualification.

### \* Result of Phase 3: (g)

	MAX	MIN	AVER	RANGE	S	Cpk
Wire mill	9.3	7.5	8.4	1.8	0.45	3.26
Ball shear	37.4	25.6	30.5	11.8	2.98	1.73
Wire roover	8.0	5.3	6.9	2.7	0.56	1.76
Loop height (mil)	8.48	7.20	7.86	1.28	0.23	N/A
Package warpage (mil)	2.9	2.7	2.8	0.2	N/A	N/A
Plating thickness (u-inch)	581.18	410	170	494	N/A	1.72
Composition (%)	84	80	4.02	82.7	N/A	2.37
Solderability	Pass					
Physical dimension test	Pass					

### Result of ball placement: (mil)

Bx	2.64	Sx	0.06	Tx	0.02	Cx	0.00
----	------	----	------	----	------	----	------

By	2.57	Sy	0.06	Tx	0.01	Ty	0.07
Cpk(X)		1.51		Cpk(Y)		1.47	

\* Result of Qualitor: (g)

	MAX	MIN	AVER	RANGE	S	Cpk
Wire mill	8.8	7.3	8.1	1.5	0.39	>3
Ball shear	38.7	26.0	31.4	12.7	3.19	1.71
Wire neck	8.0	6.0	7.1	2.0	0.49	2.11
Loop height (mil)	8.06	7.02	7.67	1.04	0.25	N/A
Package warpage (mil)	2.94	2.15	2.628	0.79	N/A	N/A
Plating thickness (u-inch)	581.1	410.8	170.38	494	3.1	1.72
Composition (%)	84.24	80.22	4.02	82	3.27	2.37
Solderability	Pass					
Physical dimension test	Pass					

Result of ball placement: (mil)

Bx	2.68	Sx	0.05	Tx	0.02	Cx	0.06
By	2.67	Sy	0.06	Ty	0.06	Cy	0.04
Cpk(X)		1.42		Cpk(Y)		1.52	

Bx: Ball size (x)  
 By: Ball size (y)  
 Tx: Target error  
 Ty: Target error  
 Sx: Ball size standard deviation (x)  
 Sy: Ball size standard deviation (y)  
 Cx: Target error standard deviation (x)  
 Cy: Target error standard deviation (y)

Result shows significant improve of ball placement Cpk, the trial run of production is successfully.

Following analysis will show the Cpk trend of the three phase evaluations and XC Qualitor.

By	2.57	Sy	0.06	Tx	0.01	Ty	0.07
Cpk(X)		1.51		Cpk(Y)		1.47	

\* Result of Qualitor: (g)

	MAX	MIN	AVER	RANGE	S	Cpk
Wire pull	8.8	7.3	8.1	1.5	0.39	>3
Ball shear	38.7	26.0	31.4	12.7	3.19	1.71
Wire pier	8.0	6.0	7.1	2.0	0.49	2.11
Loop height(mil)	8.06	7.02	7.67	1.04	0.25	N/A
Package warpage(mil)	2.94	2.15	2.628	0.79	N/A	N/A
Plating thickness(u-inch)	581.1	410.8	170.38	494	3.1	1.72
Composition(%)	84.24	80.22	4.02	82	3.27	2.37
Solderability	Pass					
Physical dimension test	Pass					

Result of ball placement: (mil)

Bx	2.68	Sx	0.05	Tx	0.02	Cx	0.06
By	2.67	Sy	0.06	Ty	0.06	Cy	0.04
Cpk(X)		1.42		Cpk(Y)		1.52	

Bx: Ball size(x)

Sx: Ball size standard deviation(x)

By: Ball size(y)

Sy: Ball size standard deviation(y)

Tx: Target error

Cx: Target error standard deviation(x)

Ty: Target error

Cy: Target error standard deviation(y)

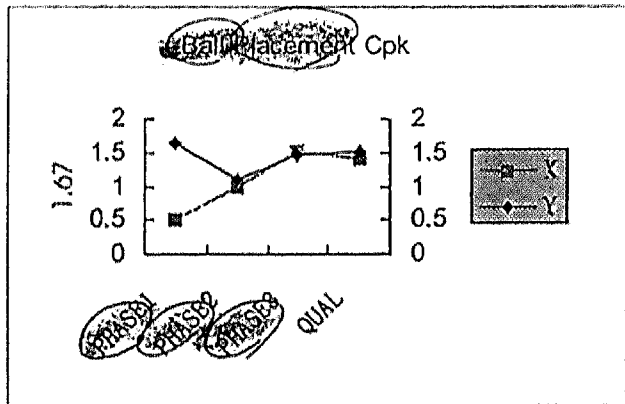
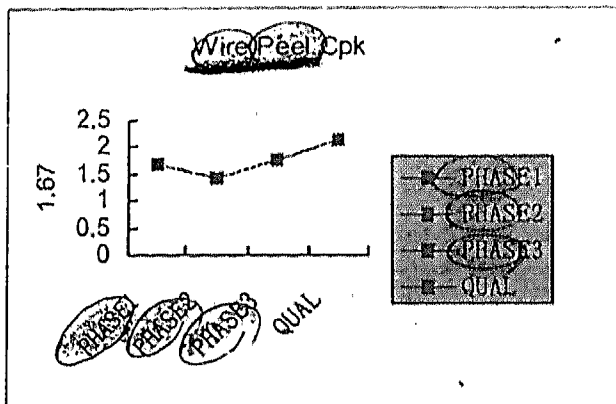
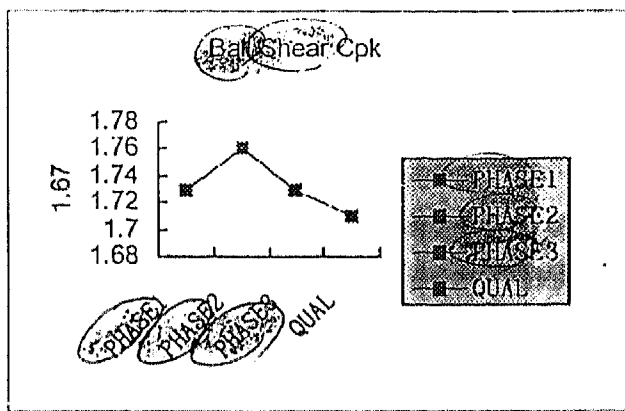
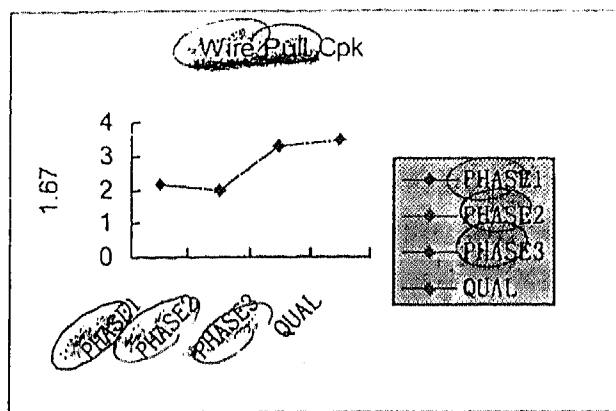
Result shows significant improve of ball placement Cpk, the trial run of production is successfully.

Following analysis will show the Cpk trend of the three phase evaluations and XC Qualitor



## ANALYSIS OF EVALUATION

The data trend of the key data valve shown as following charts



Based on the confirmation run on 1488 turbo, significant difference on displacement capability was seen on 56L SDIP product, the trial run also shows that the assembly line can deal the production of 100 micron level and pitch device, it is the first lot of fine pitch material tested in TianJin plant, this experience is very helpful for further evaluation.

## MARK:

- \* Although the evaluation shows good result, there still some points need improve. Ball placement still need improve, and if OLP (off line program) is available it will be helpful for Cpk improvement.

- \* The assembly parameter definition requires more study on DOE.
- \* The gold wire of FA type is not a fine pitch type, so, it better to evaluate a fine pitch type wire.
- \* The overall performance of material still expect the XC Qual lot result.

## ERLOOK:

The definition of what is considered fine pitch has changed very quickly. A few years ago, manufacturers were struggling to reach 115  $\mu m$  bonding pitch; today, 90  $\mu m$  is a growing application that is producing excellent yield in many production environments. An 80  $\mu m$  process is in qualification for QFPs, and feasibility studies for 70  $\mu m$  QFPs and BGAs have produced very good results. So, the evaluation of our plant is low level study compare with the fashion, it is urgent for MCEL to catch up with the leader level.



## Abstract

With the rapid advancement in wire bonding technology, ultra fine pitch (UFP) bonding with 60µm bond pad pitch (BPP) and below has fast become a reality. While the standard capillary design meets many current industrial needs from their proven reliability, demands for small ball size formation with large wire size in UFP bonding application requires a different tool design and configuration to contain the amount of gold squashed out during bonding. Using an unconventional approach in bonding tool design, a small hole to wire clearance for larger wire size with adequate chamfer diameter (CD) have been achieved.

Research and development on special tool design for UFP bonding on QFP and BGA material has been carried out to address the issue of small ball formation with large wire size. This paper discusses the bonding tool design aspects to control the desired MBD with the use of 25µm Au wire on a 60µm BPP platform. The intent is to establish the design feasibility to be used on the 50 and 40µm BPP at a later stage. Comparison of various bonding responses between standard and new bonding tool design obtained in both laboratory and manufacturing environment was also demonstrated.

## 2.0 Introduction

In UFP bonding, the most difficult tasks are the small ball consistency with a reliable stitch formation. In most cases, the eventual mashed ball diameter (MBD) is only 5 to 8µm smaller than the bond pad opening (BPO). Such tight constraint on the ball bonds would require a consistent small ball formation, high PRS resolution, high positional accuracy and a tight

control on the bonding tool dimensions. In addition, the use of large wire diameter (23 or 25µm) requires the hole diameter to be at least 30µm for a consistent looping. These constraints, together with those problems like open wire, bond lift off, looping performance, surface contamination, etc, have now become a critical process control requirement to achieve a stable wire bond process yield.

## 3.0 Objective

The main intent of this study is to establish and demonstrate the actual bonding response capability of the UFP capillary with the new design concept on a 60µm BPP platform. Reliability performance of the bonded wires is analysed through etching test and cross-sectioning after the temperature cycle test.

## 4.0 Experimental Setup

The evaluation was performed on a high frequency wire bonder using test chip die attached on BGA 256 substrate and QFP 208 copper lead frame with silver coating.

Special capillary for 60µm BPP was used based on the capillary design consideration (See next section). SPT capillary, DFXE-332B-AZM-1/16XL was used for the BGA device and DFXE-302Q-AZM-1/16XL for QFP device.

A 25µm diameter gold wire was used for this purpose.

For the optical inspection and measurement, a high power microscope of 0.5µm resolution was used for ball height, ball size, and loop height measurement.

Ball shear strength and stitch pull test was performed on the shear tester. For the ball shear test, the shear height was set at 3µm.

All responses and measurements were taken with a sample size of 25 readings.

Temperature cycling was performed at -150°C to +150°C for the BGA device. Ball shear and wire pull reading were taken at 100, 500, 1000, and 2000 cycles.

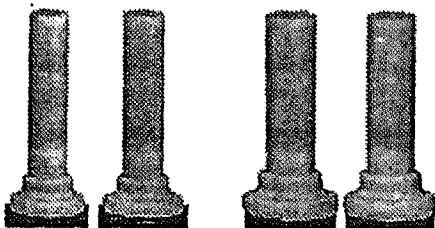
#### 4.1 Capillary Design Considerations

For the ultra-fine pitch bonding, the given BPP and BPO requires a much smaller wire diameter (WD) of 20µm and below. Although this offers an advantage in cost reduction and a simple and straight forward capillary design, the problem takes place in wire sweeping during wire bonding and molding process. The solution has reverted back to use larger wires ranging from 23µm to 25µm. However, various problems arise on using larger WD on a smaller BPO as explained below.

Firstly, for a WD of 23µm, the minimum hole size need to be at least 28µm. Considering a tolerance of +2/-0 µm, the minimum CD need to be at least 34µm for a reliable stitch bond. Such a CD size will almost be impossible to achieve an average ball size of 38µm for a 50µm BPP bonding.

Secondly, considering that the smallest Free Air Ball (FAB) size at 1.4 times the wire diameter (WD) that the current bonders can attained consistently, the deformed ball size cannot be further reduced as shown in Figure 1.

Figure 1: Ball sizes comparison for larger wire size



To address the above-mentioned issues, a unique capillary configuration known as DFX capillary has been designed to contain the amount of gold squashed out during bonding. Together with high precision impact force

control on the bonder, such design has proven to be able to control the desired mashed ball and hence reduce the ball size to a smaller dimension. The effect of such capillary design is illustrated in Figure 2.

In addition to the special capillary design configuration, consistent ultrasonic transfer is crucial for the ball size formation. This can be achieved by using the slimline bottleneck capillary with higher tip breakage resistant and consistent dimension repeatability.

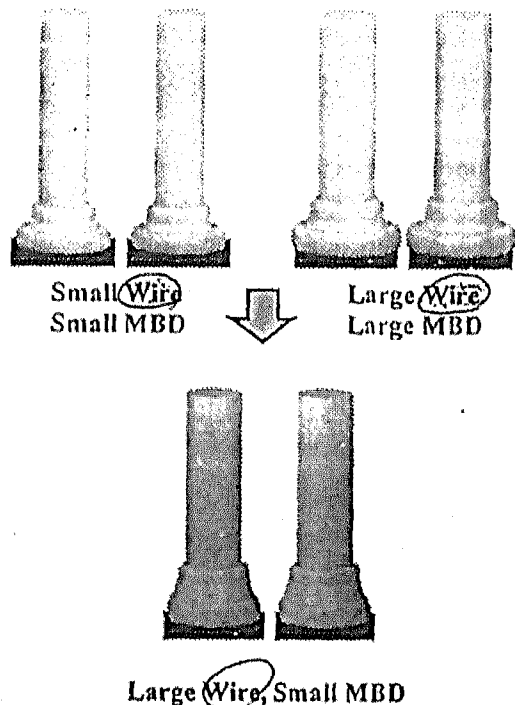


Figure 2: Special capillary configuration for small ball/large wire capability

#### 4.2 Results & Discussion:

A comparison study was carried out to check on the performance of both the Standard and the new DFX capillary. Results were then discussed based on the bonding responses performance as well as the intermetallic coverage.

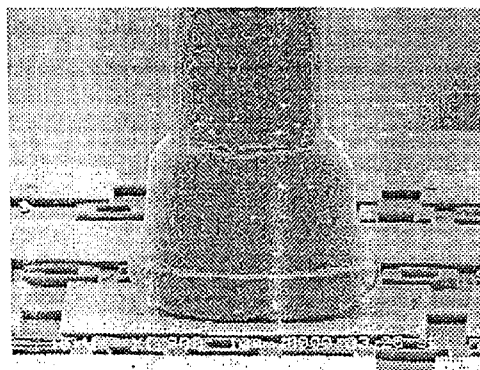
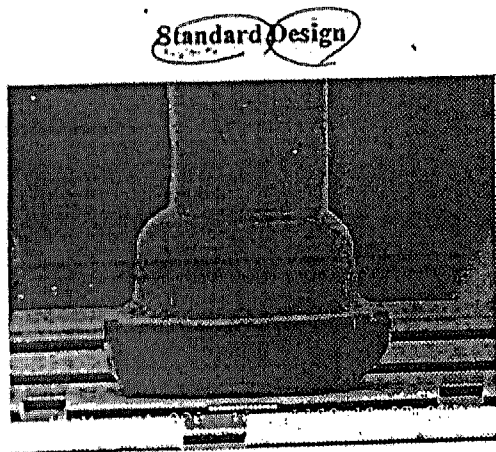
##### 4.2.1 Bonding Response

A design of experiments (DOE) was conducted to determine the optimized process window for both the standard and DFX design.

capillary on a QFP platform. A selected single point parameters was used for bonding response comparison with the result as shown in Figure 3 and 4.

Capillary Design	Standard Design	DFX Design
Device	QFP 208	QFP 208
Capillary Type	SIBNE-30ZA	DFXE-30ZA
Wire Diameter $\mu\text{m}$	23	23
Ball Dmtr $\mu\text{m}$		
Average	42.6	39.2
Std Dev	0.59	0.56
Ball Shear Strength gm		
Average	15.4	11.9
Std Dev	1.04	0.66
Ball Shear Stress $\text{N}/\text{mm}^2$		
Average	106.4	96.8
Std Dev	5.3	3.9
Wirepull Strength gm		
Average	5.8	5.7
Std Dev	0.2	0.2

Figure 3: Bonding response comparison for standard and DFX design capillary



DFX Design Capillary

Figure 4: SEM picture for standard and DFX design capillary

#### 4.2.2 Inter-metallic Analysis

Inter-metallic analysis was analyzed through the etching test to further understand the effect of the new capillary design on the inter-metallic formation. From the pictures shown in Figure 5, no significant difference was observed between the standard and DFX capillary

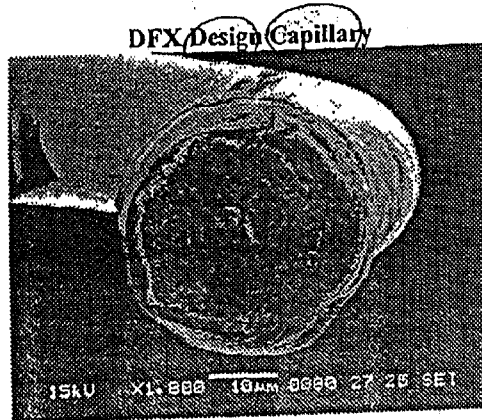
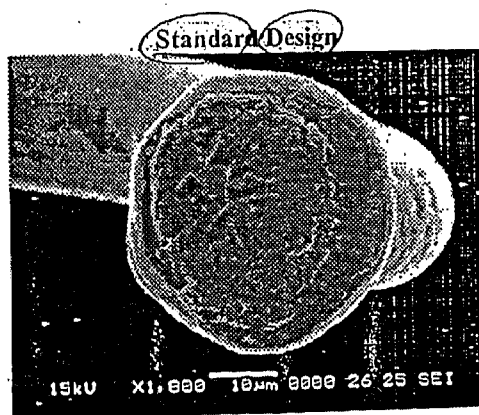


Figure 5: Intermetallic analysis for standard and DFX design capillary

From the bonding response and inter-metallic analysis it can be seen that the DFX design capillary is capable of producing a smaller ball size as compared to the standard design with a minimum ball shear stress of 90 N/mm<sup>2</sup> (6g/mil). Hole and CD dimensions remain the same for both capillary designs.

Having validated such design concept, a similar experiment was conducted with the new DFX design but with a larger hole and CD dimensions. The main purpose is to investigate the possibility of using a bigger hole diameter for larger wire application while maintaining the average bonded ball size at 42µm.

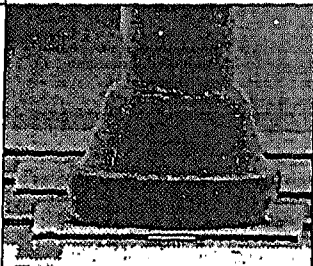
Capillary Design	DFX Design
Capillary Type	DFXE-33ZQ
Wire Diameter µm	23
Ball Dmtr µm	
Average	41.9
Std Dev	0.62
Ball Shear Strength gm	
Average	15.8
Std Dev	0.75
Ball Shear Stress N/mm <sup>2</sup>	
Average	112.5
Std Dev	4.2
Wire Pull Strength gm	
Average	5.6
Std Dev	0.3
SEM Picture	

Figure 6: Bonding response for DFXE-33ZQ

Results from the various bonding responses have indicated that a similar ball size can be achieved with a larger CD and hole diameter with acceptable bond quality. Therefore, a larger wire size can be used with such a design feature for UFP application with controlled ball size.

### 4.3 Reliability Analysis

Having understood the bonding behavior of the DFX design, reliability study was conducted with temperature cycling at condition -150°C to +150°C for a standard 256 BGA device on various bonded ball thickness. Again, Esec3018 with 125KHz was used for this purpose.

Since the evaluation is mainly to check on the reliability of the different ball thickness resulted from the new capillary design, important parameters such as Bond Force, Bond Power and Bond Time were kept constant whilst three different Free Air Ball (FAB) parameters were used. Details of the evaluation parameters is as in Figure 7.

	Eval #1	Eval #2	Eval #3
1 <sup>st</sup> Force	280mN	280mN	280mN
1 <sup>st</sup> Time	15ms	15ms	15ms
1 <sup>st</sup> Power	23.1%	23.1%	23.1%
2 <sup>nd</sup> Force	530mN	530mN	530mN
2 <sup>nd</sup> Time	15ms	15ms	15ms
2 <sup>nd</sup> Power	25.50%	25.50%	25.50%
Auto FAB	40	42	44

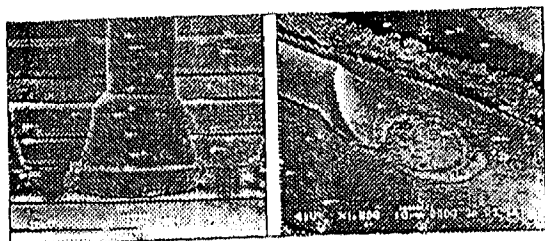
Figure 7: Evaluation layout

All samples were then subjected to the temperature cycling at condition -150°C to +150°C for 100, 500, 1000 and 2000 cycles. Responses were taken both after wirebonding process as well as after each cycle.



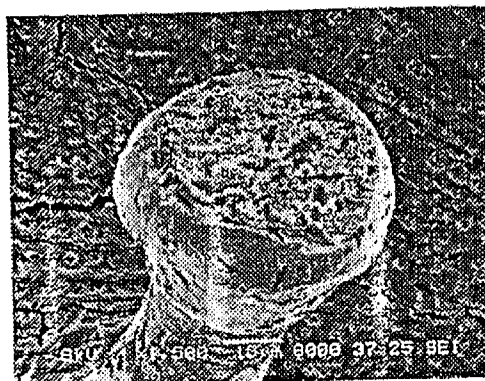
Eval #1

Eval #2



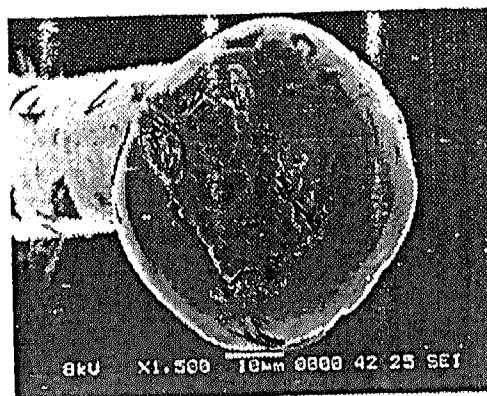
Eval #3

Stitch bond



Ball Height = 6µm

Process	Response	Auto Free Air Ball (FAB)		
		40.00	42.00	44.00
After WB	Ball Dmtr (µm)	Av:46.33 SD:2.17	Av:49.21 SD:1.49	Av:50.62 SD:1.78
	Ball Hgt (µm)	Av:5.50 SD:1.76	Av:11.35 SD:2.25	Av:15.80 SD:1.94
	Wirepull (gm)	Av:8.45 SD:0.24	Av:8.27 SD:0.19	Av:8.45 SD:0.22
	Wireage (gm)	Av:6.21 SD:0.35	Av:5.68 SD:0.42	Av:5.88 SD:0.55



Ball Height = 16µm

Figure 10: Intermetallic analysis for different ball heights

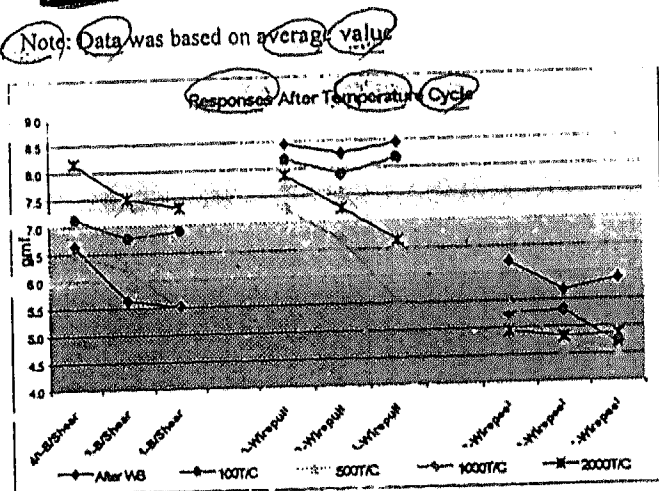


Figure 9: Responses after temperature Cycle

With the same bonding parameters, a smaller FAB setting result in a lower ball height but with a higher ball shear reading. This may be due to the efficient transfer of the ultrasonic energy through the capillary to the smaller amount of squashed gold that helps to develop the intermetallic formation between the Al pad and the Au ball. This observation was verified with an etching test on those units with different ball height readings as shown in Figure 10.

Result indicates that the inter-metallic coverage for the thinner gold ball is approximately 15% more than for the thicker ball. A sufficient coverage of inter-metallic is very crucial in the UFP bonding that requires small and thin bonded ball to cater for the narrow pitch requirement and at the same time did not sacrifice on the bonding performance.

In addition, the degradation of the interface between the bonded ball and the Al pad during temperature cycle was also studied by monitoring the ball shear strength. Fluctuation in the ball shear stress was observed at each read out with the highest reading recorded at 2000T/C. No interface degradation was observed for all units. In fact, there was an increase in the ball shear stress at certain read out.

On the other hand, wirepull and wirepeel strength using the new capillary design concept were comparable to the standard design before temperature cycle test. However, a gradual decrease in the pull and peel strength was observed in most cases but still beyond the above the 4gm minimum limit. Such observation has little impact on the FAB setting since the stitch quality was basically controlled by the FA, OR and T dimensions of the capillary.

In addition to the various bonding responses, a cross section on the ball bond was performed on units for eval/1 with the results as shown below Figure 11.

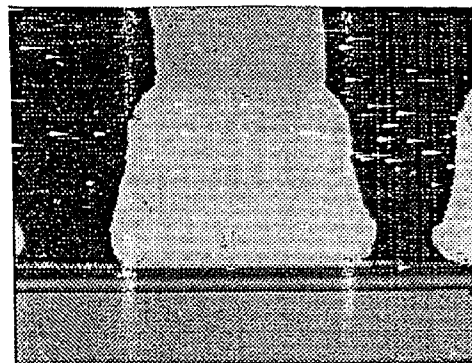


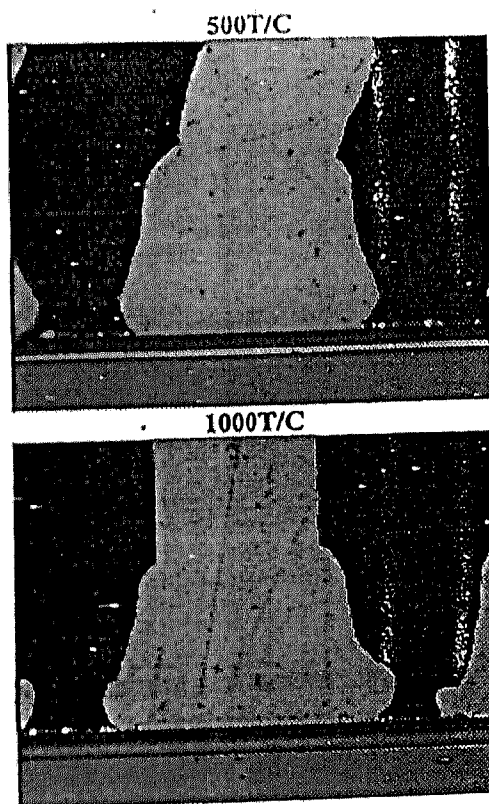
Figure 11: Cross section analysis

Measurement for the inter-metallic thickness revealed that compound thickness varies from 1.5µm to 3µm with no significant difference between 0 and 2000T/C.

On the overall, temperature cycling effect did not have significant impact on ball height variation. Likewise, stitch performance remains within the acceptable quality after temperature cycling.

## 5.0 Conclusion

Wire bonding experiment with the new capillary design concept for ultra-fine pitch bonding has shown that the ball and stitch bonds can be bonded with equivalent quality as compared to the standard design. The bondability and reliability tests have confirmed that the new capillary design can be introduced for volume production without any bonding reliability issue. Results from the bonding test have also demonstrated that a minimum ball size of 10% larger than the CD dimension can be achieved in a production environment for a 25µm wire size on a 60µm BPP. The findings and reliability data provide a useful platform for such design to be used on even smaller pitch bonding application, which required a small ball size formation with large wire size.



2000T/C

## 6.0 Future Development

With the development and verification of the new capillary design on a 60µm BPP, the emphasis by the assembly houses is to incorporate such capillary design for their 50µm BPP using 23µm wire size. In-house